GeoE.171.007

Report on play and prospect evaluation

in HotLime's case study areas.

HotLime Deliverable 3.1

pooling D3.1.1, D3.1.2, D3.1.3 and D3.1.4

2021-03-31

HotLime Deliverable # / WP / due month	D3.1 / WP3 / M30
Dissemination Level	Public
Partner / Person in charge	TNO / J.G. Veldkamp
Authors	See Imprint
Approved	LfU / G.W. Diepolder, PL
Submitted to MT	2021-04-08

This document is part of a project that has received funding by the European Union's Horizon 2020 research and innovation programme, grant agreement number 731166.

Imprint

Collator and editor: J.G. (Hans) Veldkamp (TNO), WP3 Lead
Author(s) of chapters as stated in the sub-headline of the chapters.

Recommended citing

Veldkamp, J.G. & HotLime Team (2021): Report on play and prospect evaluation in HotLime's case study areas. - HotLime Deliverable 3.1: 93 pp. https://repository.europe-geology.eu/egdidocs/hotlime/hotlime_deliverable_31.pdf

Disclaimer

All information provided in this report and eventually via the EGDI dissemination platform serves as a link between the geosciences community and policymakers, authorities and the interested public. It is made available to inform about HotLime's results for the convenience of interested persons and organizations. Albeit the HotLime consortium believes the information to be reliable, mechanical or human errors remain possible. The HotLime consortium, thus, cannot guarantee the accuracy or completeness of the information provided. Neither the HotLime consortium nor any of the sources of information shall be liable for errors or omissions, or for the use of this information, including any liability or expense incurred, claimed to have resulted from the use of the HotLime reports. The information in this report and as eventually provided via EGDI web services is subject to the usual uncertainties of research and shall not be relied on as the basis for doing or failing to do something.

The use of trade names in this report is for descriptive purposes only and does not imply endorsement.

List of abbreviations and acronyms used in the text

AZU	Croatian Hydrocarbon Agency
BHP	Bottom Hole Pressure
BHT	Bottom Hole Temperature
CAPEX	Capital Expenditure
D#	Deliverable #
E&P	Exploration and Production
EB	Empordà Basin
EC	Electrical conductivity
EGDI	European Geological Data Infrastructure
ES-DMA	Ensemble Smoother – Multiple Data Assimilation
GJ	Gigajoule
GLF	Girona Limestone Formation
HIP	Heat in Place
KBMZ	Clinical Hospital New Zagreb geothermal system
LCOE	Levelized Cost of Energy
M	Month (of GeoERA implementation)
Ma	Million years
masl	Meters above sea level
NAFB	North Alpine Molasse Basin
NN	Above sea level
NWECB	Northwest European Carboniferous Basin
OPEX	Operational Expenditure
PBS	Pannonian Basin System
PDF	Probability density function
SRP	(GeoERA) Scientific Research Project
SRTM	Shuttle Radar Topography Mission
T#	Task number
TDS	Total Dissolved Solids
TIN	Triangulated irregular network

UDG	Ultradeep Geothermal
UNFC	United Nations Framework Classification
URI	Uniform Resource Identifier
UTC	Unit Technical Cost
WP	(HotLime) Work package
ZGF	Zagreb Geothermal Field

Contents

Summary

Limestones and dolomites constitute potential geothermal reservoirs. In order to facilitate the estimation of their potential, they can be classified into different plays on basis of their heat transport mechanism. Once grouped into plays, their heat content can be calculated using the straightforward method of Muffler and Cataldi (1978). While being an easily applicable method which allows the comparison of different areas, this does not provide information about the amount of energy which can ultimately be produced from them, nor about the certainty of the estimate. For this, resource classification methods exist which estimate the size of the resources and reserves which can be produced over its lifetime. The most well-known and recent one is the one defined by UNFC which classifies the resources / reserves using 3 axes: level of confidence of the estimate (G-axis), project feasibility (F-axis) and socio-economic feasibility (E-axis).

For the 10 HotLime pilot areas it was concluded that so much uncertainty exists about the level of confidence of the estimate (resources and reserves) that application of the UNFC classification is not useful. This is especially valid for the lack of data regarding developing projects, and reservoir quality data required to estimate producible resources. Therefore, emphasis was put on the calculation of the heat-in -place using a set of common reservoir parameters. Figure 1 shows the results in terms of the min-P90-P10-max values encountered in the pilot area. The maps on which the data of Figure 1 are based are available through the EGDI platform (www.europe-geology.eu). For selected pilot areas an attempt was made to apply the UNFC classification.

Significant uncertainty exists regarding the size of the HIP if deterministic values area are used. In order to visualize this uncertainty a HIP calculation tool was developed which allows to calculate a HIP from a digital geological model using stochastic methods. The tool is available from this link.

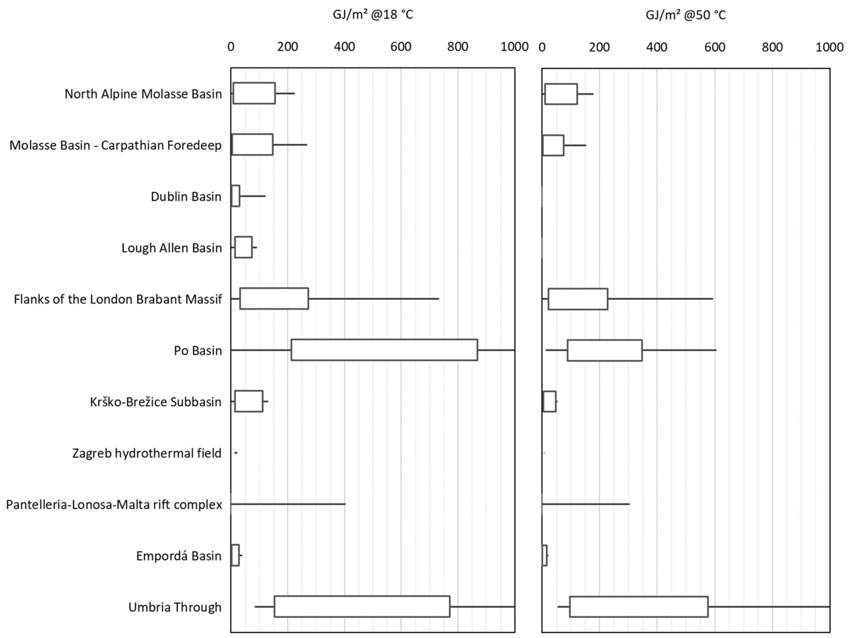

Figure 1 *HIP values for the 10 pilot areas expressed as min-P90-P10-max values for a return temperature of 18°C (left) and 50 °C (right). Note that for the Dublin and Lough Allen basins the HIP for a return temperature was not calculated because the reservoir temperature is mostly below 50°C. For the Zagreb hydrothermal field, no 3D model exists. Therefore, the min and max values were taken from the min and max thickness and temperature values of the Mladost and KBNZ installations. For the Pantelleria-Lonosa-Malta rift complex, a 3D model was not available either. The HIP values were calculated using estimated thickness and temperature values.*

1 Introduction

Author: J.G. Veldkamp (TNO)

1.1 Objective and scope of work carried out

The objectives of the work package 'Play and prospect evaluation' were to provide means to quantitatively and qualitatively assess the expected amount of geothermal energy which can be produced, rank the assessed carbonate plays and classify them. To this end, a workshop was organized in March 2019 in Utrecht to discuss the methodology to be followed. During this workshop, methods to calculate resources and reserves, such as DoubletCalc and ThermoGIS, and to classify them, such as the United Nations Framework Classification (UNECE 2016) were demonstrated and discussed in order to find a common ground on which analyses of the test areas could be performed by all partners. During this workshop, it was decided that the UNFC classification could not be applied to the geothermal reservoirs of the majority of the participating countries because of a lack of sufficient data. Instead, it was then decided that all partners focus on an evaluation of their respective geothermal limestone reservoirs and apply a common heat-in-place (HIP) calculation (Muffler & Cataldi 1978) using common rock parameter settings in order to be able to compare the results, thereby leaving it open to individual partners to possibly apply more sophisticated methods leading to a more detailed view on prospectivity.

Description of work

The work in WP3 is pooled into one task as it builds upon the mapping results of HotLime WP2 (Diepolder et al. 2019, Rupf et al. 2020, Diepolder & HotLime Team 2020), emerging in different geological situations and to a different viability (depending on the data situation), feeding into a iterative process for generic and representative evaluation, classification and ranking. The task focuses on the development of simple and easy-to-use to sophisticated flow performance and resource assessment models for deep carbonate rocks and applying them to the reservoir models that result from WP2.

To this end, applicable (readily available) fast models will be selected based on (public domain, in-house and/or commercial reservoir simulators. This task should be lined up with activities of GE2-Geo4Sure for methodology and classification (see WP6, Task 6.2), however this had to be cancelled as Geo4Sure was not funded, thus implemented. The assessment of carbonates in the latter project is also terra incognita. Therefore, initially, in particular, fast- and/ simplified model approaches will be considered, which allows fast swift computation of the reservoir performance and resulting resource assessment. These models need to be able to incorporate the static model input (resulting from WP2): reservoir depth, thickness and temperature, and, in particular the detailed and anisotropic representation of 3D permeability for karstified and/or fractured reservoirs, building from input from WP2. Results from more detailed interaction effects (chemical, mechanical, thermal) are taken into account in a simplified yet representative way Setting up a quantitative conceptual methodology (tool) for carbonates that incorporates relevant properties and processes affecting flow, taking into account coupled processes of chemical, thermal and mechanical reactions in order to estimate the doublet performance to be fed into the assessment tool must therefore be developed.

Preferably, the static model also incorporates the uncertainty of the major reservoir properties (usually permeability), in order to calculate a geothermal power expectation curve. Results from more detailed interaction effects (chemical, mechanical, thermal) may be considered in a simplified yet representative way. It should also include assessment of sensitivities, which in turns feeds into ways to optimize well completion and ways to stimulate wells and mitigate unsolicited flow performance. To this end the tasks develops representative scenarios of predictive models for (fractured) carbonate reservoirs and templates for model parameterization (under uncertainty).

The deliverables D3.1.1. and D3.1.3 are jointly reported in Chapter 2.

The deliverable D3.1.2 is reported digitally on the EGDI platform (www.europe-geology.eu). The results are described in Chapter 2.

Deliverable D3.1.4, a stochastic HIP calculation tool, was achieved by the Institut Cartogràfic i Geològic de Catalunya and is reported in Chapter 3.

2 Resource calculation and classification (D3.1.1 / 3.1.3)

Authors: J.G. Veldkamp, J. ten Veen, M. Vrijlandt (TNO)

The play concept was originally devised by the oil and gas industry, where a play refers to hydrocarbon occurrences sharing the same source, reservoir and seal. In a similar fashion, one can think of a geothermal play of having a common heat sourcing mechanism (convection or conduction) and reservoir. Various systems for the classification of geothermal plays and, within the plays, prospects have been proposed in the past, usually based on oil and gas systems. Recently, more systems were adapted for specific use in the geothermal industry. A classification in plays serves to identify areas with common characteristics where geothermal exploration and production can take place in similar fashion. Van Wees et al. (2020) state that the adoption of a play concept for geothermal exploration has many advantages, like a reduction of cost, and production of more resources. Once plays have been identified, one can estimate the amount of energy, the resource present in the plays, and, ultimately, calculate how much energy can be produced from it over time.

2.1 Plays

The highest level of organisation is the play type (Moeck et al. 2020). Moeck et al. (2014) state that 90% of the world's geothermal resources belongs to just two convection dominated play types (magmatic or plutonic), whereas convection dominated type are less than 10%. Van Wees et al. (2020) define a geothermal play as 'geothermal potential based on the presence of water in a formation with comparable geological characteristics'. The CANGEA geothermal reporting code (Deibert et al. 2010) uses the term 'Geothermal Play' as 'an informal qualitative descriptor for an accumulation of heat energy within the earth's crust. It can apply to heat contained in rock and/or in fluid. It has no connotations as to permeability or the recoverability of the energy'. Moeck et al. (2020) refer to it as a 'group of lithologically related stratigraphic units having a chance for heat charge and reservoir within a play type' (Figure 2). Hence, geothermal potential in the same play relies on similar geological controls (rock type, porosity / permeability) and heat transport mechanisms (convection vs. conduction) (Moeck et al. 2020).

In HotLime, potential target aquifers were identified without paying overly attention to the type of play they are in. In the Moeck et al. (2015, 2020) system they belong to the main 'conduction-dominated' (CD) type, which contains various play types. For the German HotLime testbed area, this is for instance the 'Foreland basin play type' CD2a, and for the Dutch / Belgian testbed area it would be the CD1.

Term	Definition	Example
Geothermal play type	Patterns in heat charge system, permeability structure and fluid type related to a specific geologic setting, that resemble each other closely geologically, allowing worldwide analogue comparison	German Molasse Basin as part of the North Alpine Foreland Basin, the play type *foreland basin with conduction-dominated heat transport*
Play	Group of lithologically related stratigraphic unit having a chance for heat charge and reservoir within a play type	Upper Jurassic carbonate formation within the play type *foreland basin*
Play segment	Subdivision of a geothermal play. Fields and prospects that share common geological controls and thus a common probability-of-success profile	Carbonate platform or platform slope of Upper Jurassic carbonate formation of the Molasse Basin
Play level	Structural or stratigraphic level of a play; portrays plays at different depths	Mainly Kimmeridgian of the Upper Jurassic at 2 to 5 km depth of the Molasse Basin
Play element	Geologic controls within a play segment bounded by a change in the depositional environment	Reef facies, laminated facies, normal faults, karst in the Upper Jurassic carbonates in the Molasse Basin

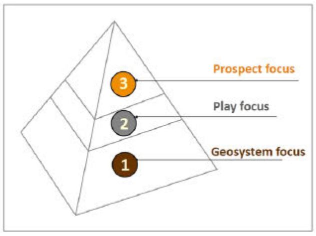

1 **Geologic system analysis as a whole**
- plate setting
- tectonostratigraphic framework
- geosystem history
- rocks and fluids
- stratigraphic sequences
- play identification

2 **Understanding the geothermal play in the geologic system**
- play level identification
- play mapping
- play quantification
- play element
- summary play maps
- common risk segment maps
- exploration targets
- prospect selection

3 **Play level analysis in prospect area**
- geophysical evaluation on prospect scale
- geological model building
- volumetrical model
- selection of drilling targets
- technical risk evaluation
- confidence assessment for a range of models and prospects
- play execution activities

Figure 3. The exploration play pyramid, illustrating the steps of play-based exploration (modified from Royal Dutch Shell, 2013).

Figure 2 Definition of terms required for play-based exploration of geothermal resources and exploration play pyramid. From: Moeck et al. 2020.

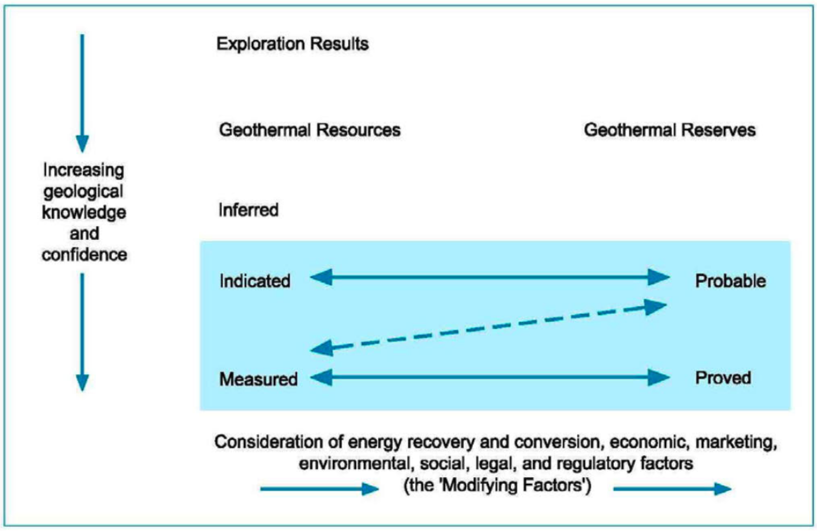

Figure 3 Relationship between Exploration Results, Geothermal Resources and Geothermal Reserves. source: Australian Geothermal Energy Association (2010). The Geothermal Reporting Code. 2008 Edition (copied from: the Canadian geothermal code for public reporting, 2010 edition, https://www.cangea.ca/uploads/3/0/9/7/30973335/canadiangeothermalcodeforpublicreporting.pdf).

2.2 Resources and reserves

In order to be able to predict future geothermal energy production, and to make geothermal energy more attractive for investors, numerical estimates of the size of the available energy are a requirement. Australia, using a system originating from the mineral resources industry (Lawless et al. 2010), and Canada, using the Australian code as a basis have been pioneers in the classification of resources and reserves. Both use a two-dimensional matrix (Figure 3), one axis being the amount of geological knowledge, and the second axis named Modifying Factors which relate to energy recovery and conversion, economic and other factors.

The difference between a *resource* and a *reserve* is the commerciality – for a resource this is not yet established, for a reserve the commerciality is feasible. In the initial stages of exploration, when uncertainty is high, a resource is *inferred*, and with exploration continuing and uncertainty decreasing, this turns into *indicated* and finally *measured*. For reserves, there is not equivalent to inferred, and instead the classes are *probable* and *proved*, similar to the terms used in the oil and gas industry (Deibert 2010). Recently, the United Nations Framework Classification on Reserves (UNFC), using the 2009 classification for fossil energy and mineral reserves and resources as a basis, made a refinement to the Australian and Canadian codes by introducing a third axis (UNFC 2016). In the UNFC classification (Figure 4), the three axes refer to socio-economic feasibility E, project feasibility (F) and level of confidence of the estimate (G which corresponds to the vertical axis of the Canadian scheme of Figure 3). A potential project will plot somewhere in the cube. Hence, if the level of confidence, the project feasibility and the socio-economic viability are all high, a project is considered commercial (green cubes in Figure 4) – but a project may also be commercial if the level of confidence is not on the highest level, hence the three green cubes. The full definition of the axes is:

- **E: Economic and social viability of commercial extraction** (degree of favourability of social and economic conditions in establishing commercial viability of project, e.g. market prices, relevant legal, regulatory, environmental and contractual conditions).
- **F: Field project status and project feasibility** (maturity of studies and commitments necessary to implement project). These extend from early exploration efforts before a deposit or accumulation has been confirmed to exist through to a project that is extracting and selling a commodity and reflect standard value chain management principles.
- **G: Geological knowledge** (level of confidence in the geological knowledge and potential recoverability of the quantities).

Given the fact that most testbed areas within HotLime are in the early stages of exploration with no or few projects developing yet, the classification will plot mostly around G4-G3 (low level of confidence), with a low project feasibility (F4-F3). This makes the application of the scheme less relevant, and, given the lack of data describing the reservoir quality, challenging at the same time. An exception to the rule may be the German Alpine Foreland Basin, where a growing number of projects have been realized, all but three highly successful, some considerably overachieving the expected viability.

A

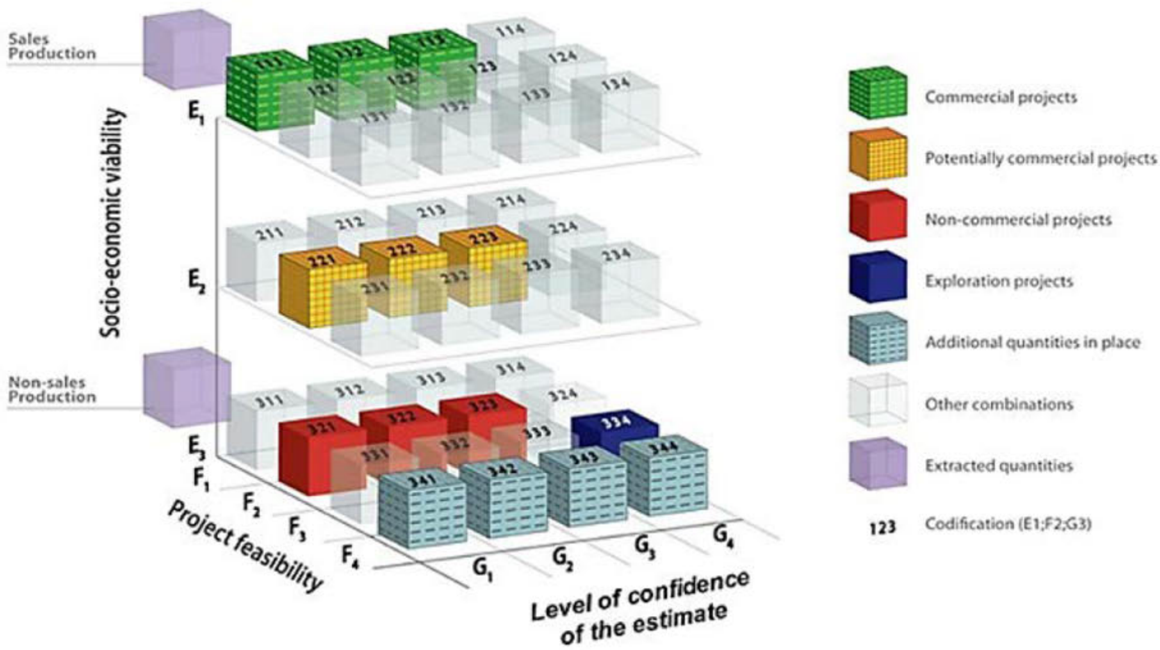

Figure 4 UNFC classification axes and categories (from Falcone and Conti, 2020).

Therefore, within HotLime, it was decided to focus on the geothermal base assessment using a common applicable methodology which is less data demanding, rather than working on the application of a methodology that cannot be applied to most testbed areas due to a lack of data.

The volumetric 'Heat in Place' (HIP) method, developed by the United States Geological survey (USGS) and reported by Muffler & Cataldi (1978), with subsequent revisions and reformulations (Williams et al. 2008, Garg & Combs 2010, 2011, 2015), is the most globally used evaluation technique to estimate the available heat from deep geothermal reservoirs among geological services, research centres and companies in general. A HIP estimation is the first and the key step of any geothermal project in early exploration stages. This method calculates the heat in energy per unit area, which is present in a geothermal aquifer, with respect to an arbitrary cooling temperature which is usually set to surface or ambient temperature. The method requires estimates on reservoir depth and thickness, temperature, and the reservoir rock properties specific heat, density, porosity, and water specific heat and density. The HIP is the maximum theoretically extractable heat energy in the reservoir and is defined by equation 1:

$$Q_{total} = [(1-\phi)c_{pr}\,\rho_r+\phi c_{pw}\,\rho_w]*h*(T_r-T_{ref}) \qquad \text{eq. 1}$$

Table 1 lists the parameters and the common parameter values that were adopted in order to achieve HIP values that can be compared across pilot sites.

Table 1 Rock thermal properties used for the heat in place calculation.

	description	unit	value
Q_{total}	energy content for a column of reservoir rock	J / m²	
ϕ	bulk porosity	fraction	0.05
c_{pr}	specific heat capacity for the carbonate reservoir rock (matrix)	J / kg.K	860
c_{pw}	specific heat capacity (water) for the pore fluid (brine)	J/ kg.K	3800
ρ_r	rock matrix density of carbonate rock	kg/m³	2700
ρ_w	density of low TDS water at about 100°C	kg/m³	1040
h	reservoir height	m	-
T_r	average reservoir temperature	°C	-
T_{ref}	reference (injection) temperature	°C	18, 50

The HIP was calculated for all testbed areas. Additionally, for three pilot regions (the Netherlands, Croatia and Slovenia) the UNFC classification was tentatively applied.

2.3 Upper Jurassic carbonates of the central North Alpine Molasse Basin (Germany and Austria, T2.1)

Authors: J. Großmann (LfU), A. de Witt, I. Rupf (LGRB), C. Porpaczy (GBA)

2.3.1 Description of the pilot area

For a detailed description of the reservoir please refer to HotLime Deliverable 2.0, Summary report of mapping and characterization. Here, only a summary is given.
Please note: Middle Triassic Muschelkalk, occurring in the western part of case study area, in HotLime D2.0 described a reservoir, has not been considered any further as it turned out a thin arenaceous marginal facies all over its distribution area, thus, by definition, not representing a hot lime reservoir.

Case study area T2.1 comprises the central part of the North Alpine Foreland Basin (NAFB), also known as Molasse Basin and the adjacent Swabian-Franconian Alb within the territories of Baden-Württemberg, Bavaria and westernmost Upper Austria.

Stretching over more than 1000 km along the northern fringes of the Alpine Mountain Belt from Grenoble in France to almost Vienna in Austria, the basin features highly productive aquifers at depth. Especially in the NAFB's middle part, these aquifers host enormous utilizable hydrothermal resources, considered holding the highest geothermal potential in Central Europe (Paschen et al. 2003, GeoMol Team 2015).

The case study area itself sprawls 400 km in W-E direction with a maximum N-S extend of 170 km, covering overall roughly 47,700 km², about 13,000 km² on Baden-Württemberg territory, 33,300 km² in Bavaria, and 1,400 km² on Austrian territory.

The asymmetric orogenic foreland basin is filled with Tertiary deposits and resting on a footwall of south dipping Mesozoic sediments and a Paleozoic crystalline basement. To the south, the NAFB is bounded by the Alpine-Carpathian Orogen. To the northwest of the NAFB, the Tertiary basin fill pinches out and the Mesozoic sedimentary sequence crops out in the South German Scarplands. To the northeast, the basin terminates at the Variscan basement inlier of the Bohemian Massif.

Carbonates from the Upper Jurassic represent the targeted geothermal reservoir in the study area. Deposited in a tropical shelf sea environment with up to 600 m thickness, they show strong regional variation of facies realms like reefs and other bioherms, lagoons and basins. A major early Cretaceous regression event ended deposition. From Cretaceous to early Tertiary the carbonates experienced intense weathering and deep karstification under humid conditions. This created considerable secondary permeability in the carbonates and, hence, the Upper Jurassic (Malm) became the most prominent reservoir of the Central North Alpine Foreland Basin.

The tilted block, fault-bounded to the SW, Landshut-Neuötting crystalline rise represents a major structural element in the study area. The basement fault block strikes NW-SE and continues into Austrian territory, where it is named Central Swell (Zentrale Schwellenzone). Due to Cretaceous reactivation uplift, the Upper Jurassic was completely eroded across most parts of the crystalline fault block. In consequence, the area of the Landshut-Neuötting crystalline rise had to be excluded from the reservoir model.

Within hydrothermal sedimentary energy systems, the Molasse Basin is assigned to the CD2-Foreland basin play type/ orogenic belt type where the heat transfer is conduction dominated and the geologic controls are litho- or biofacies and faults or fractures.

Characteristic properties of this type are high to low permeability of marine sediments, infiltration fluids and temperatures below 160°C (Moeck et al. 2014).

When calculating the HIP, for the sake of comparability, only an average value for the porosity was assumed and facial differences within the Upper Jurassic were not modelled and considered. Thus, the indices (a, c, or d) according to Moeck et al. (2014) cannot be determined more precisely.

2.3.2 Input data

For the preparation of a consistent heat-in-place model across the T2.1 area, LGRB and LfU produced a joint structural 3D model of the Upper Jurassic carbonate reservoir horizon (Diepolder & HotLime Team 2020) including the minor Upper Austria share (Donner 2019). Likewise, the calculation of the heat-in-place parameter was carried out separately at first (Table 2) and was integrated into a regional heat-in-place model across the whole T2.1 area later on. For the area of Upper Austria, heat-in-place was modelled together with the area of Bavaria at LfU.

2.3.3 Results

In general, the parameters listed above show a rather heterogeneous distribution in the model area of Baden-Württemberg and a more homogeneous distribution in the model area of Bavaria/Upper Austria (discussed below).

Considering the areal distribution of the Upper Jurassic carbonates, the heat-in-place model excludes the area of the Nördlinger Ries, the Landshut-Neuötting crystalline rise and the Bohemian Massif, except for the small area of 'Ortenburg Depression' where carbonate rocks were preserved from erosion. For injection temperatures of 18°C and 50°C (Figure 6), the modelled heat-in-place parameters show a N-S trend of increasing heat-in-place towards the Alpine orogenic front. In the whole modelling area, maximum heat-in-place of 224 GJ/m² (T_{inj} = 18°C) and of 178 GJ/m² (T_{inj} = 50°C) can be observed. The isoline, which defines minimum heat-in-place, is oriented WSW-ENE and perpendicular to the dip direction of the Upper Jurassic carbonates. With increasing T_{inj} the heat-in-place isoline migrates south, where the reservoir lies at greater depth and includes higher temperature. Unlike the clear orientation of the minimum heat-in-place isoline in the western and in the central parts of the study area, the shape of the isoline is more complex in the eastern part of the modelled area, towards the crystalline platform of the Bohemian Massif. In the very south of the model area, directly north of the Alpine orogenic front, heat-in-place magnitudes show more variety as well.

In contrary to the fairly homogenous distribution of temperature and depth values, the Upper Jurassic carbonate reservoir displays a rather heterogeneous distribution of thickness values in the modelled area. In particular, this is observable in the South of the modelled area, where constrained areas of high thickness coincide with areas of maximum heat-in-place.

Table 2 Input data and workflows for heat-in-place modelling approaches.

data and workflow	LGRB (covering Baden-Württemberg)	LfU (covering Bavaria and Upper Austria)
3D horizons and fault network	Manual fault surface modelling and iterative horizon modelling with SKUA Structural Modelling Workflow • Well data sets, digital (3319 wells) • 112 2D-Seismic Lines (total length ~1600 km) • One ~136 km 3D-Seismic (Moenchsrot)	Construction of a grid with regional cross-sections that integrate all available depth data (wells, outcrops, legacy contour maps, 3D models, fault network). Seismic-based fault interpretations were included from the GeoMol Framework Model (GeoMol Team 2015) and revised based on results from the HIKE project.
temperature data	GeoMol temperature model (GeoMol Team 2015)	
heat-in-place modelling workflow	• Export of Point Data Sets with depth and temperature information • ArcGIS-workflow with raster interpolation and calculation for 500 x 500 m seized cells	• SKUA SGrid from top and bottom horizons (triangulated meshes) with displacements at faults • Grid cells with volume defined as 500 m x 500 m x thickness of reservoir [m] • Grid cells attributed with temperature data (catchment of temperature data from voxet model closest to SGrid cell centers) • Calculation of heat-in-place parameter in each grid cell • Export of parameters (heat-in-place, thickness of reservoir, depth of top of reservoir, temperature) to ArcGIS as Point Data Sets
raster interpolation	• Merge of Point Data Sets provided by LGRB and LfU • Raster interpolation (spline with barrier) using barrier polygon (HotLime Case Study Area 1) • Correction of artefacts from raster interpolation (e.g. negative heat-in-place value, negative thickness value, etc.) • Preparation of map series with raster colour schemes, defined by maximum and minimum representative for all HotLime project areas	

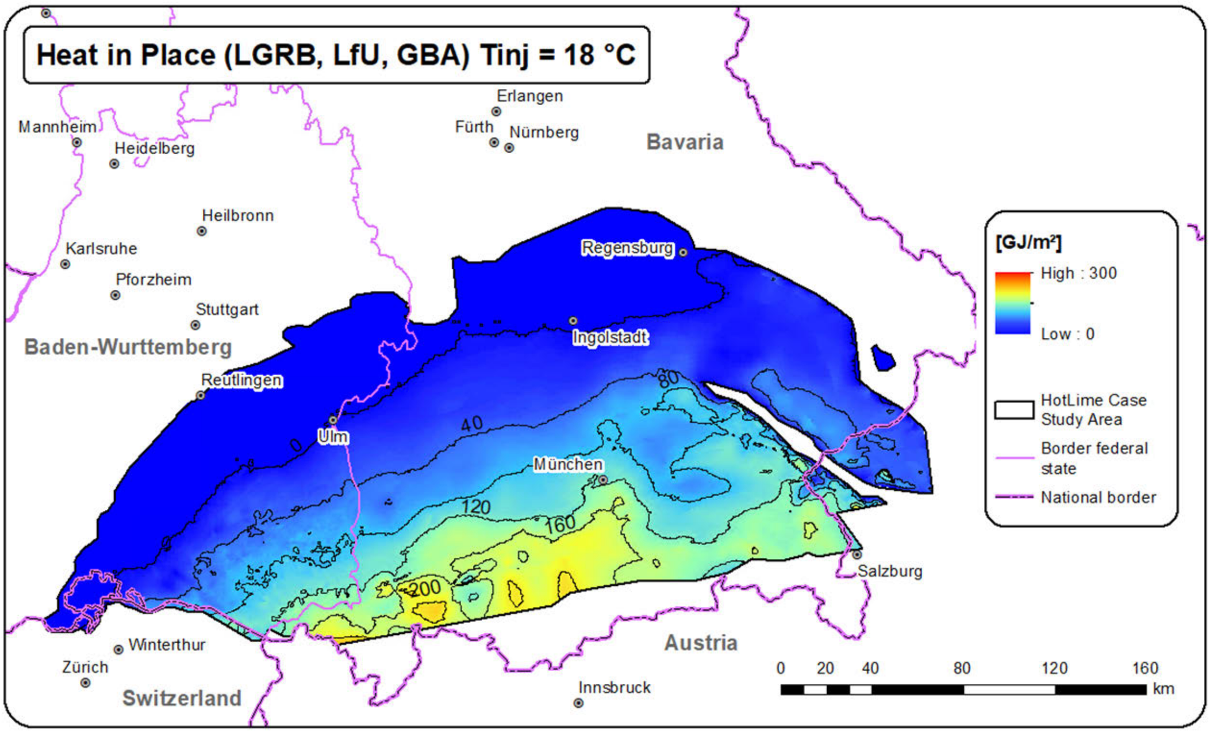

Figure 5 *Heat-in-place with reinjection temperature at 18 C, contour lines with 40 GJ/m² spacing.*

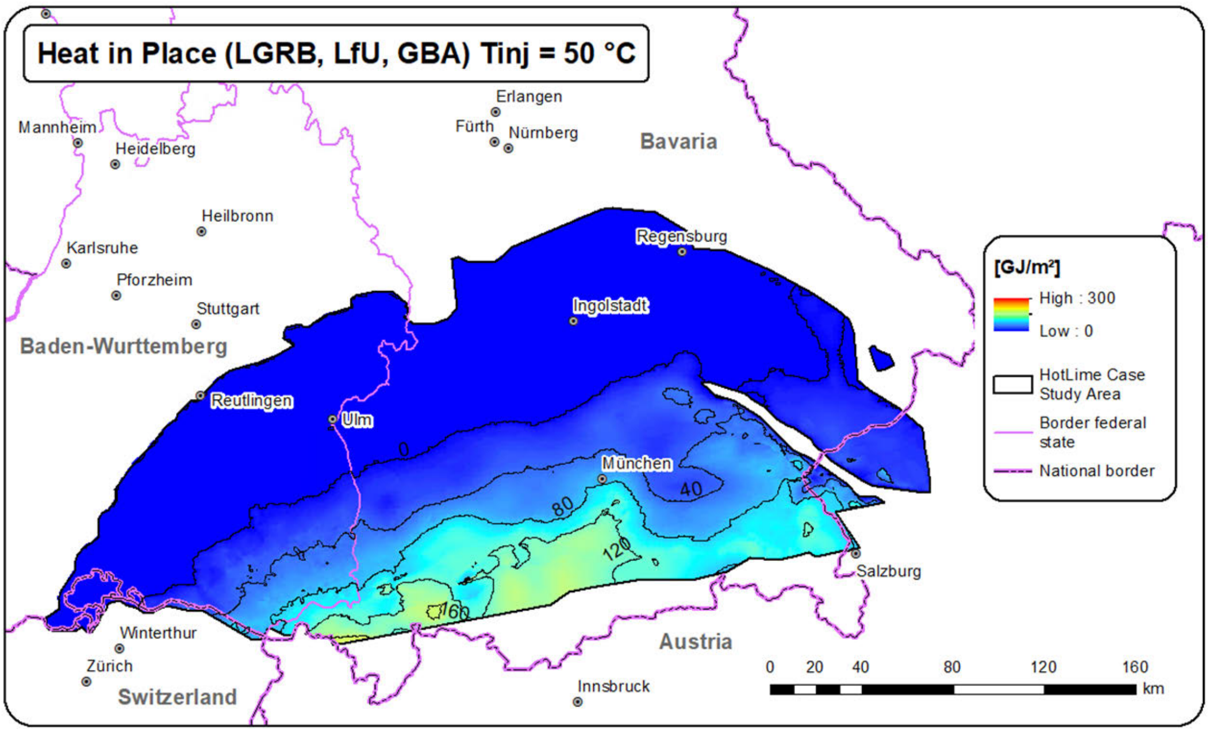

Figure 6 *Heat-in-place with reinjection temperature at 50 C, contour lines spaced at 40 GJ/m².*

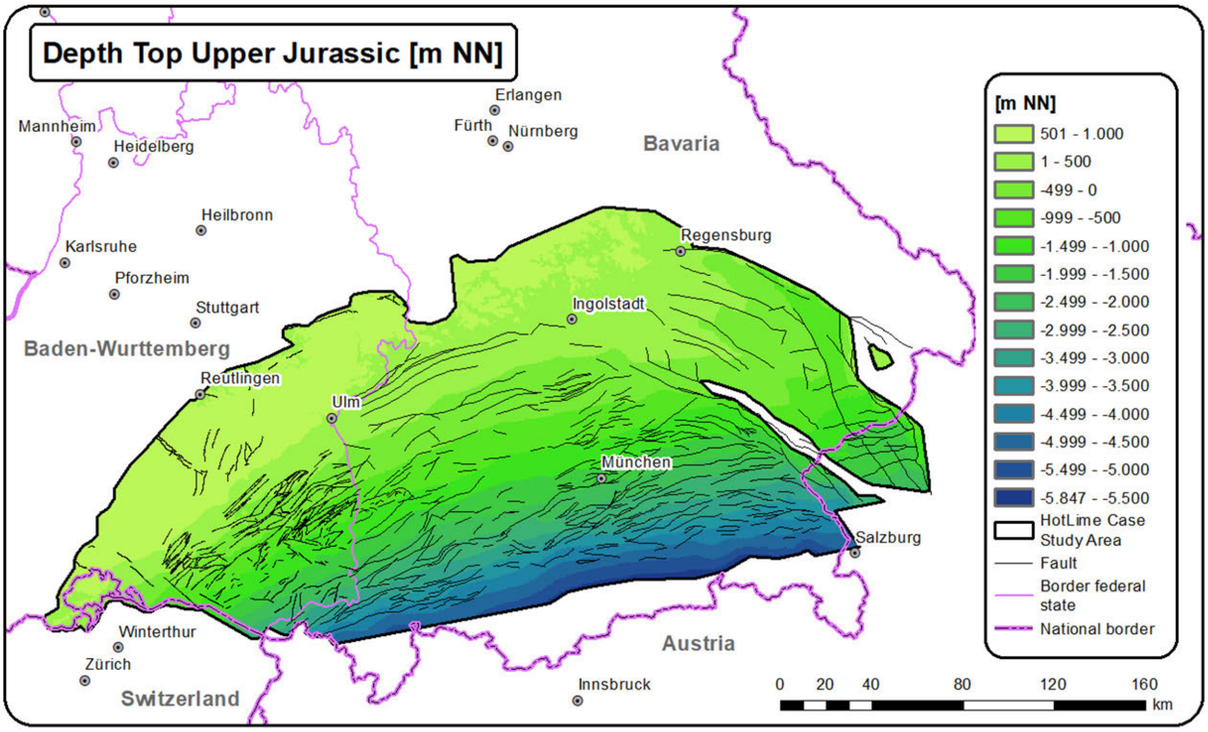

Figure 7 Depth of the top of the Upper Jurassic (NN: above sea level).

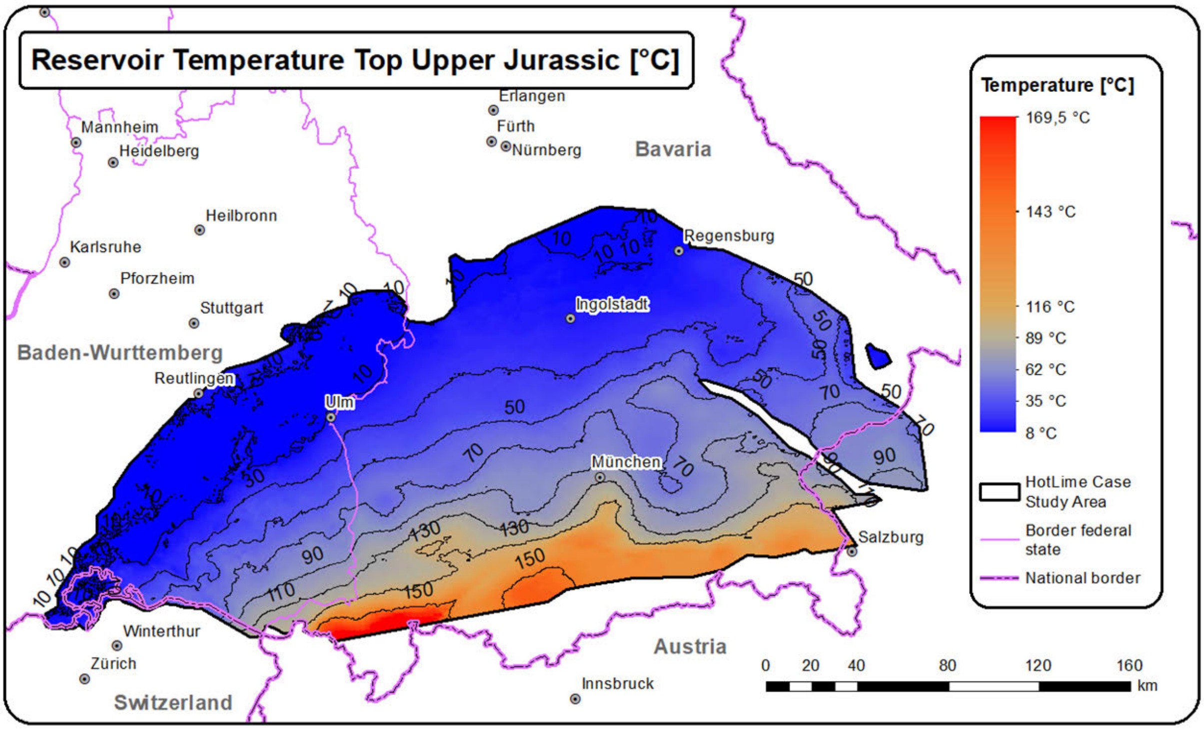

Figure 8 Temperature at the top of the Upper Jurassic, isotherms spaced at 20°C.

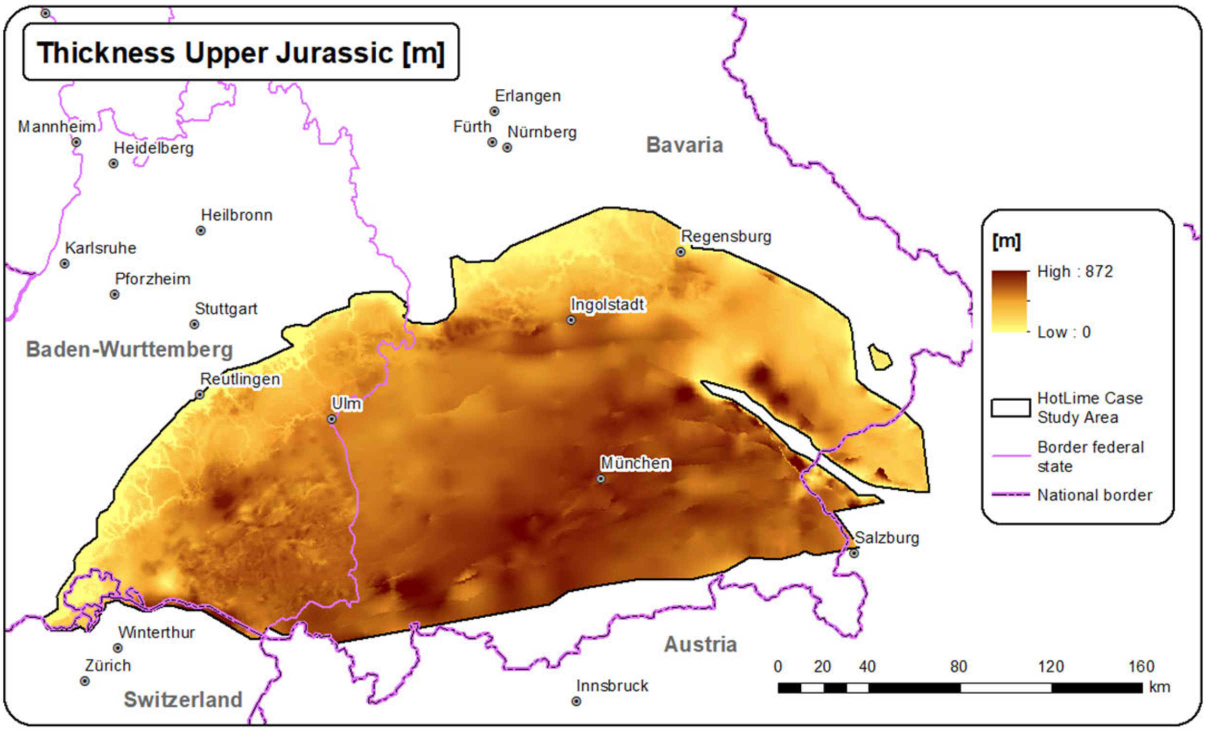

Figure 9 *Thickness of the Upper Jurassic as geothermal reservoir.*

Parallel to the trend of increasing heat-in-place towards the south, the depth of the top of the reservoir (Figure 7) and the reservoir temperature (Figure 8) increase. The deepest value for the top of the Upper Jurassic unit is at -5847 m a.s.l. The highest temperature according to the included temperature model is 170°C in the very southeast of the modelled area.

The modelled thickness of the Upper Jurassic carbonate reservoir shows minimum values along the northern and the north-eastern edge of the model area (Figure 9). Here, the carbonate units crop out in the Swabian-Franconian Alb. Towards the east, the thickness of the Upper Jurassic reservoir decreases incrementally towards the south-western margin of the Bohemian Massif, where is terminates at the Danube Fault System. Additional areas of minimum thickness emerge southwest and northeast of the Landshut-Neuötting crystalline rise, where the Upper Jurassic units were tectonically uplifted and eroded. The maximum thickness of 872 m is located east of the Landshut-Neuötting crystalline rise.

In contrast to the fairly homogenous distribution of temperature and depth values, the Upper Jurassic carbonate reservoir displays a rather heterogeneous distribution of thickness values in the modelled area. In particular, this is observable in the South of the modelled area, where constrained areas of high thickness coincide with areas of maximum heat-in-place.

2.3.4 Uncertainties

Uncertainties in the heat-in-place model are difficult to quantify. One major aspect of uncertainty comes with a regionally highly varying availability of reliable underground data in the modelled region. The density in the distribution of deep wells and of 2D/3D seismic data is high in the basin center and diminishes almost entirely towards the basin margins.

While in the north-western part of Baden-Württemberg the 3D modelling was based on outcrop and drilling information, the southern section was mainly based on borehole information and seismic interpretation. Due to the heterogeneous nature of the seismic data ensemble and the lack of metadata on the original processing, the uncertainty of the interpretation itself can be as high as one full wavelength in time domain (corresponding to approximately 50 m). Further uncertainty concerning the interpretations in depth domain arise from possible variations of the seismic velocities, including the static correction used for harmonizing the seismic data to a common reference level. Together with ambiguities from far distance interpolation of 3D horizon data, the resulting Upper Jurassic reservoir thickness, and thus the calculated volume of the reservoir for the HIP calculation, can be either underestimated or overestimated. Accordingly, the modelled maximum reservoir thickness of 872 m is much higher than the expected maximum thickness of 600 m.

The 3D modelling approach in Bavaria/Upper Austria was primarily based on depth data only. Consequently, uncertainties from seismic interpretation and time-depth conversion have to be considered for the geometry of the fault network, which was imported from the GeoMol Framework model (GeoMol Team 2015) and revised in its eastern part (Donner 2019). Considering the applied explicit modelling approach, where a grid of regional cross-sections was constructed first, and horizons and faults were modelled in 3D afterwards, uncertainty naturally rises with increasing distance from the cross-sections. Consequently, the resulting parameter maps show an overall higher heterogeneity in the area of Baden-Württemberg, where a dense grid of interpreted seismic horizon lines and widely scattered well markers was included in the 3D reservoir geometry.

In addition, the average temperature of the rock as an input variable for calculating the heat-in-place according to Muffler & Cataldi (1978) was subject to different calculation methods. In the model of Baden-Württemberg it represents the mean value of the temperatures at the top and the base of the reservoir ($(T_{top} + T_{base}) / 2$). In the model of Bavaria/Upper Austria, temperature data was extracted from the GeoMol temperature voxet cube, closest to each cell center of the reservoir SGrid volume.

Additional uncertainty for heat-in-place is based on a lack of porosity data in the Upper Jurassic carbonate reservoir. Especially in the deeper surface, formation porosity data is only available from deep wells, which mostly cluster in areas constrained to oil and gas fields or deep geothermal plays in the Munich area. Consequently, the distribution of known facies types is hard to map in the deeper subsurface and facies variation can only be documented on regional scale (e.g. Birner et al. 2012, Birner 2013). In addition, intense karstification, faulting and fracturing contribute considerably to secondary porosity, which significantly influences the overall porosity used for calculating heat-in-place after Muffler & Cataldi (1978). Other parameters like the specific heat capacity can vary significantly across the whole reservoir as well. Before carrying out more detailed studies, the mentioned parameters require thorough revision regarding other available data on local scale.

2.3.5 Assessment of the HIP results in terms of geothermal potential (where to go, and where not to go)

The produced heat-in-place model with both scenarios of T_{inj} = 18°C and T_{inj} = 50°C represents a regional-scaled basic concept for locating deep geothermal prospect areas in the NAFB. Depending on the calculated scenarios, areas of unproductive heat-in-place are generally located in the North of the basin and can be excluded from any deep geothermal prospecting endeavours. With higher reinjection temperature, these unproductive areas extend south. In the south, where the carbonate reservoir reaches its highest depth, heat-in-place shows its highest magnitude. Here, any deep geothermal production can only be realized by drilling extremely deep wells, which naturally implies high risk and cost. Few anomalies that show heat-in-place of 150 - 200 GJ/m² stretch north, towards the basin centre where the Upper Jurassic unit is located at shallower depth (-3000 to -2500 m a.s.l.). They coincide with areas of higher reservoir thickness, which most likely refer to the distribution of specific carbonate facies types like reef bodies. These areas represent promising prospecting regions, as the amount of stored heat-in-place likely balances deep drilling risk and cost. Here, a local more detailed heat-in-place study would allow for quantifying the reservoir potential more accurately.

2.4 Upper Jurassic carbonates in the Molasse Basin – Carpathian Foredeep transition zone (Austria and Czechia, T2.2)

Authors: C. Porpaczy (GBA), J. Franců (CGS)

For a detailed description of the reservoir please refer to [HotLime Deliverable 2.0](), Summary report of mapping and characterization.

Geothermal resource assessment in pilot area T2.2 between Austria and Czechia was based on a deterministic Heat in Place method, with input parameters for density, porosity and heat capacity provided by project lead LfU in order foster comparability of results between all HotLime pilot areas throughout Europe.

Top and Base Layers of the modelled Upper Jurassic Limestone reservoir in the Molasse Basin- Carpathian Foredeep transition Zone and a SRTM90 digital elevation model were used to calculate the required input parameters for the cross border pilot area (Figure 10). Furthermore, a regional geothermal gradient of 2.8°C/100m was taken from a previous study dealing with geothermal potential assessment in the north-eastern part of Austria to estimate temperature values for the top and base horizons of the Upper Jurassic strata (Götzl et al. 2012).

The SKUA-GOCAD™ Software suite was used to calculate values for depth below surface topography, thickness of reservoir and temperature at top and base Upper Jurassic on a 2D-grid (Figure 40). Depth, thickness and temperature information derived from modelled TIN Layers were then imported as point sets into ArcGIS Pro. In the GIS environment, a mastergrid with 500x500m cells was created and populated with the data from the 3D model. Based on a workflow provided by LGRB, the average temperature for the reservoir (temperature top + temperature base/2) and Heat in Place was subsequently calculated using the Tool "Raster Calculator" in ArcGIS Pro.

In HotLime WP2, the Upper Jurassic reservoir appears in two distinct depositional environments, reflecting a marginal reef carbonate facies towards the west and an overlying basinal facies in the eastern part of the pilot area. However, these facies were only mapped in the static model and not put into consideration for geothermal potential assessment, due to lack of petrophysical data. The border between those facies (Mušov line) is shown in the thickness map (Figure 11).

The calculated HIP results varied between negative and positive values for both reinjection temperature settings. Subsequently, negative values were discarded, as they depicted areas where injection temperatures exceeded the estimated reservoir temperatures due to shallow and thin Upper Jurassic strata. The final max. values were estimated to be 269 GJ/m² for 18°C and 154 GJ/m² for 50°C reinjection temperatures. In both cases, the respective HIP reflects the thickness and depth variations of the reservoir, with max. values located at the south-eastern margin of the pilot area. In this region, Upper Jurassic units are descending towards the deeper parts of the Molasse Basin and are covered by the foremost thrust units of the Alpine-Carpathian Orogen approaching from southeast. However, considering potential geothermal usage, the area exhibiting the highest HIP values remains sparsely populated in

Austria. On Czech territory, the town of Mikulov (population ~7530) is located close to the Austrian border in the easternmost pilot area, showing a more favourable location for possible geothermal energy usage.

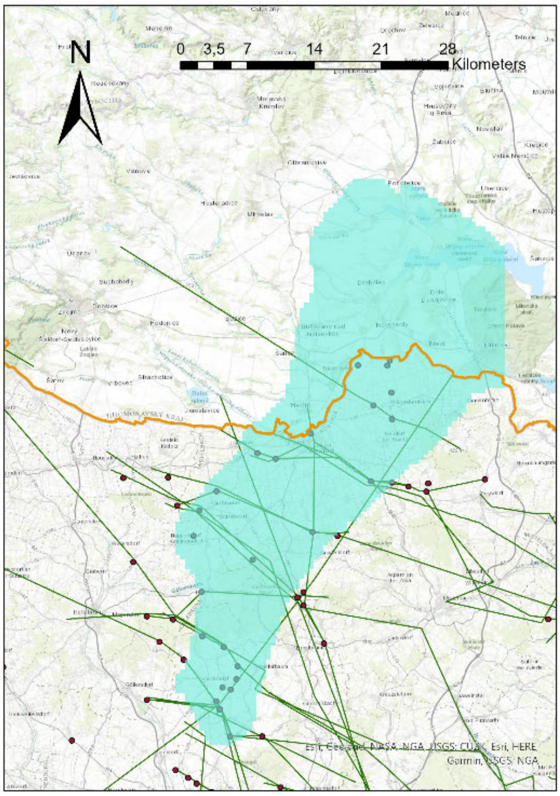

Figure 10 *Wells and Cross Sections in Austria available for modelling. Partner CGS provided 3D Layers of Top and Base Upper Jurassic on Czech side, but without information on input data for modelling. Austrian/Czech border indicated in orange. For further description of input data sets, see HotLime Midterm report (https://repository.europe-geology.eu/egdidocs/hotlime/hotlime_deliverable_20.pdf).*

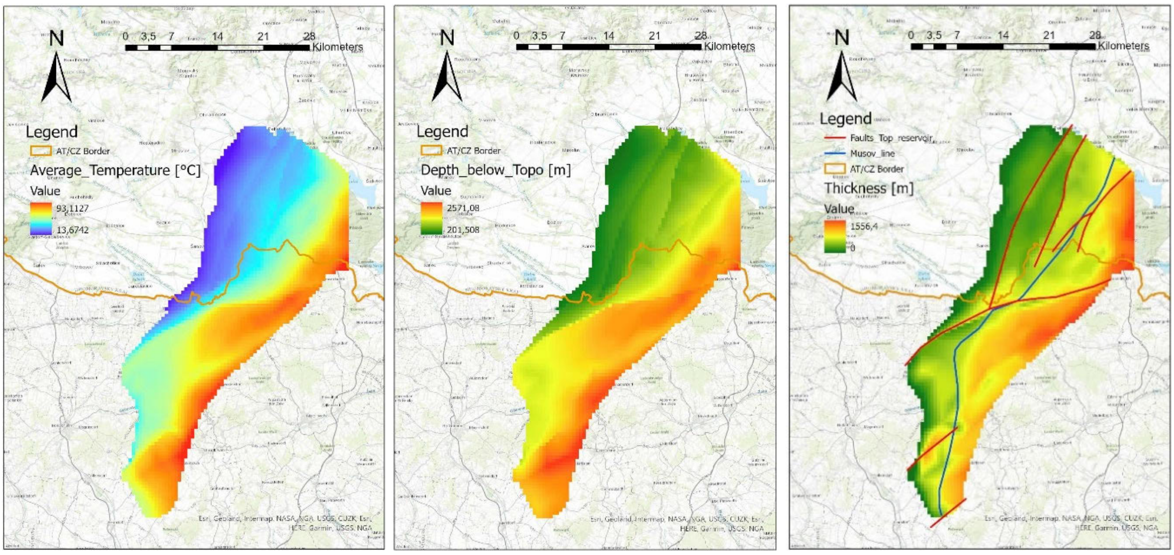

Figure 11 *Maps showing Average Temperature, depth below topography and thickness of the Upper Jurassic units in the cross-border area Austria/Czechia. Mušov line and faults at the top of the reservoir are depicted in the thickness map.*

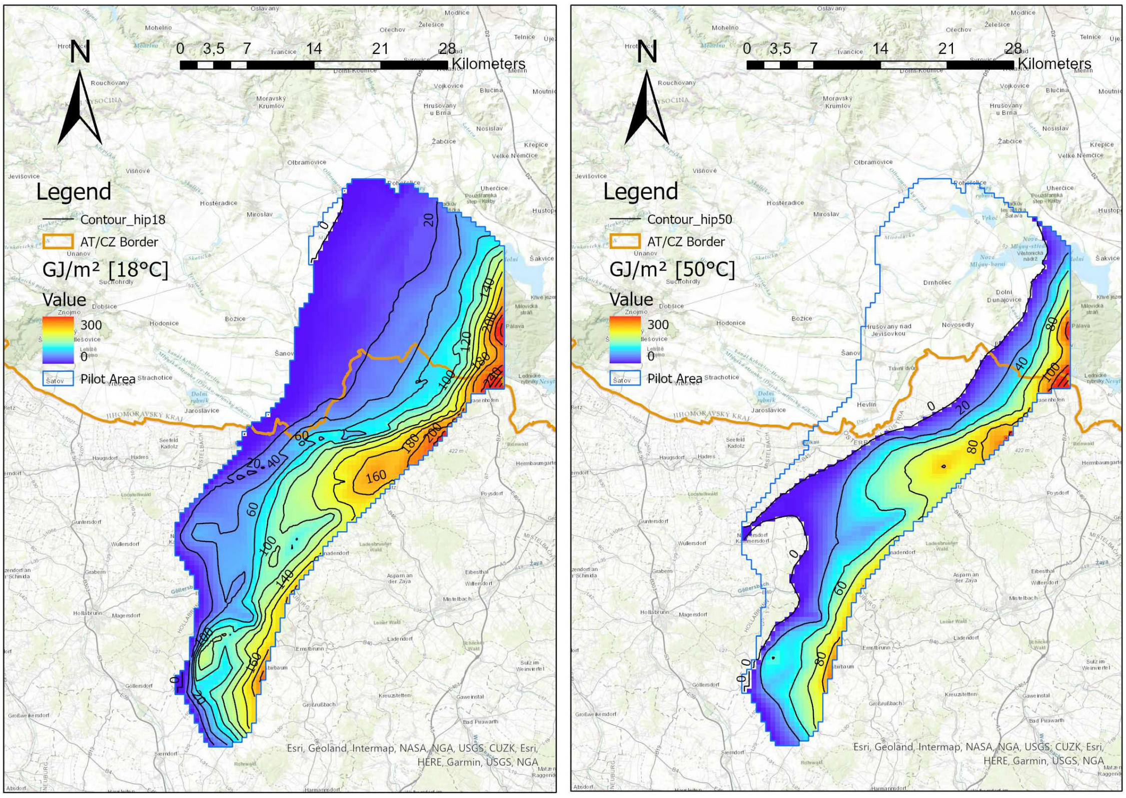

Figure 12 *HIP calculated on a 500x500m reservoir grid. Left: 18°C injection temperature. Right: 50°C injection temperature. Highest values in the southeast correspond with areas of increasing sedimentary thickness towards the deeper areas of the Molasse Basin.*

2.4.1 Uncertainty of results

A quantitative assessment of uncertainties for the HIP maps shown in Figure 12 remains difficult as input data were only available for static modelling and distributed unevenly throughout the pilot area. In general, resulting data from the Austrian side is considered as being more reliable as the location and quality of wells and sections used for 3D model construction was thoroughly evaluated. All results for the Czech Part of the pilot area are bases on top and base layers of the reservoir, which were stitched together with the horizons modelled in Austria. However, no information on the input data which was considered in modelling on the Czech part of the pilot area was available.

2.4.2 Recommendations for future research & exploration

Taking the results from the calculated HIP maps into account, future research should be conducted in the border area in the vicinity of the town of Mikulov (population ~7530), where Upper Jurassic carbonates are located at depth of ca. 2300 - 2500m below surface. If population size is sufficient for commercial viability of hydrothermal heat production has to be evaluated, as exploration for deep geothermal resources usually requires 3D seismic surveying and - if available - geological legacy data from the E&P Industry. This makes hydro-geothermal exploration a costly and high-risk endeavour, which only pays off if local heat demand is given and systematic use of the reservoir over a long time period can be expected.

2.5 Carboniferous carbonates in (a) Lough Allen Basin and (b) Dublin Basin (Ireland, T2.3)

Authors: R. Rogers, B. Mozo, S. Blake, B. McConnell (GSI)

2.5.1 Dublin Basin

For the determination of volumetric heat in place in the Dublin Basin the HotLime consensus values for porosity, heat capacity and reference temperature were used. The other values required for the equation were determined from the 3D model.

The target reservoir is defined as the carbonate sequence between the base surface of the Ballysteen Formation and the base surface of the Tober Colleen Formation (incorporating the Ballysteen Formation and the Waulsortian Formation; see T2.3 in HotLime Deliverable 2.0 (Rupf et al. 2020) for further information). Using these two surfaces the thickness of the reservoir was calculated as a raster and the reservoir volume was derived for individual cells of 500x500m (Figure 13).

The temperatures at the top of the reservoir were initially determined using the depth to the top of the reservoir and an estimated average geothermal gradient for Ireland of 25°C km^{-1} (Goodman et al. 2004). The temperature maps were then refined by incorporating available data from a 1.3 km borehole near Newcastle (Figure 14), and existing knowledge of thermal springs in the central region of the basin. Measurements from the deep borehole in Newcastle, near the southern margin of the basin, recorded a bottom-hole temperature of 46°C and a maximum thermal gradient of 32.4°C km^{-1} (SLR, 2009). Thermal springs (i.e., those with average surface temperatures significantly elevated with respect to average annual groundwater temperatures) are recorded in several places in the centre of the Dublin basin, and are commonly associated with either NE-trending Carboniferous normal faults or N-trending Cenozoic strike-slip faults (Blake, 2016). The large NE-trending faults are older and extend deep beneath the basin, and so have the potential to provide deep permeability for thermal fluids, particularly where the structures are karstified.

The elevated Newcastle geothermal gradient was applied within a 2.5 km buffer zone surrounding both the southernmost fault (basin boundary) and the NE-trending fault in the centre of the basin (Figure 14) as these faults have been demonstrated as hydrothermal circulation conduits. Outside of these zones the national average gradient was used. The average reservoir temperature is determined by averaging the top reservoir temperature and bottom reservoir temperature in a 500x500m aerial extent.

The Dublin Basin study area shows the highest thermal potential in the northwest of the basin, with some potential in the south and southeast between the fault zones with elevated thermal gradients in Figure 15. The southern fault zone itself also displays higher heat in place that the basin average, particularly near the coast. Blank spots in the Dublin Basin heat in place maps are artifacts of interpolating the surface depths from the 3D model.

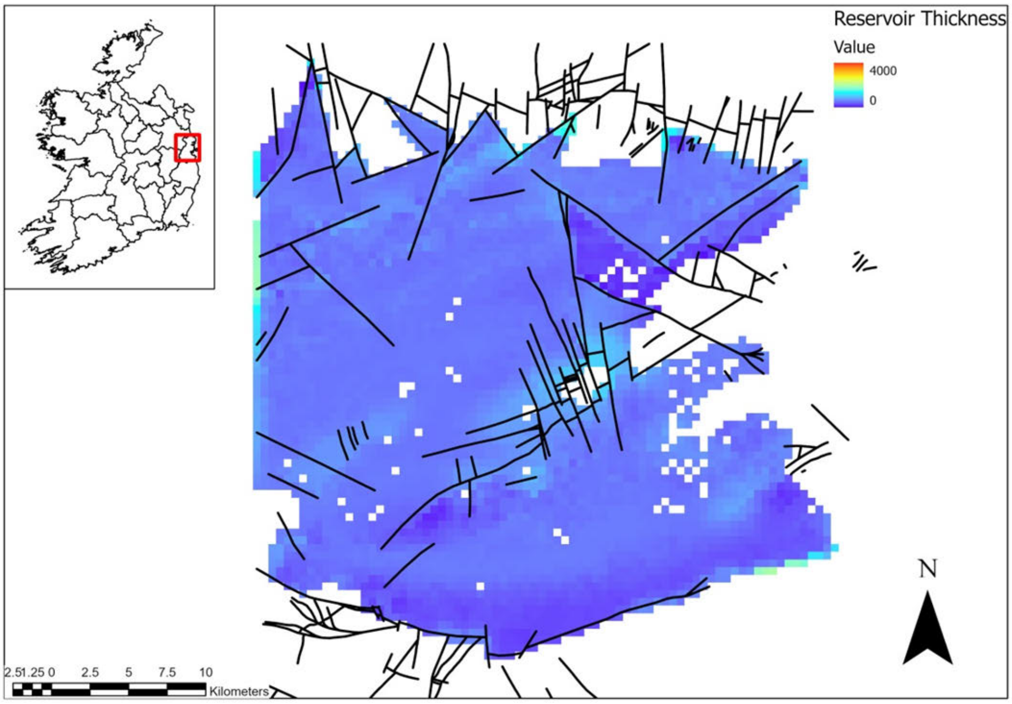

Figure 13 Reservoir thickness in the Dublin Basin.

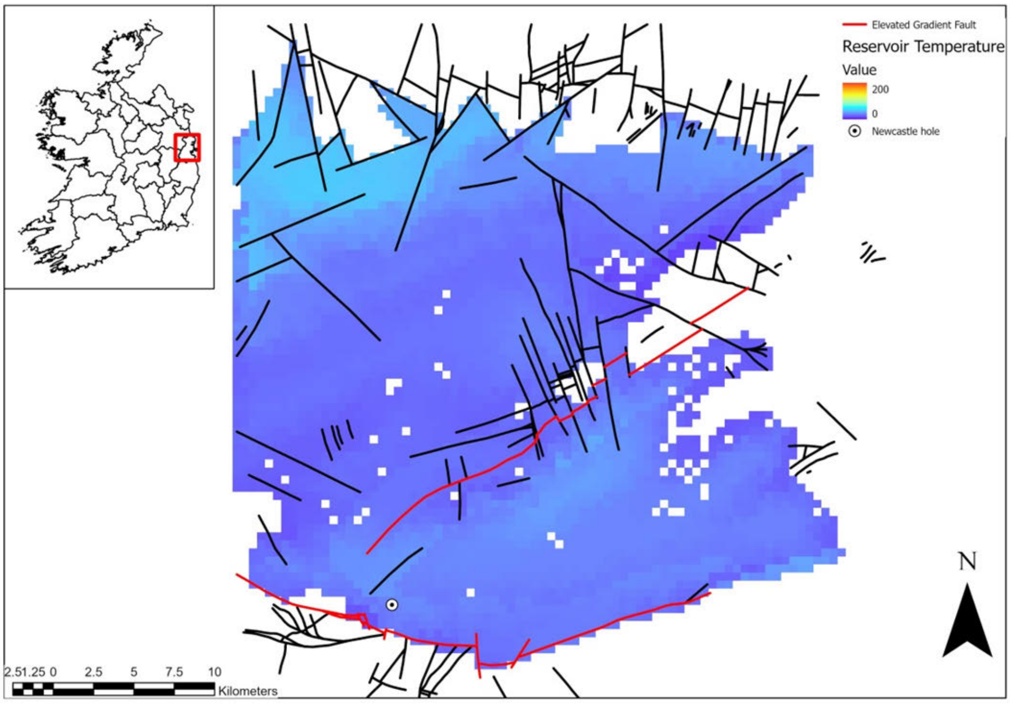

Figure 14 Average reservoir temperature in the Dublin Basin.

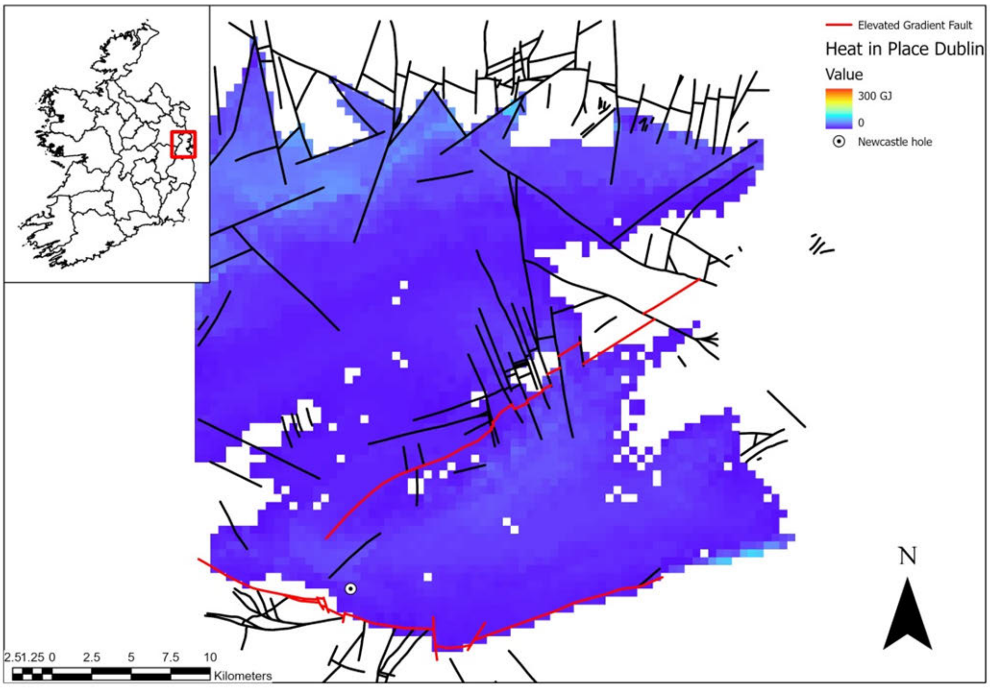

Figure 15 *Heat in place in the Dublin Basin. Maximum value of 121 GJ/m².*

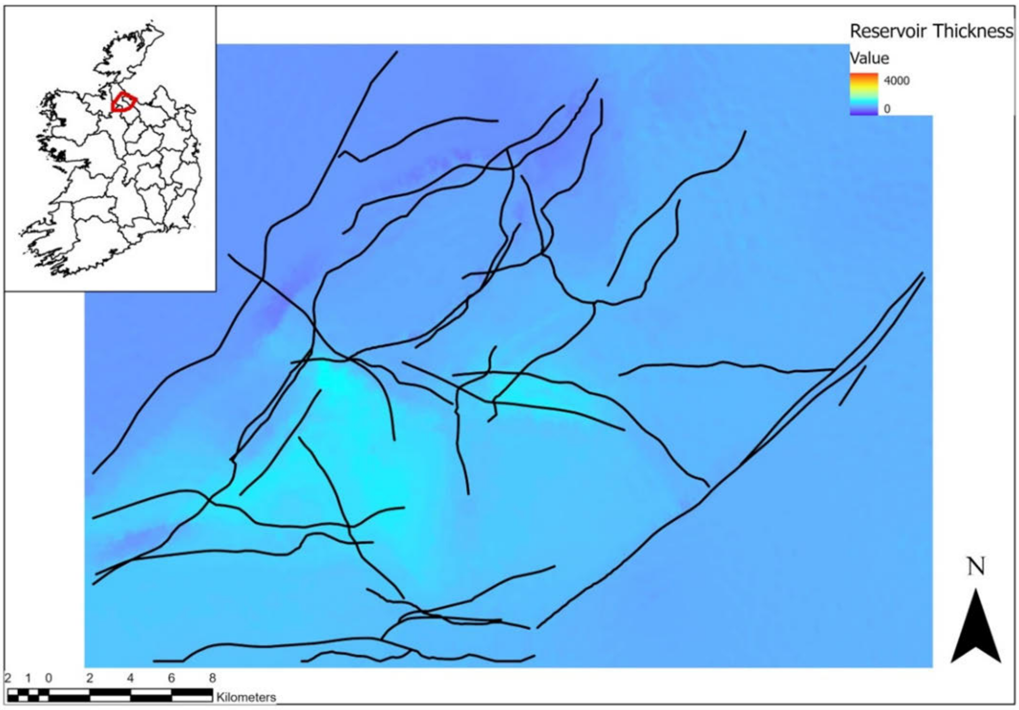

Figure 16 *Reservoir thickness in the Lough Allen Basin.*

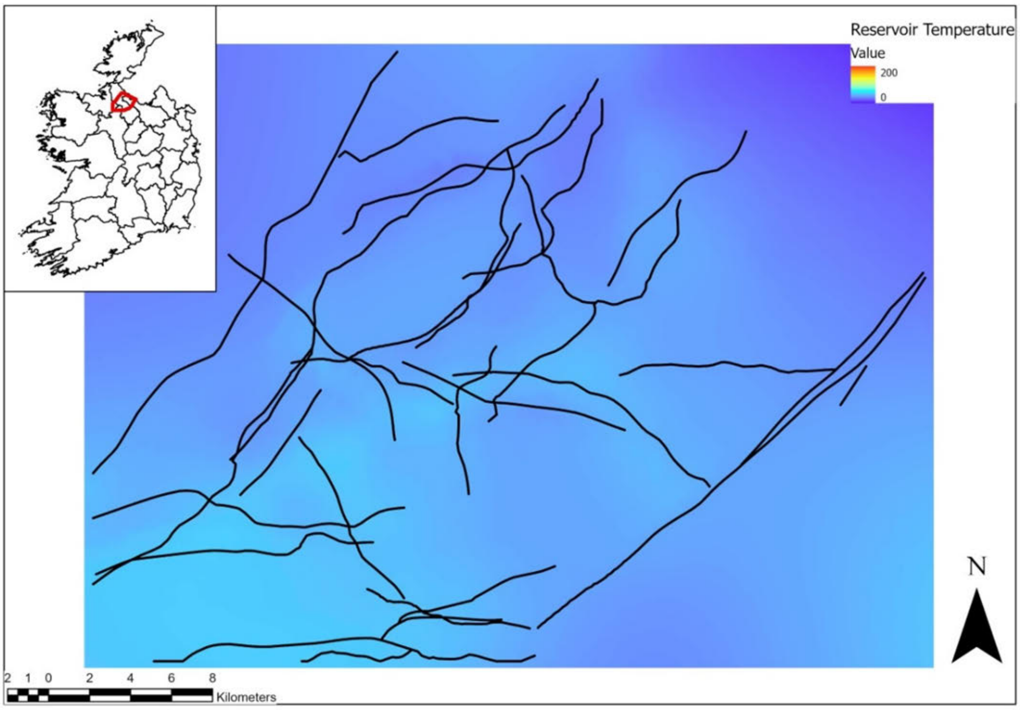

Figure 17 Reservoir temperature in the Lough Allen Basin.

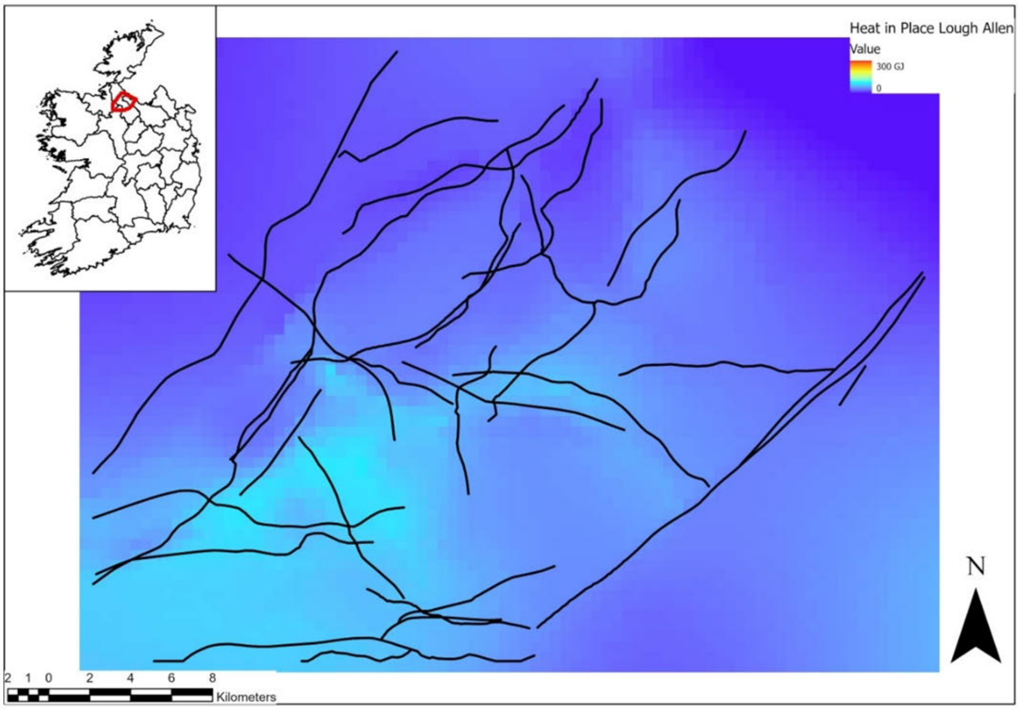

Figure 18 Heat in place in the Lough Allen basin. Maximum value of 91 GJ/m².

2.5.2 Lough Allen Basin

For the determination of volumetric heat in place in the Lough Allen Basin the HotLime consensus values for porosity, heat capacity and reference temperature were used. The other values required for the equation were determined from the 3D model.

The target reservoir is defined as the carbonate sequence between the base surface of the Kilbryan Limestone Formation and the base surface of the Mullaghmore Sandstone Formation (see T2.3 in HotLime deliverable D2.0 (Rupf et al. 2020) for further information). Using these two surfaces the thickness of the reservoir was calculated as a raster and the reservoir volume was derived for individual cells of 500x500 m (Figure 16).

Reservoir temperatures in the Lough Allen Basin were calculated using the same method as in the Dublin Basin; top and bottom temperature surfaces were calculated using the average geothermal gradient for Ireland of 25°C km^{-1}. The average reservoir temperature is determined by averaging the top reservoir temperature and bottom reservoir temperature in a 500x500m aerial extent (Figure 17).

The Lough Allen Basin study area shows the highest thermal potential in the southwest (Figure 18). This is due to a combination of reservoir thickness and overall depth of reservoir in this area. In the case of this study, the heat in place estimates may be weighted too heavily on reservoir geometry. Porosity and permeability are not fully understood in the area.

2.5.3 Discussion

While the drawbacks of performing heat in place calculations with a lack of data are apparent, as a first pass de-risking exercise the heat in place information has value. The maps of the Lough Allen and Dublin basins will allow identification of targets for future data generation, as well as allowing comparison to conditions in existing well-defined reservoirs in the HotLime partner countries. While heat in place in the two case study reservoirs would be considered low compared to a global average, both reservoirs contain large volumes where the temperatures could easily be expected to be sufficient for district heating purposes.

Further development of geothermal resource estimation in Ireland will require a detailed study of the porosity and permeability of deep Irish carbonates, including the variation in both parameters in relation to faults. The understanding of geothermal potential will be furthered by geophysics and drilling to further characterise the overall geometry of the basins and highlight significant fault zones, particularly for the centre of the Dublin basin. The methodology outlined in this report to determine heat in place using existing data could also be applied to other carbonate regions of Ireland, e.g., the Clare basin in the southwest.

2.6 Dinantian carbonates at the flanks of London-Brabant Massif (Netherlands, T2.4)

Authors: J.G. Veldkamp, J. ten Veen, M. Vrijlandt (TNO)

2.6.1 Description of the pilot area

For a detailed description of the reservoir please refer to HotLime Deliverable 2.0, Summary report of mapping and characterization. Here, only a summary is given.

The Northwest European Carboniferous Basin (NWECB; Figure 19) developed in the Devonian and Carboniferous in response to lithospheric stretching and Late Carboniferous flexural subsidence (Kombrink et al. 2008) in between the southern margin of the Old Red Continent to the north and the Variscan orogeny to the south, which more or less agrees with the southern margin of the Rhenohercynian Zone (Ziegler, 1990a, b; Oncken et al. 1999; Burgess & Gayer, 2000; Narkiewicz, 2007). The basin consisted of a series of WNW-trending half-grabens in the southern North Sea, in which a thick pile of Devonian and Lower Carboniferous sediments was deposited sourced from the Mid German Crystalline High in the south and the Old Red Continent in the north. The resulting horst-and-graben tectonic style steered the occurrence of isolated carbonate build-ups on intra-basinal highs. Throughout the Dinantian period the London-Brabant Massif played a vital role as a relatively stable high at the southern border of the Carboniferous Basin (Figure 19; Kombrink et al. 2010). Due to tectonic activity, the high underwent uplift, fracturing, emersion, and karstification at several moments during the Dinantian.

The main types of carbonate build-ups are microbial mud-mounds (Bridges et al. 1995), the product of an M-Factory type of carbonate deposition. The depositional environment changed during the Dinantian in response to the main tectonic basin-forming phases and variations in sea level, which is reflected by the different types of carbonate mud-mounds that developed through time (Bridges et al. 1995). For the southern Netherlands and Belgium which constitute the HotLime testbed area, Dinantian carbonates developed on the northern flank of the London-Brabant Massif (Reimer et al. 2017, Mozafari et al. 2019, Figure 20). Here, a Tournasian low-gradient carbonate ramp system is succeeded by a succession in which the carbonate ramp system evolved to a rimmed shelf setting. Subsidence of the northern margin of the London-Brabant Massif resulted in a landward shift of the shallow-marine facies belts, while the formation of normal faults resulted in a 'staircase' shaped shallow-water platform–slope–basin profile, associated with large-scale re-sedimentation processes. In conjunction, the slope angles steepened and at the deeper parts of the slope and within the basin characteristic 'Kulm' shales (Kombrink, 2008; Aretz, 2016) were deposited. After deposition, the limestone deposits were frequently exhumed and reburied. A first period of regional exhumation occurred at the end of the Dinantian, which seems to be associated with porosity enhancing meteoric karstification; possibly limited to the paleo-shelf edge. The most intense alterations seem to be present as a deep leached horizon below the Cretaceous unconformity at the top of the Dinantian sequences. In addition, clear evidence for hydrothermal fluid migration is found locally, enhancing reservoir properties at some places while occluding porosity at others.

In the Moeck et al. (2020) play type classification (Figure 2), the Dinantian limestones can be considered a play. The various facies units of Figure 20 can be considered play segments. Play elements could play a role for the definition of prospects, but currently not enough information about the reservoir exists to enable such detailed subdivision.

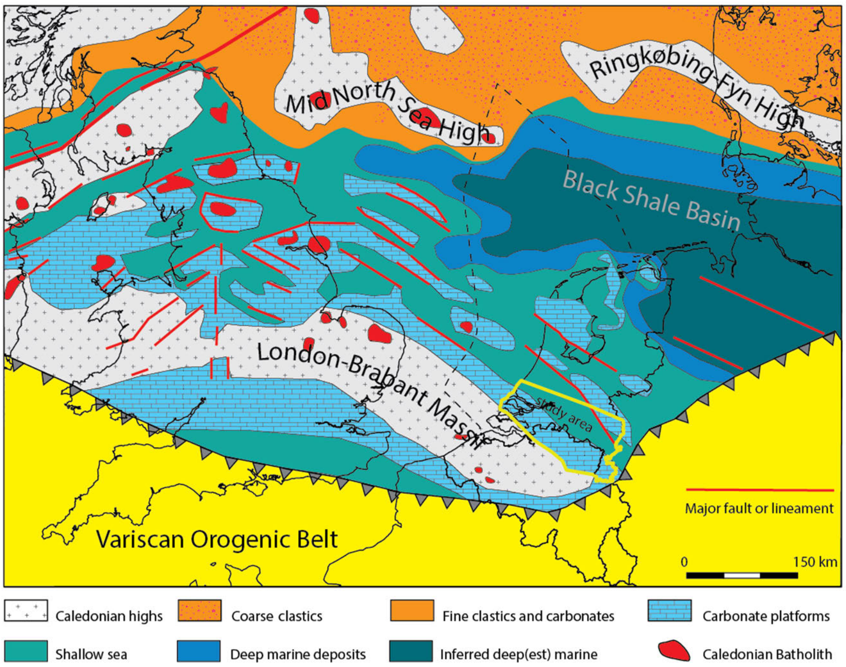

Figure 19 *Northwest European map of Dinantian palaeo-geography. Study area marked by yellow box. Modified after van Hulten (2012) and Reijmer et al (2017). Northwest European Carboniferous Basin (NWECB) roughly indicated with blue-green colours.*

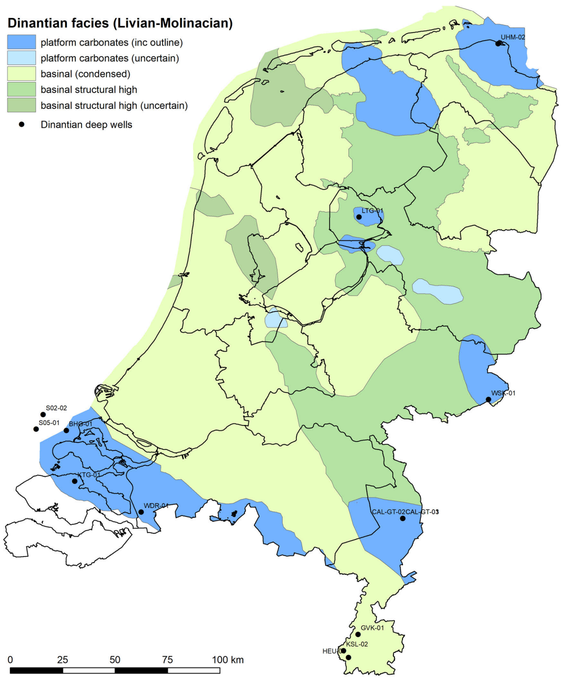

Figure 20 *Dinantian facies map (modified after Mozafari et al. 2019), only available for the Dutch part of the pilot area.*

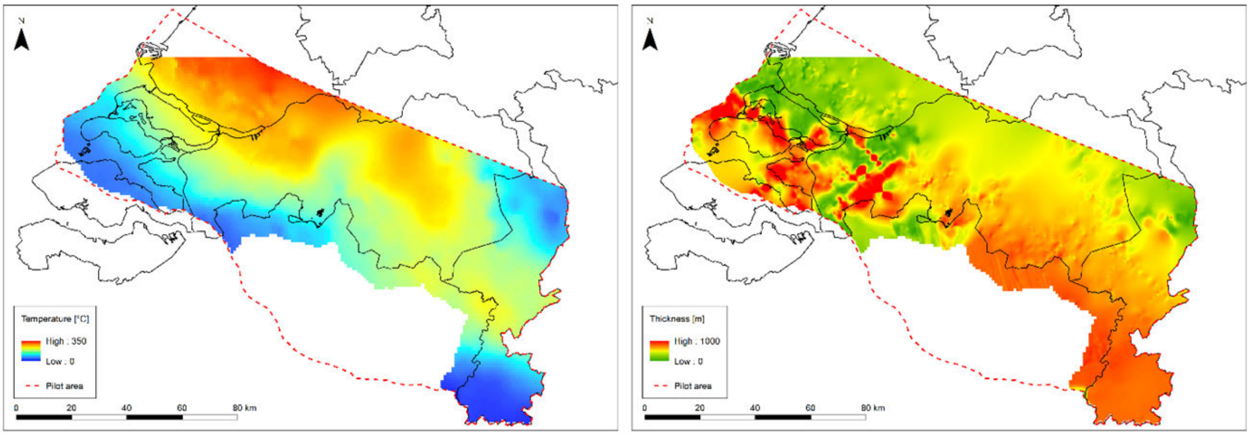

Figure 21 *Thickness (left) and temperature (right) of the reservoir used for the HIP calculation.*

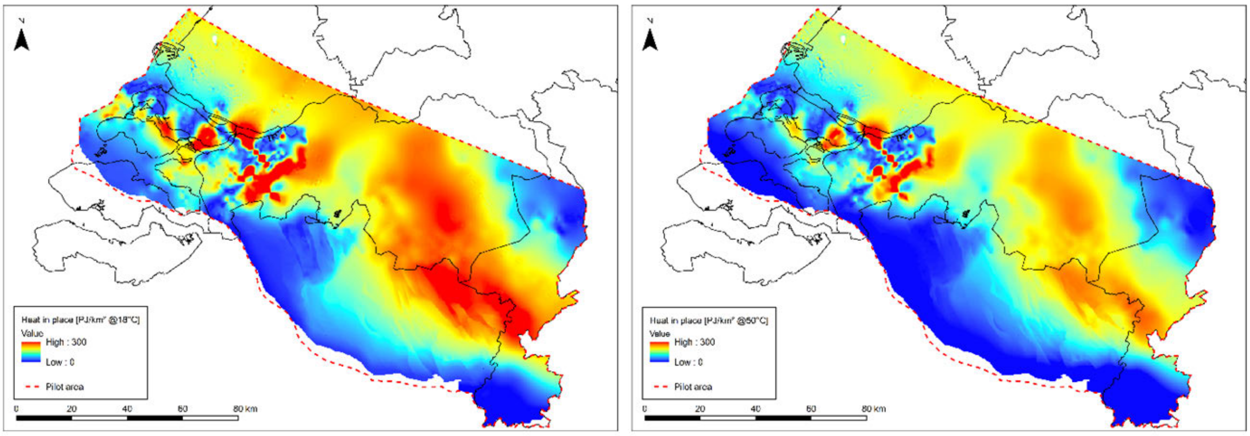

Figure 22 *Heat in place using a return temperature of 18°C (left) and 50°C (right).*

2.6.2 Heat in place

A heat in place calculation was carried out using the Muffler and Cataldi (1978) method and the parameter values presented in Table 1. For the Dutch part of the pilot area, the updated maps published in ten Veen et al. (2019) and Veldkamp et al. (2019) were used. For the Belgian part of the testbed area the results of the GeoHeat-App project (GEOHEAT-APP, 2014) were used and merged with the Dutch part. The resulting heat in place values range between 48 and 301 GJ/m² for a return temperature of 18°C (p10, p90), and 21 and 255 GJ/m² for a return temperature of 50°C. The higher values are determined by the deep burial in the Ruhr Valley Graben and associated high temperatures, as well as by the large thicknesses in some areas.

2.6.3 Resources calculation using the ThermoGIS method

ThermoGIS is an online tool, which is used to calculate the geothermal potential of the Netherlands for direct heat application (Vrijlandt et al. 2019, www.thermogis.nl). It builds on four pillars for calculating a potentially achievable geothermal power for 28 identified clastic aquifers, varying in age between

Carboniferous and Cenozoic. For geothermal exploration and production, it is an important step forward from the heat in place calculation towards potentially producible resources.

1. A 2.5D layer cake model of the subsurface having depth and thickness based on seismic interpretation for the main horizons (Digital Geological Model - DGM - Kombrink et al. 2012) and isopach interpolation for the intermediate aquifers and aquitards,
2. Reservoir quality maps for the aquifers resulting from interpolation of petrophysical well data (porosity and permeability) (Pluymaekers et al. 2012). The net-to-gross ratio is still considered to be constant.
3. A temperature model (Bonté et al 2012, Veldkamp et al. 2019). The model contains temperatures on a regular 3D grid. An initial version is calculated by solving the heat equation using temperature as top and bottom boundary conditions, and the DGM-model as structural framework. Thermal properties are assigned to the model layers based on lithological content. The initial model is then calibrated to temperature data resulting from measurements in deep wells by using an ensemble smoother (ES-DMA)
4. An economic model which calculates the discounted cashflow over the lifetime of the doublet, using estimates about CAPEX and OPEX, interest rates, energy prices and subsidy levels (van Wees et al. 2012).

For each XY location in each aquifer a standardized doublet is optimized by varying the distance between the producer and injector wells at reservoir level, and the drawdown pressure. A higher drawdown pressure ensures a higher production, but also increases the cost via the pump OPEX. Furthermore, it should be kept below legal thresholds to ensure reservoir integrity. The well distance should be chosen in such a way to prevent early thermal breakthrough (minimum 30 years), while at the same time a large distance increases the required pump pressure. An optimal business case is imposed by minimizing the cost of the produced energy (LCOE) within the calculated pump pressure and well distance boundaries.

Permeability is the most important factor determining the achievable flow rate. Therefore, a standard deviation map of the permeability is used to calculate the uncertainty of the predicted geothermal power in terms of p90, p50 and p10 maps. The permeability maps are generated from abundant reservoir quality information such as well tests, petrophysical evaluations, and core plugs.

Output maps of ThermoGIS include the heat in place (GJ/m²), potential recoverable heat (GJ/m²), geothermal power (MW_{th}) and the economic potential in terms of the odds of being able to produce energy against economic rates (cost price less than market price plus subsidy). Note that the provided maps in the current ThermoGIS version do not represent reserves in terms of the Australian and Canadian codes, or of the UNFC.

Whereas ThermoGIS was applied to the clastic reservoirs relevant for geothermal exploration in the Dutch subsurface, the Dinantian limestones were not included yet. Partly this is because of the deep burial in a large part of the country (Figure 21), making the rocks an unattractive target for exploration, and partly because a full set of the required input maps (depth, thickness, reservoir quality, temperature) did not exist previously. During the execution of the Ultradeep Geothermal (UDG) project (see www.nlog.nl/scan), a substantial effort was undertaken to improve the knowledge of the Dinantian limestones in the Netherlands. This resulted in updated versions of the depth and thickness maps (ten Veen et al. 2019) and the temperature map (Veldkamp et al. 2019). Further, facies and diagenesis were described from available core material and petrophysical well logs (Mozafari et al. 2019, Carlsen 2019). This resulted in, among other things, a Dinantian facies map. A reconstruction of burial and structural development was made (Bouroullec et al. 2019), and a fracture characterization study was performed (Van Leverink and Geel 2019). A reservoir quality map, however, was not an output of the project. In contrast to siliciclastic systems, the lateral and vertical distribution of the permeability is difficult to predict because it is highly variable. This, in combination with the sparse amount of available reservoir quality data, introduces major uncertainty in the calculation of the resource. However, the improved knowledge of the reservoir enables to generate a first conceptual reservoir quality map. Note that this is a fundamentally different kind of reservoir quality map that is being used in ThermoGIS for the siliciclastic reservoirs. The latter is based on measured reservoir quality data and geological knowledge, and less on concepts, whereas the former is based largely on concepts and less on measured data.

The assumptions extracted from the UDG reports which were used for generating a Dinantian permeability map are the following:

- Although a large amount of core material exists, permeability measurements were only performed on a small amount of these plugs, possibly because the plugs had very low permeability due to their low porosity (Carlson 2019). A relationship between core porosity and permeability was therefore not established. For the higher porosity intervals, a clear relationship between porosity and permeability is unlikely to exist because of the heterogeneity in the karstified and / or fractured sections.
- The matrix porosity of the reservoir is very low, usually below 2% and along long intervals below 1%. The permeability in these sections if in the order of micro-Darcies. Hence, it is considered unsuitable for geothermal production. However, all wells have short intervals with increased porosity. However, all wells have short intervals with porosities between 2 and 6%, and some wells with porosities up to 25-32 %.
- Multiple periods of subareal exposure and hence karst are documented. The most prominent period of compression tectonics and related subaerial exposure and associated karstification occurred from the Late Jurassic through the Early Cretaceous. Karst permeability possibly exists where Cretaceous chalk deposits directly overly the Dinantian (although karst pores may have been filled with impermeable sediment). This occurs along the North-western edge of the London Brabant Massif (for example the Kortgene well KTG-01 had flow to surface without lift, and Brouwershavense Gat BHG-01 an S05-01 with nitrogen lift. For KTG-01, the better reservoir quality is also due to the fact that here it has the mostly dolomitic base of the Dinantian, with better porosity.), and the south-western part of the province of Limburg (the well Geverik GVK-01 has higher porosities over longer intervals). The horst block east of the Californië doublets may also qualify as such, but this does not follow from the current DGM-Deep model because a thin section of Paleozoic deposits is considered to be present between the Dinantian and the Mesozoic rocks.

The above-mentioned information was used in the following way to derive an assumed permeability map:

- The transmissivity of the karstified subcrops is arbitrarily set to 100 Dm – in the Southern part of the Netherlands where the carbonates are buried very shallowly, porosity was observed up to 50%. This may appear to be a high value it the light of the mentioned porosity observations, but it is emphasized here that on the one hand the porosity – permeability relationship could not be established, and on the other hand that the KTG-01 well flowed to the surface without artificial lift, indicating good permeability.
- Fault and fracture permeability is observed in outcrops bordering the Netherlands, in Germany (Hastenrath quarry in the Aachen area) and Belgium (Mol doublet), and in well data. The Californië doublets are a mixture of fracture and (associated?) karst permeability. The Belgian gas storage facility in Loenhout also has karst permeability. Hence, fractures *may* be associated with karst, but fractures may also be cemented. A safe assumption for this type of karst is to allow a broad range for such fractures, but the shape of the distribution is hard to establish. Cemented fractures will then concern the downside (low permeability), open fractures (Californië geothermal system) the upside.
- A set of fault lines was obtained from the HIKE project results (Figure 23). Most were not mapped all the way down to the Dinantian but rather to the depth of the Permian, but they are considered to possibly cut through the Dinantian. It is unknown if fracture permeability exists along these faults. Proven recent activity of the faults, for instance if Cenozoic layers are offset by them, increases the odds of the fractures being open. In contrast, faults that have proven offset in younger strata may not reach all the way down to the Dinantian. Therefore, preferably, faults should have 'offset labels' which enable to identify when it was active. Alternatively, a hand-drawn map showing areas with a higher degree of tectonic disturbance may help identifying sets of faults more apt to fracture permeability, but such a map does not currently exist.
- The direction of the faults is considered to play a role (Figure 24). The NNW-SSE fault direction (as for instance near the Californië doublet, Figure 23) is approximately perpendicular to $S_{h,max}$. This direction is considered to have a higher permeability than the WNW-ESE running faults that border the Ruhr Valley Graben and the West Netherlands basin (Figure 24). Azimuths are between 0° and 180°, but mostly between 90° and 180°. All faults between 135° and 180° are considered to belong to the NNW-ESE group.
- The fault and fracture permeability is considered to decrease with increasing distance from the fault, i.e., with increasing distance from the fault core. The width of the damage zone is hard to assess and likely to be variable, but several 100s of meters may be a reasonable estimate. The Hastenrath quarry may serve as an example of the width of the damage zone (Reith 20xx), in accordance with the Californië wells, of which GT-01 and GT-03 are located towards the fault core, and GT-02 away from the fault core. For the WNW-ESE direction, the maximum distance is an arbitrary 500m. The maximum transmissivity is 300 Dm (@center of fault), based on values observed in the Californië doublet. The minimum transmissivity is 0.1 Dm (at 500m distance from the fault center, on both sides). For the WNW-ESE direction the maximum transmissivity is an arbitrary 100 Dm.

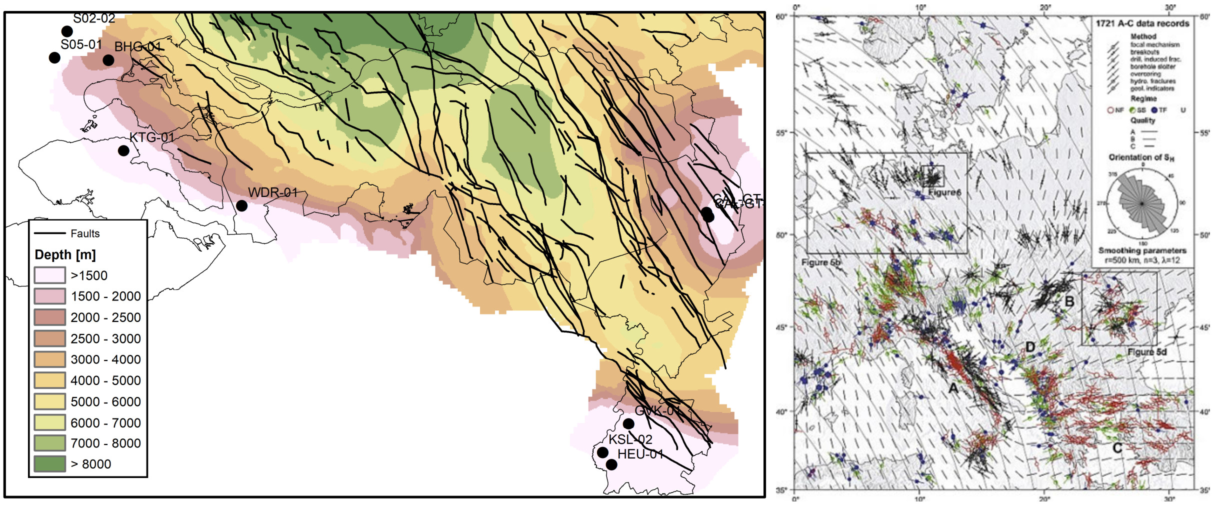

Figure 23 *Left: Main fault directions overlaid on the depth to top Dinantian. The Californië doublets are located in the north-eastern part of the area. Right: NW Europe stress map showing Sh_{max} (from Heidbach et al. 2007).*

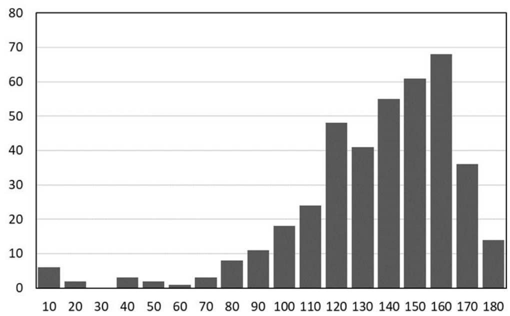

Figure 24 *Fault azimuths.*

- Depth dependence is also assumed. Depths shallower than 2000m are assigned the transmissivity described above. Depths deeper than 4000m are assigned a transmissivity which is 1% of the assigned transmissivity. Between 2000 and 4000m there is a linear decrease.
- The background transmissivity (no karst, no fault) is an arbitrary 0.0025 Dm which results from an assumed 500m average thickness (the approximate average thickness in the study area) and 5 micro-Darcy permeability.
- More distal facies units are assumed to have a lower net-to-gross, but this is yet to be implemented. Also, the fine-grained, clay-rich distal facies may well contain open fractures.
- The standard deviation of the permeability is set relatively low at 25%.
- Porosities were adopted from the UDG petrophysics report (Carlsen 2019). The porosity values are 1% for the background (KTG-01, O18-01, S05-01, S02-02, UHM-02, LTG-01, WSK-01), 9% for the NNW-ESE faulted zones (CAL-GT-02), decreasing to an arbitrary 3% to the outer boundaries of the fault zones. For the WNW-ESE faults, this is arbitrarily set to 50% of the NNW-ESE faults.

It is acknowledged that the above-mentioned assumptions regarding the permeability of the Dinantian rocks in the Dutch subsurface are to a large extent arbitrary and have very large associated uncertainty. The resulting map should therefore be considered tentative, and merely serve as a first step towards the construction of a more detailed reservoir quality map of the Dinantian reservoir in the Netherlands. Together with the depth, thickness and temperature maps used for the HIP calculation, the permeability map was entered in ThermoGIS to calculate the potential geothermal power (Figure 25). The largest potential appears to be alongside the boundary faults of the Ruhr Valley Graben, and in areas where the Dinantian is overlain by sediments of the Cretaceous Chalk Group.

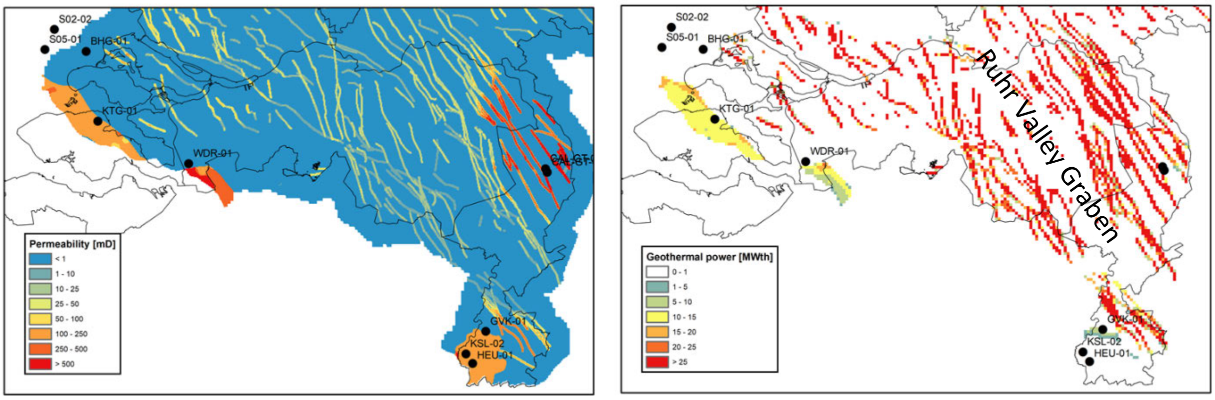

Figure 25 Tentatively calculated fault permeability (left) and resulting tentative geothermal power (right).

The tentative geothermal power map is a step further from the heat in place but does not yet provide an answer to the question how much energy can be produced over time. On the other hand, owing to the use of an economic model which determines whether the LCOE is below an economic threshold, and because production flow rates are calculated, it is possible to determine the technical lifetime of the doublet (years to thermal breakthrough), and the amount of energy a doublet, located at a certain XY location, will be able to produce (Mijnlieff et al. 2019). For the doublet it is then possible to calculate a recovery factor – the amount of energy produced by it throughout its lifetime, divided by the heat in place. This factor will not be the same for each location within the reservoir. Therefore, in order to be able to calculate the total amount of energy which can be produced from the entire play, another assumptions need to be made: the amount of doublets that will theoretically fit in the play area, and a sorting factor determining how spatially efficient doublets are laid out in the subsurface in reality. In case there are already doublet systems in operation in the area, their energy needs to be subtracted from the total, like for instance the Californië doublets in the Netherlands. Table 3 lists the tentative resources that were calculated from the ThermoGIS potential maps. Note that the HIP is calculated with reference to the surface temperature of 10 °C (average surface temperature), in contrast to the common HIP calculation carried out for all HotLime pilot areas. The potential recoverable heat (PRH) is calculated according to Kramers et al. (2012) as 1/3 of the HIP. The recoverable heat is calculated as the PRH with a cut-off where the unit technical cost (UTC) is larger than the specified 'unit technical cost cut-off'. The potential resources are calculated while considering the sorting factor, annual load hours and lifetime before thermal breakthrough. A UTC cut-off is used to go from potential resources to resources.

Table 3 Tentative resources of the Dinantian limestone [PJ].

HIP	Potential Recoverable Heat	Recoverable Heat	Potential Resources	Resources
3183456	995328	72671	62652	46005

In terms of the three UNFC classification axes (see Appendix 1), the resources of the Dinantian limestone in the Netherlands shown in Table 3 have a low socio-economic viability after the shut-in as a result of a minor seismic event in one of the Californië doublets (E3). Given the high uncertainty regarding reservoir quality and hence amount of resources, the G-axis will be G4. Due to the low socio-economic feasibility, projects are not being developed. The F-axis is therefore F4.

2.6.4 Conclusions

The resulting map of Figure 25 is the first exercise towards a regional calculation of the geothermal power of the Dinantian limestones in the Netherlands. The actual values contain considerable uncertainty due to the assumptions that had to be made regarding the karst and fracture permeability, given the lack of measured data. The map should therefore be interpreted with appropriate caution. The added value of the map lies therefore not in the fact that it claims to represent the 'true' potential geothermal power, but that it was shown that the ThermoGIS approach to calculating geothermal resources can be applied to limestone reservoirs, bringing the resources calculation a step further than a single calculation of the heat in place, and enlarge awareness of the geothermal potential of this reservoir. It is understood that the best guess assumptions which led to the permeability map can be improved upon, which will be helped if exploration is intensified.

2.7 Upper Triassic to Middle Eocene carbonates of the Po Basin (Italy, T2.5)

Author: F.C. Molinari (SGSS Regione Emilia Romagna)

2.7.1 Description of the pilot area *(for detailed reservoir description see Rupf et al. 2020)*

The calculation of the Heat in Place (HIP) was based on the geological and temperature model elaborated in WP2 and on the petrophysical parameters obtained from data available in the bibliography and representative of the carbonate sequence mapped.

In particular, the BHT data belonging to 46 E&P wells falling both inside and partially outside the pilot area were analysed and corrected using analytical methods. BHT-data (Bottom-Hole Temperatures) are measured during geophysical borehole logging surveys, mostly using analogous maximum temperature thermometers.

The assignment of the parametric values for the calculation of the HIP in the modelled carbonate sequence, analysing the data present in the E&P well profiles, was based on two main facies groups:

- Mainly carbonate facies
- Mainly dolomite facies

The limestone-prevalent part (hlu5_lime), Jurassic to Middle Eocene, is made by mud-to-packstone, marl, with common cherty nodules and thin beds, nodular limestone and cherty limestone, sedimented in pelagic environments including deep basin (thicker successions), (intra-basinal) morpho-structural highs (plateau and ridges; thinner successions) and slopes; since Aptian basin environment (locally slopes) prevailed.

The dolomite prevalent part (hlu5_dol) is made by dolostone and calcareous dolostone, dolomitized grainstone-to-mudstone, with local anhydrite intercalated mainly in the eastern areas, dolomitic limestone. The succession sedimented in shallow water carbonate platform environment. Norian-Rhaetian and Lower Jurassic. Based on this macro-subdivision it was decided to assign, where possible, to each group of facies a different Specific Heat Capacity (c_{pr}) [J/kgK] (Hantschel & Kauerauf, 2009). Above all, on the basis of the existing data, it was not possible to make further differentiations of the other parameters, in particular the bulk porosity (fluid filled voids).

Table 4 Available data in the pilot area.

pilot / study area		number of wells		number of individual datum points		
name	area km²	total	BHT	total	BHT uncorr	BHT corr
T 2.5 – Po Basin	21,177	46	46	394	160	234

Table 5 Specific Heat Capacity parameters.

unit	lithological composition	specific heat capacity (c_{pr}) [J/kgK]
Carbonate Unit (hlu5_lime): Limestone facies	chalk, 75% calcite	840
Carbonate Unit (hlu5_dol): Dolomite facies	typical	860

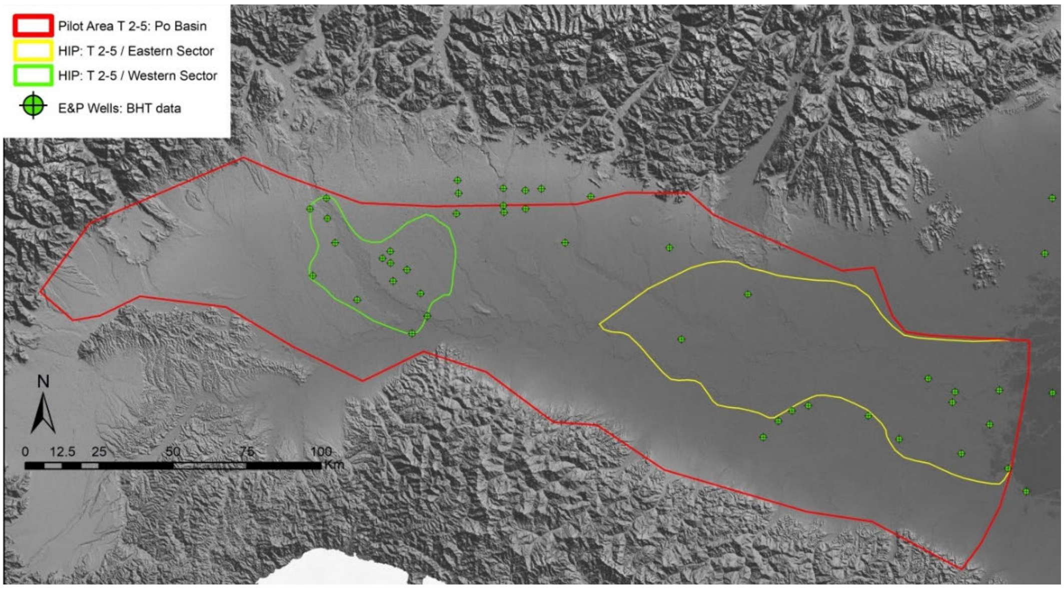

Figure 26 *Outline of the pilot area.*

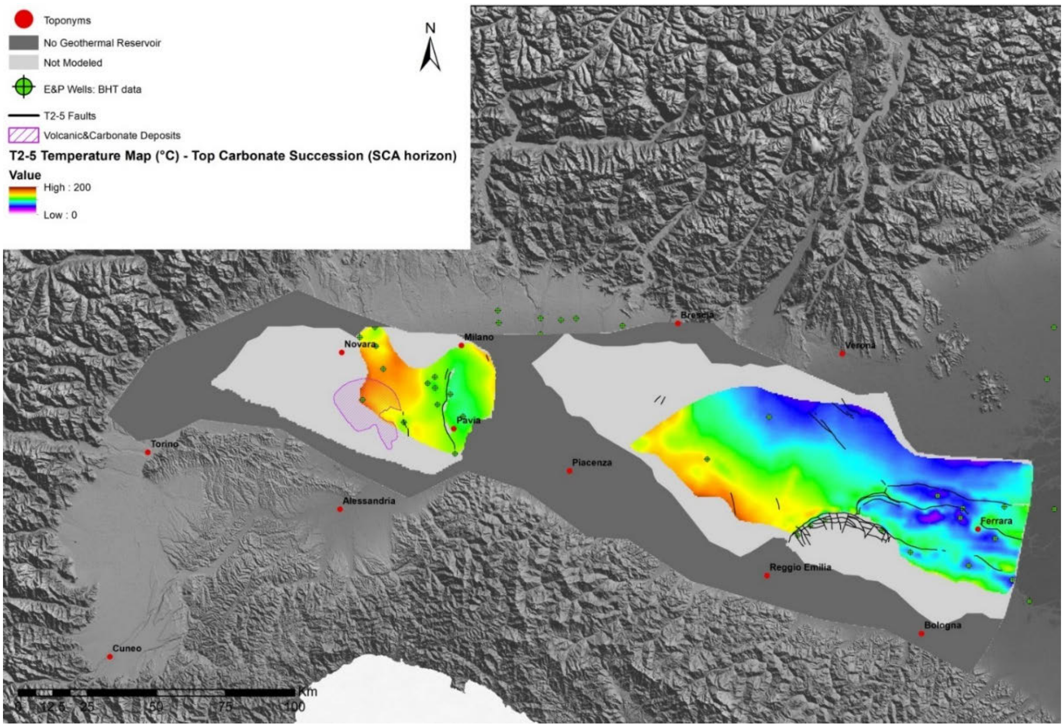

Figure 27 *Temperature map of the roof of the carbonate sequence shows that in the eastern area there are relatively low temperatures (45-50°C / 60-80°C) both in the central-northern sector of the Venetian monocline and in the other structural sectors relating to the top of the Ferrara Folds hanging walls (HW1, HW2 and HW3). In the southern sector of the Venetian monocline (FW3), due to the high depths, temperature values to about 160-180°C are obtained. While in the western area it is noted that in the footwall sector (FW) there are overall high temperatures (130-170°C) due to both the depths and the geothermal gradient which is higher than in the eastern area. Also, in the HW sector ("Lacchiarella" structural high) there are generally high temperatures (105°C /120 ° C) even if lower than in the FW sector.*

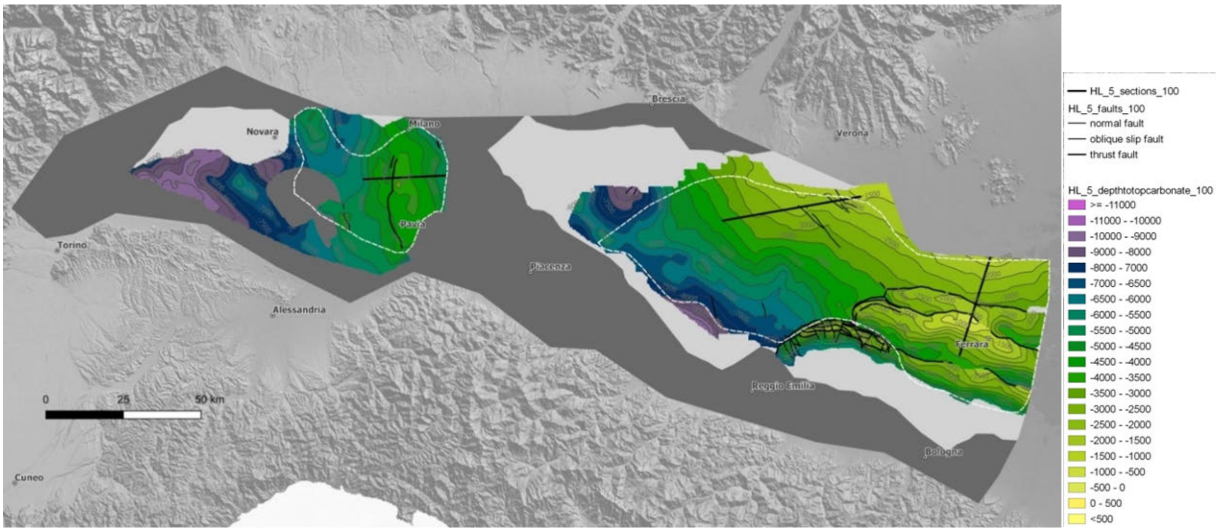

Figure 28 The depth of the top of the carbonate sequence shows how the minor depths relative to the roof of the carbonate succession are in the northern sector of the Venetian monocline and in the other structural sectors relating to the Hanging walls of the Ferrara folds (eastern sector) and the upper structural part of Lacchiarella (eastern sector).

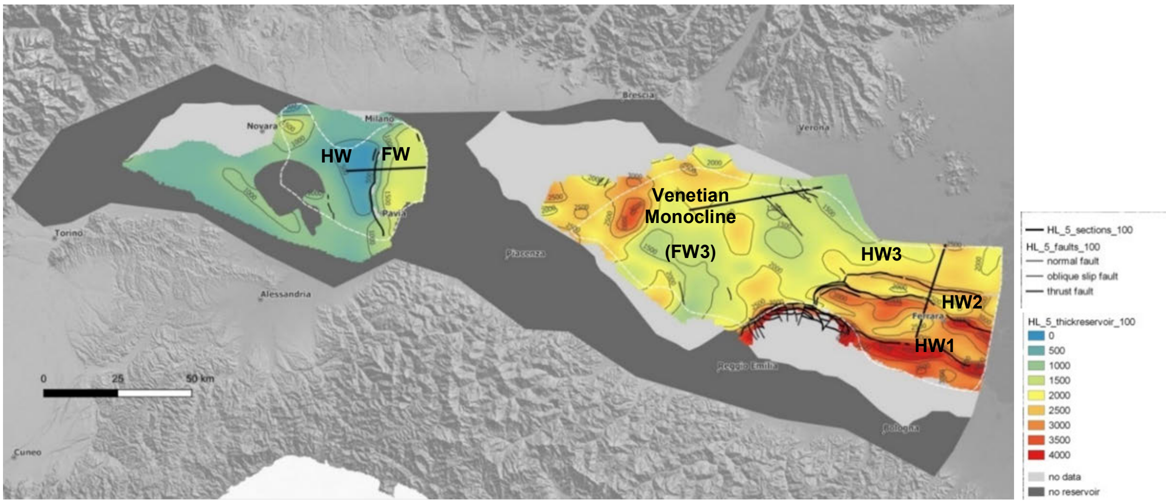

Figure 29 The thicknesses of the carbonate sequence shows that in the eastern sector the smaller thicknesses of the carbonate succession correspond to the Venetian monocline (1000-2000 meters), while above all in the hanging wall sectors of the Ferrara folds (HW1 and HW2) there are greater thicknesses (3000- 4500 meters) also due to the tectonic doubling of the carbonate succession. While in the western area it is noted that in the footwall sector (FW) there are low thicknesses (400-1000 meters) due to the condensation of the carbonate succession.

2.7.2 Geological model and temperature model

Below are the main structural maps obtained from 3D modelling with related comments for:

- Depth of the top of the carbonate sequence
- Thicknesses of the carbonate sequence
- Temperatures map of the roof of the carbonate sequence

The areas in which it was possible to model and process the structural maps are distinct in a western and an eastern sector.

2.7.3 Heat in place

Eastern Sector

In the eastern sector of the pilot area, both for the thicknesses present and on the basis of the interpretation of the E&P wells data, it was possible to differentiate the succession in an upper portion with predominantly carbonate facies (hlu5_lime: depositional environments of locally slop/basin) and in a lower portion with predominantly dolomitic facies (hlu5_dol: shallow water carbonate platform environment). On the basis of the well data it was possible to differentiate the thicknesses of the lower portion with predominantly dolomitic facies which has average thicknesses of about 2200-2300 m in the HW1 and HW2 sectors while in the HW3 sector there are average thicknesses of about 1100-1200 meters up to get to sector FW3 (Venetian Monocline) with thicknesses of about 800-900 meters. The thicknesses of the Dolomite facies influenced the distribution of the HIP values, also for having higher specific heat capacity values compared to the carbonate facies .

Western Sector

In the western sector, through the analysis of well data, the chronostratigraphic subdivision between the carbonate and dolomitic facies is attributable to that present in the eastern sector with the difference that in the interpretation of the seismic profiles / well data and therefore in the elaboration of the geological model it was not possible to physically differentiate the two groups of facies. In this sector, however, the thicknesses of the carbonate facies are generally prevalent compared to the dolomitic ones, so it was decided to use a unique value of Specific Heat Capacity (c_{pr}) [J/kgK] equal to 840 (Carbonate Rocks: Limestone facies). In the western sector the average thicknesses are about 500-700 meters in the FW sector and 1000-1200 m in the HW sector. The thicknesses and the Specific Heat Capacity values influenced the distribution of the HIP values, which in general are much smaller than those present in the eastern sector.

The no-data areas represent the sectors in which, depending on the geological-structural setting or on the distribution of the data, it was not possible to process the geological model or the temperature model.

The distribution of the thicknesses and the depth of the roof of the carbonate succession explain the strong variability (range) of values in the HIP maps.

The factor that therefore most influences the distribution of HIP is mainly the highly heterogeneous geological setting in both sectors and especially in the eastern sector; while only secondarily is it due to the geothermal gradient which is on average slightly superior in the western sector (mean geothermal gradient:~2.7-2.8°C/100 m) compared to the eastern one (mean geothermal gradient:~2.1-2.2°C/100 m).

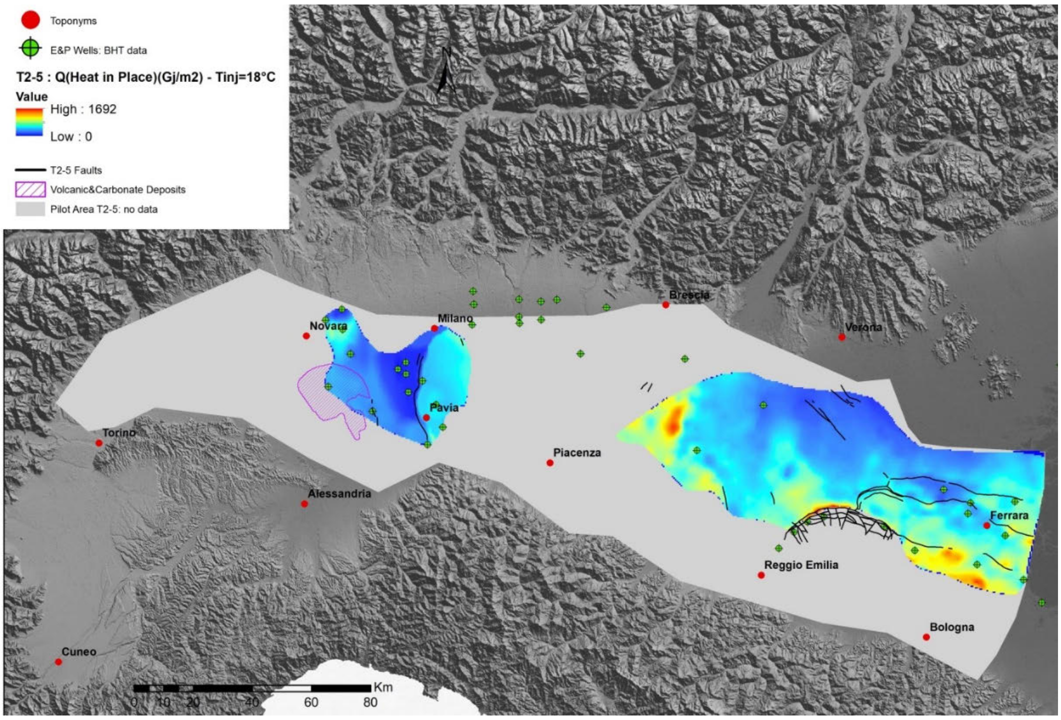

Figure 30 *Heat in Place (HIP) (Tref 18°C).*

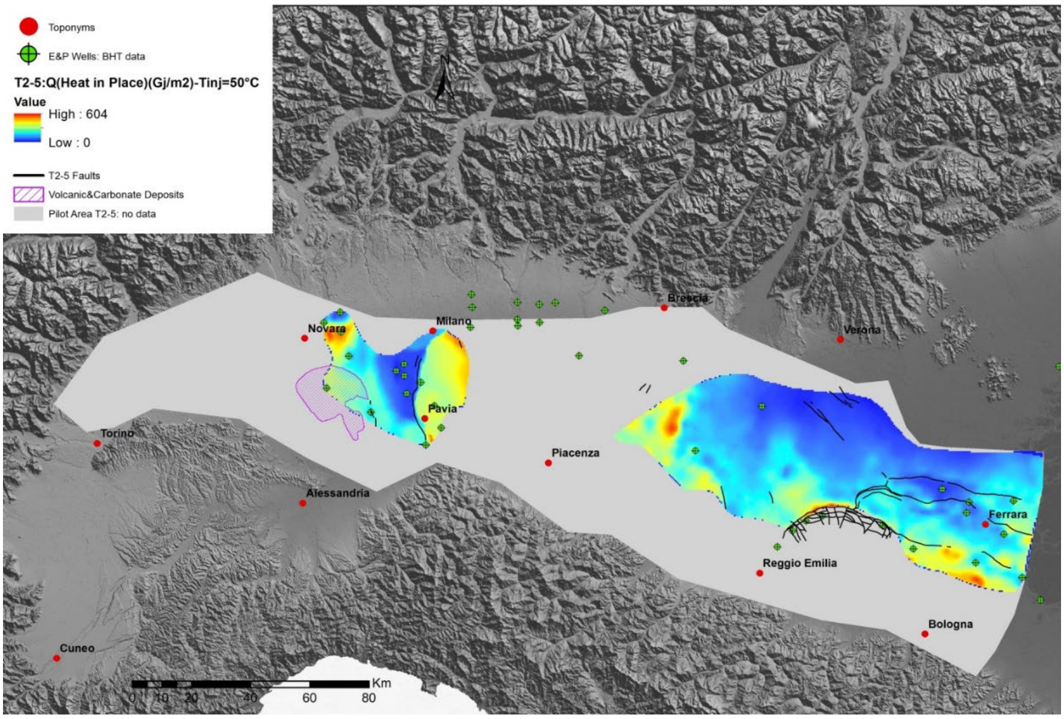

Figure 31 *Heat in Place (HIP) (Tref 50°C).*

2.8 Triassic carbonates of the Krško-Brežice sub-basin (Slovenia, T2.6)

Authors: D. Rajver, D. Šram, J. Atanackov (GeoZS)

2.8.1 Description of the pilot area: the Čatež geothermal field and its immediate surroundings

The Krško basin with its thermal springs is a syncline, filled with low permeable Tertiary and some Quaternary sediments. The measured geotherms reflect predominantly a conductive temperature field but in the syncline basement convective thermal field is predominant in the Čatež fault zone which can extend to a depth of at least 2 to 3 kilometers beneath the surface, but not all the way within the Triassic carbonate rocks (dolomite, limestone), because it could also have formed within the other lithology of older age. There are 11 relatively deep boreholes which reached the geothermal aquifer and were drilled inside the Čatež fault zone. They all finished with their bottom parts in the Triassic dolomite, limestone with dolomite and/or dolomite breccia rock type. The reservoir rock type is predominantly Late (and Middle) Triassic dolomite in the deeper and shallower parts of the fault zone with possible late Triassic Dachstein limestone in shallower parts. In a wider area around the constrained Čatež fault zone the top of the geothermal aquifer may be presented also with Jurassic carbonate rocks (limestone and dolomite).

In the Čatež fault zone the highest borehole temperatures have been logged, up to 64°C. Circulation of meteoric water (mostly subvertical) into a few kilometers deep fractured Čatež fault zone is the only heating possibility for thermal water in the Čatež field (Figure 32). Water circulation is probably the deepest there than elsewhere in the Krško basin (Rajver & Ravnik, 2003). Geological and thermal settings are further described in detail in WP2 report (Rupf et al. 2020).

The current users in the Čatež fault zone (or Čatež geothermal field) are: Terme Čatež d.d., AFP Dobova and Paradiso Dobova, and all of them use energy for heating. The utilization of thermal water at AFP Dobova and at Paradiso Dobova has been operating since 1996 and 2010, respectively, while at the Terme Čatež d.d. much longer, already since the 1964 when the first exploration and production wells were drilled into the dolomite aquifer.

The structure (Figure 33), including the reservoir rock lithology and general geologic structure (e.g. depth (Figure 34) and thickness (Figure 35) of reservoir) is constrained from available data on the Krško syncline and a composite regional lithostratigraphic column all defined in WP2.

2.8.2 Heat in Place

The results of the Heat in Place (HIP) calculation suggest that there could be also other areas within the Čatež fault zone or in the immediate surroundings (perhaps more probable north and north-east to east of this zone) where there is pretty good probability for new exploration and exploitation wells for thermal water of at least 50 to 60°C at the wellhead, which might be successful. Within the Čatež fault zone there are possibilities for such hopefully successful wells between the Terme Čatež and small town of Dobova and beyond Dobova to the east towards the Slovenian-Croatian border.

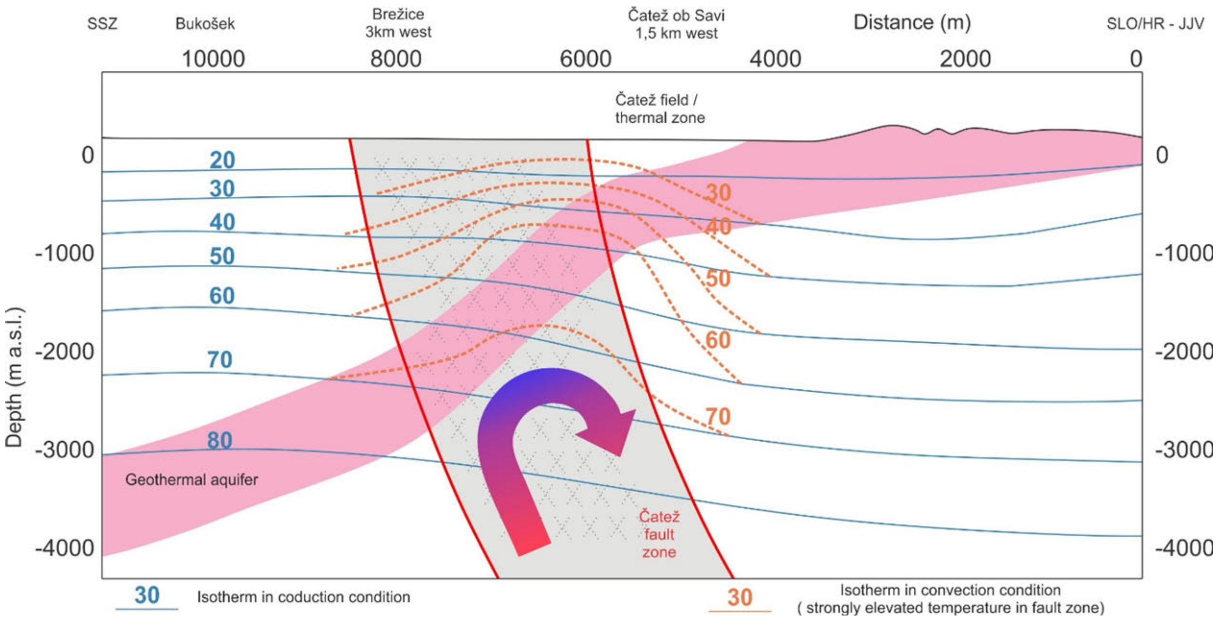

Figure 32: Typical cross-section with expected temperature and groundwater convection at the Čatež thermal field.

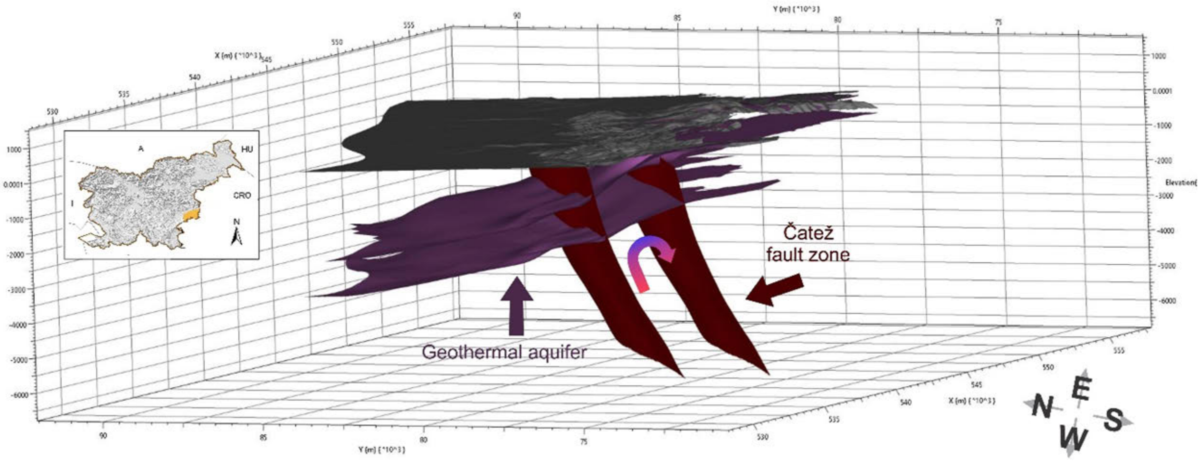

Figure 33 3D geological model of Čatež fault zone.

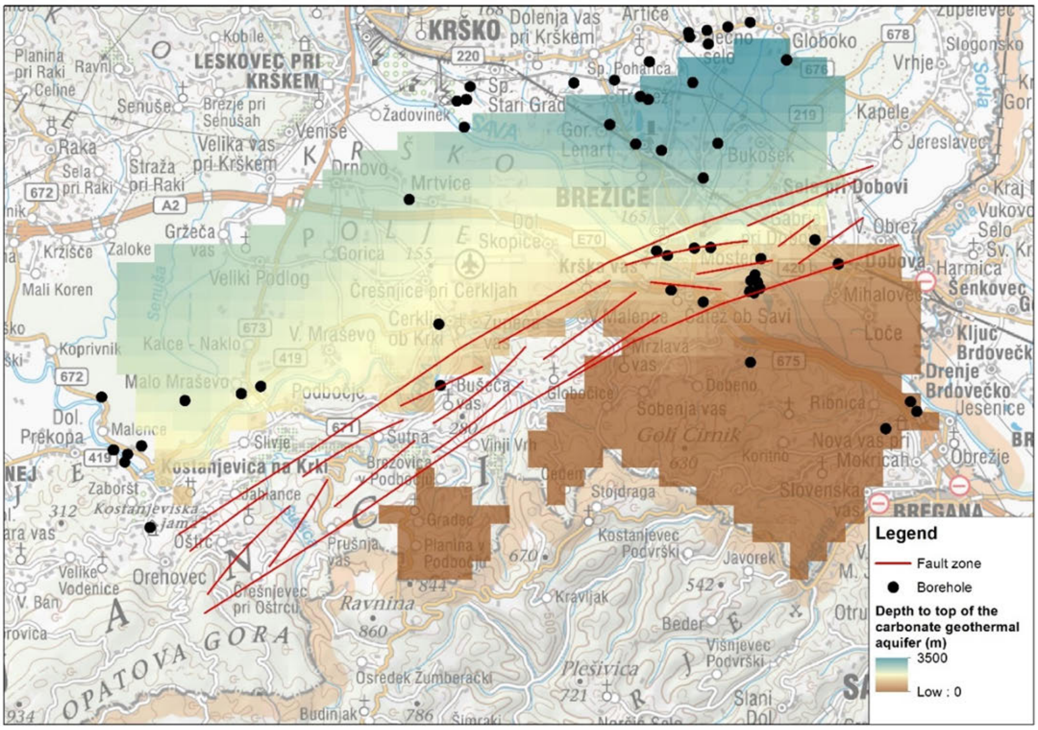

Figure 34   Depth to top of the carbonate geothermal aquifer.

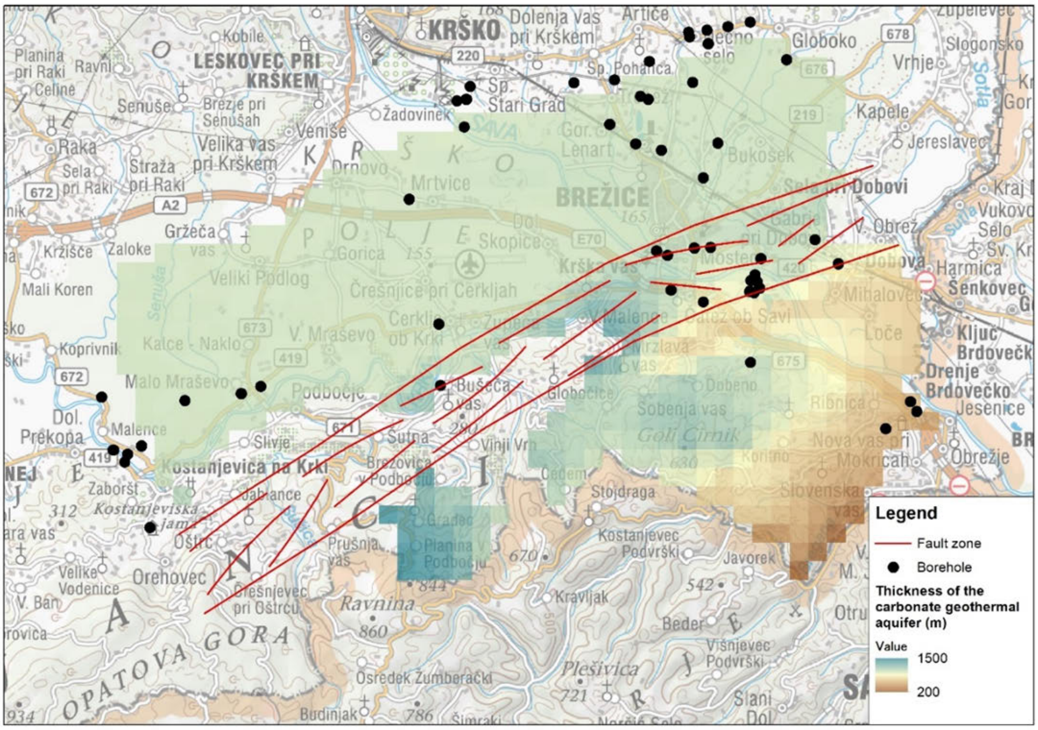

Figure 35   Thickness of the carbonate geothermal aquifer.

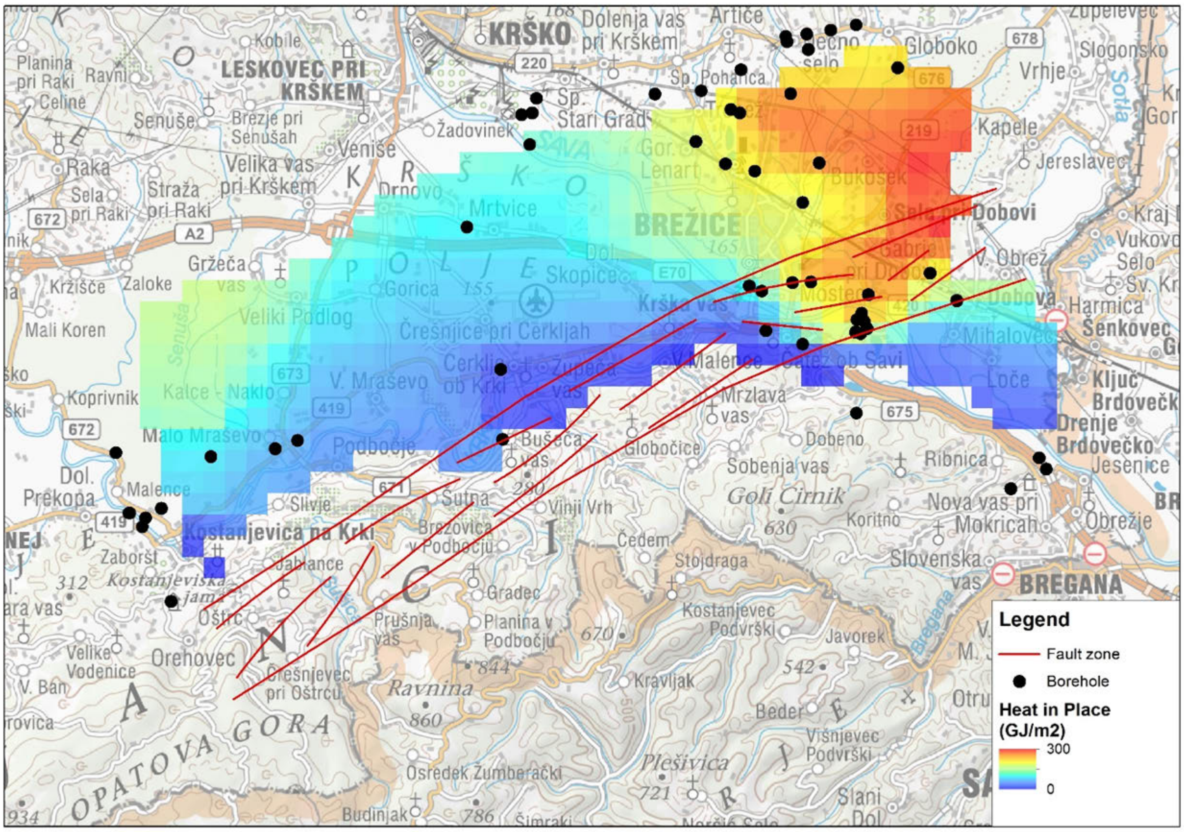

Figure 36 Estimated Heat in Place.

The total HIP at the pilot area is estimated to 6.8 EJ. Average HIP is 54 GJ/m², with maximum value of 128 GJ/m² and minimum value as low as 0.7 GJ/m² (Figure 36).

However, there are potential issues which influence the calculated HIP, as there is some uncertainty in assumed effective porosity. The effective porosity used is 5%, with no distinction between the fault thermal zone and the compact rocks (outside the fault zone), which was agreed as default value in the HotLime project.

The uncertainty is also large with regard the depth of the thermal Čatež fault zone, because no up-to-date drilled borehole has reached the bottom end of this zone; such a borehole should be at least 2.5 km deep. The fault zone is likely a deep structure, related to the formation of the Gorjanci mountains and may be structurally related to the deep, regional Sv Nedelja fault along the southern flank of the Gorjanci mountains (in Croatia). Maximum depth of the Sv Nedelja fault is estimated at approximately 19 km.

The areal extension of the Čatež geothermal field is not yet firmly delimited. We have some rough picture of an extension of the Čatež fault zone of which the Čatež field is just one part, located more in the eastern zone. However, with some earlier investigations, in the 1960's and 1970's and especially in 1996, it was possible to acquire a picture of the areal extent, mostly with geophysical methods, such as deep geoelectrical sounding, shallow temperature gradient measurements and few deep seismic reflection profiles, the latter from the previous decades (Rajver & Ravnik, 2003). We may predict that the reservoir volume is within the 2 km narrow fault zone and somehow oriented more sub-vertically and inclined to south-southeast direction. It is necessary to determine the areal extent in more detail with additional geophysical research, especially with temperature gradient survey in more new shallow boreholes (especially in direction towards north, northeast and east to southeast) and with more deep reflection seismic survey and perhaps also deep geoelectrical sounding.

2.8.3 Application of the UNFC-2009 framework system to the Čatež geothermal field

The various steps, how a certain »project« (geological commodity) is progressing along the 3 axes of the UNFC-2009 cube (E: Economic and social viability, F: Field project status and feasibility, and G: Geological knowledge) from an exploration phase to non-commercial and finally commercial projects, are a result of various decisions and steps (Nádor et al. 2018). The UNFC-2009 is a generic, principle-based system in which estimates of mineral and energy quantities (geological commodities) are classified in a numerical and language independent coding scheme according to 3 fundamental criteria, creating a 3-dimensional system (in 3 axes, see paragraph 2.2 and Appendix 1).

The Expert group on Resource Classification did not consider geothermal energy during its formulation of the UNFC-2009, but this does not in itself disqualify the UNFC-2009 as a possible template for a classification framework for geothermal energy (Beardsmore 2013).

2.8.4 UNFC-2009 classification and quantification of the present project

The production history of the three currently operating users shows for 2019 that about 96.6 TJ is produced annually at all three in total, as reported by operators and calculated according to equations for the WGC reporting (Rajver et al. 2020+1). Following is just a preliminary and a trial version of the E, F and G classifications according to instructions by Beardsmore (2013) and following few examples which are found in the Case studies by Falcone et al. (2017).

As a long-distance view into the future we would need more data to be able to calculate geothermal resources from our HIP in the sense of the UNFC classification method: to better define the temperature, flow rate and flow paths in the underground, recoverability, top of the carbonate aquifer and other characteristics of the probable geothermal energy resource outside the narrow Čatež fault zone or on the outskirts of this zone, so that the geothermal resources could be determined with a higher level of confidence. This provokes more data acquisition as mentioned before.

2.9 Miocene and Triassic carbonates of Zagreb hydrothermal field (Croatia, T2.7)

Author: S. Borović (HGI-CGS)

2.9.1 Introduction

Croatia is situated at the junction of major European tectonic units: the Alps, the Dinarides and the Pannonian Basin System (PBS) (Figure 37a). When considering the area from the perspective of geothermal resources utilization, it can be divided into two distinctive regions (Figure 37b).

Geologically, the north-eastern part of the country represents the south-western margin of the PBS, while the south-eastern part of the country is situated in the Dinarides. Favourable geothermal characteristics of the PBS are well known and demonstrated (e.g. (Dővényi and Horváth, 1988), (Horváth et al. 2015)), and its Croatian part shares these traits. Lithosphere thinning in the back-arc extensional area leads to high heat transfer from the mantle and anomalously high surface heat flow as a consequence. On the other hand, the Dinaridic area is characterized by a combination of thick lithosphere and kilometers thick carbonate platform deposits, which are also karstified - enabling deep meteoric water percolation, leading in combination to almost negligible surface heat flow. That is why, for all practical purposes, geothermal research (excluding heat pump applications) is concentrated to Pannonian part of the country.

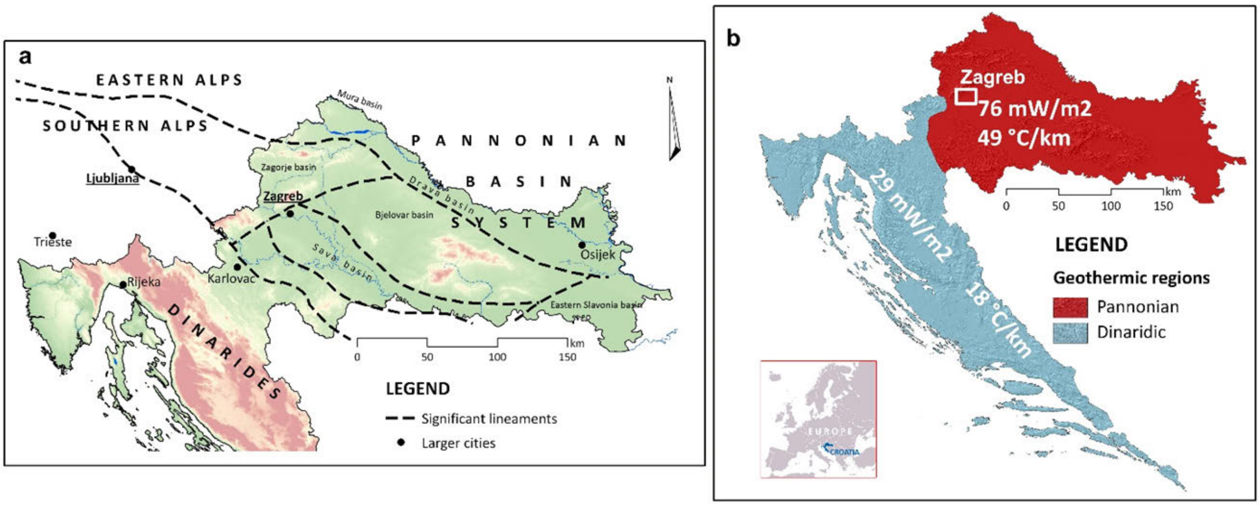

Figure 37 (a) Position of Croatia in relation to major European tectonic units (according to (Lučić et al. 2001; Tari and Pamić, 1998; Velić et al. 2012); (b) Heat flow density and geothermal gradient in different Croatian regions. Modified from (Borović et al. 2016).

There are dozens of natural thermal springs in the Pannonian part of Croatia, and they are known and utilized since prehistoric and ancient times (Schejbal, 2003). However, many more geothermal aquifers were discovered in the period from 1950-s to 1990-s, owing to extensive exploratory and drilling surveys conducted by hydrocarbon industry (in those times, the former Yugoslav publicly owned petroleum company INA-Naftaplin) - one of those being the Zagreb geothermal aquifer, object of analysis as a pilot area in the scope of HotLime project (location shown in Figure 37). The permission to use the borehole and seismic data for research purposes was obtained from the Croatian Hydrocarbon Agency (AZU).

2.9.2 Zagreb geothermal field characteristics

Zagreb geothermal field (ZGF), discovered in the 1960-s, has an area of about 54 km² and is situated in the City of Zagreb, the national capital. Considering the number of potential users (790,000 inhabitants according to the last population census in 2011, and around 100,000 households in the district heating system, DZS, 2019) it represents an example of available resource which could be put into good use. The opportunity of using the resource was recognized and the field was further developed as a geothermal field. Research and drilling continued until 1988. Although the boreholes in the external part of the field are also utilized (e.g. Lučanka and Nedelja boreholes), the main development is represented by two so called *technological systems*: Mladost and KBNZ (in the central part of the field, with the highest measured temperatures and geothermal gradients). Figure 38 shows the schematic cross-section of the Zagreb area.

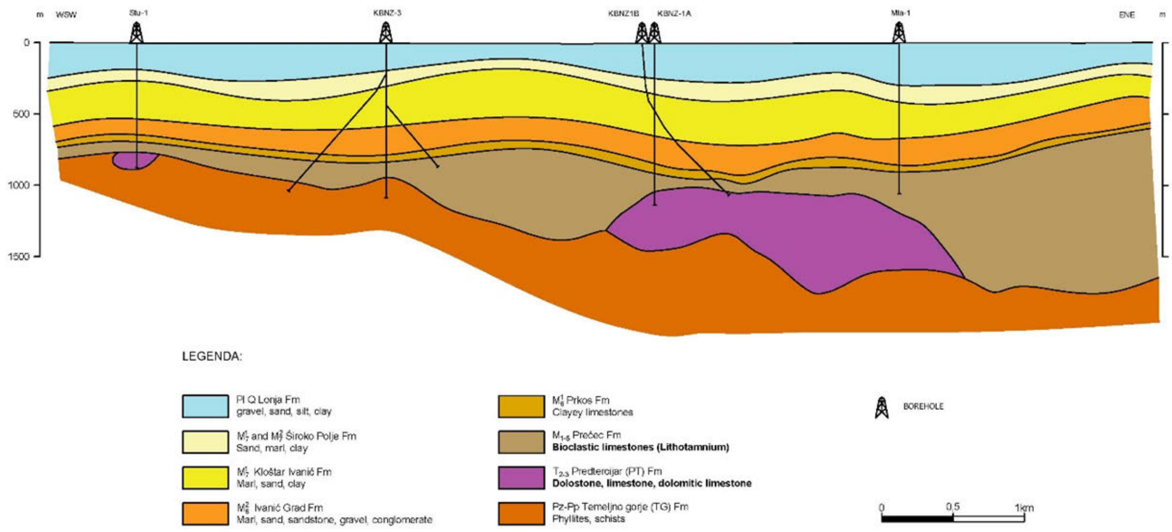

Figure 38 Schematic geological cross-section, redrawn according to Zelić et al (1995).

The main geothermal aquifers, as identified in the existing boreholes are $M_{1\text{-}5}$ Prečec Formation bioclastic (*Lithotamnium*) limestones and $T_{2\text{-}3}$ Podloga tercijara (PT) Formation dolostones, limestones, and dolomitic limestones. They vary significantly in thickness in this small area: $M_{1\text{-}5}$ from 35 to 1016+x meters and $T_{2\text{-}3}$ from 5 to 357 m. Lithothamnium limestones are characterized by primary and secondary porosity which results in good overall permeability. The Triassic carbonates have low matrix porosity so good permeability is attributed only to secondary porosity. Recorded water temperatures in the boreholes range from a minimum of 34°C up to a maximum of 78°C at Mladost technological system and 82°C in the KBNZ system.

In the majority of the boreholes the formation yielding water was the Miocene bioclastic limestone. However, the hydrochemical data suggest that water is equilibrated with the dolomitic aquifer, so for practical purposes the two formations were considered as a single hydro-stratigraphic unit.

2.9.3 Status of the data

In the area of Zagreb geothermal field 27 boreholes were drilled, 34 seismic reflection profiles were recorded, and these data were obtained from the AZU.

Firstly, it must be stated that no data base exists, containing organized information from decades of hydrocarbon exploration and exploitation in Croatia. Also, creating one was impossible until few years ago because the archive data were unavailable to the research community. Even now, as was the case for HotLime project data request, the whole procedure had to be undertaken to get the data, after which the data is obtained in the form of scanned paper reports.

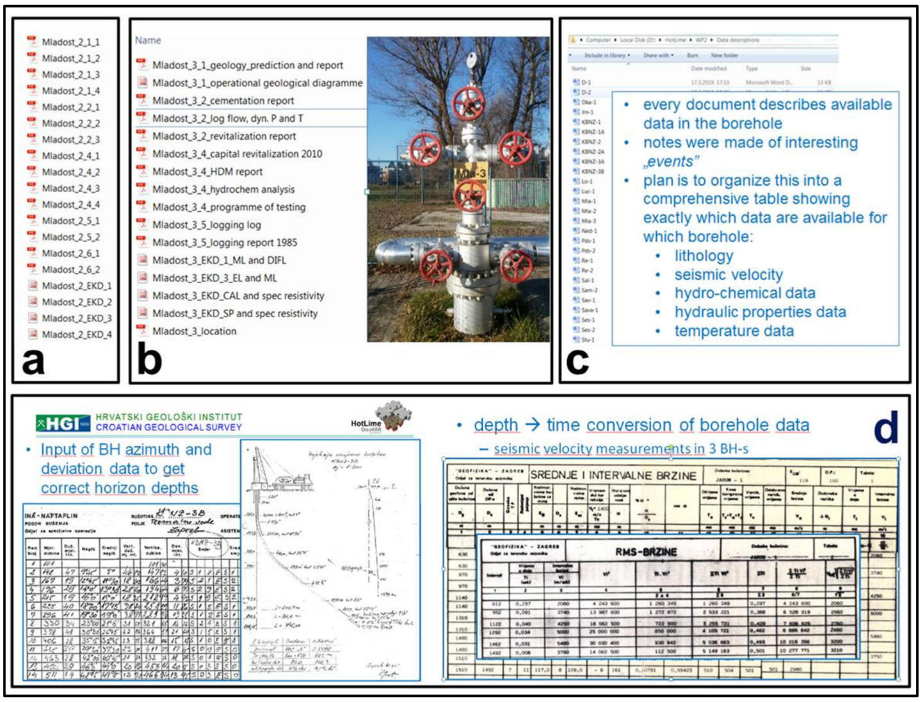

Figure 39 *(a) original data and file names; (b) renamed files; (c) created data descriptions; (d) examples of the scanned PDF documents.*

The documents needed to be inspected one by one (Figure 39a) to determine their actual content, then renamed for future use (Figure 39b), and data descriptions were done for data relevant for HotLime investigations. It is clear that it would have been wiser to start creating the full data base, but due to personnel shortages at the HGI-CGS, there is no possibility to extract all the useful data at this point. Figure 39d shows some of the data which have been delivered to us, as an example.

Owing to the fact that the data was obtained in a disorganized form as described above, the works have been progressing slower than planned. However, the initial premise of the HotLime proposal was that the partners will be starting from different levels of data availability and organization, as well as with different availability of human resources which are available and skilled in geothermal research. The goal is to bring all the partners to the higher level of expertise, considering the difference in starting points inside the project consortium.

In the light of such status of the data, the Croatian HotLime project team did not create a 3D model of the subsurface yet so the application of the 3DHIP calculation is not possible. However, due to the existing data on ZGF, we did have ample data for the originally planned type of resource estimation and classification, which is therefore presented in this report.

2.9.4 Resource estimation and classification

Probabilistic estimates (P10, P50 and P90) of possible power output were calculated for two technological systems of the ZGF: Mladost and KBNZ (Figure 40).

The estimates are based on the ZGF main mining design data (Zelić et al. 1995). Main mining design is a document which, in accordance with Croatian legislation, contains all the data on geothermal field construction, testing and interpretation. DoubletCalc 1.4.3 software (TNO, 2014) was used, which was conceived for permitting purposes in The Netherlands, and the required geotechnical input parameters were available.

Mladost is a doublet system in successful and continuous operation since 1987, so it is clearly feasible and socio-economically accepted. Mladost is a sports park, and the thermal energy is used for space and water heating. Due to its longevity, it is known that it operates on average 335 days annually, so this number was used for the calculation of energy output. The calculation was done for a 50-year period (Table 6).

The KBNZ system is situated ca. 1 km to the SSW from Mladost. Three boreholes were drilled in the area, all of them including side-tracks. The system was planned for heating of the University hospital which was being constructed at the time. However, with changing circumstances, the hospital was never completed, and the geothermal boreholes are in place, but not utilized. Possible power output was also calculated, and the annual energy output was predicted based on the same operational regime as the neighbouring Mladost system. Predicted power output for both systems is graphically summarized in Figure 41.

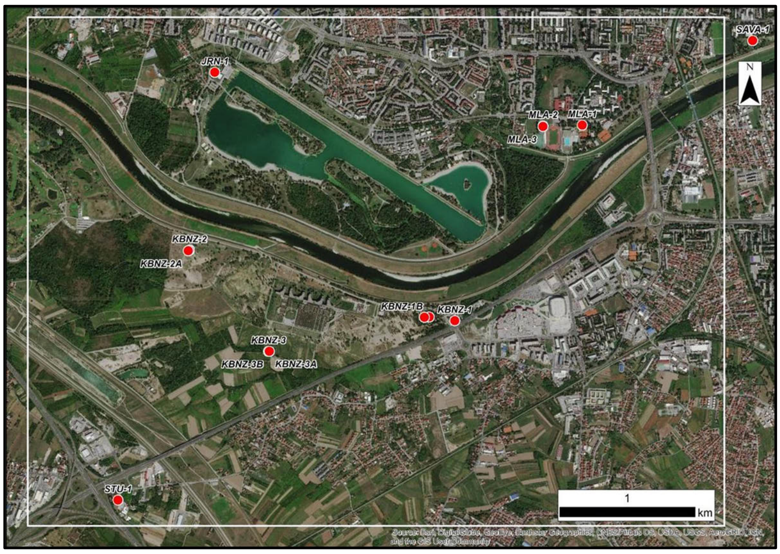

Figure 40 *Central part of the Zagreb geothermal field (satellite imagery in the background by Google Earth).*

Table 6 *Resource assessment for Mladost and KBNZ systems.*

	MLADOST		**KBNZ**	
for 50 yr	P (MW)	E (PJ)	P (MW)	E (PJ)
P10	10,90	15,77	14,96	21,65
P50	8,65	12,52	9,90	14,33
P90	4,90	7,09	5,01	7,25

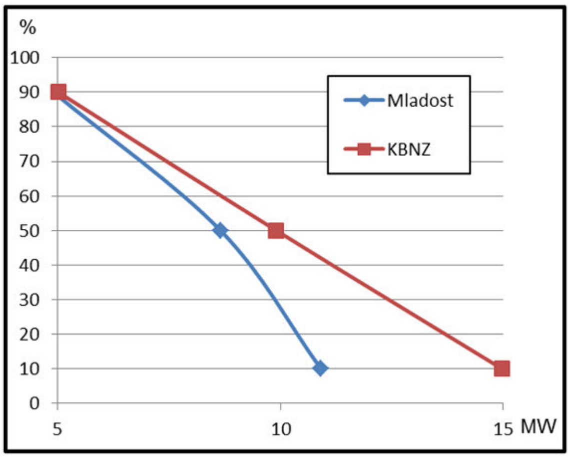

Figure 41 *Probability plot for Mladost and KBNZ systems power outputs.*

Since the UNFC-2009 classification is project-based, it was necessary to ensure the comparable level of quantification. Most of the HotLime case studies were investigations on large areas (regional scale), and a classification was therefore not applicable, i.e. all regional examples would be classified as E.3; F3.3; G4 based on notional 'standard' projects, as exemplified for the Pannonian Basin System (PBS) in the scope of DARLINGe project (Nador, 2018). Looking at the whole theoretical 'Zagreb Basin' (sub-basin of the PBS), the DARLINGe project classified the resource as mentioned above. However, since the technological systems in the ZGF are already in place: Mladost (in operation) and KBNZ (idle, but tested), these projects could be classified. In accordance with the guidelines determined at the HotLime workshop on the topic held in Utrecht, the following manuals were used: Specifications for the application of the United Nations Framework Classification for Fossil Energy and Mineral Reserves and Resources 2009 (UNFC-2009) to Geothermal Energy Resources (2016) and Application of the United Nations Framework Classification (UNFC) to Geothermal Energy Resources – Selected case studies (2017). An example is given for the operational Mladost system in Figure 42.

The Mladost system classifies as 7,09 PJ E1.1; F1.1; G1 + 5,43 PJ E1.1; F1.1; G2 + 3,25 PJ E1.1; F1.1; G3 – totally contrasting the sub-basin scale classification (E.3; F3.3; G4). This system is in successful continuous operation since 1987, so it is clearly feasible and socio-economically accepted.

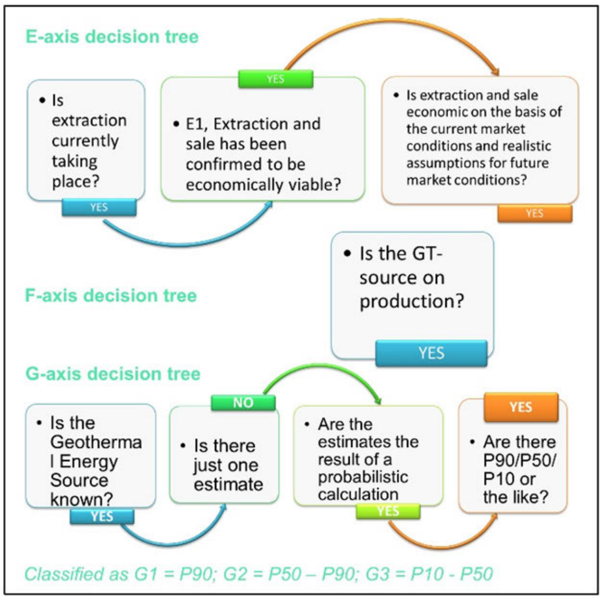

Figure 42 UNFC decision tree for E, F and G axes for Mladost technological system of the ZGF.

On the other hand, the neighbouring system KBNZ of the same geothermal field must be classified as 7,25 PJ E3; F1.3; G1 + 7,08 PJ E3; F1.3; G2 + 7,32 PJ E3; F1.3; G3 because – although all the wells are in place since 1987, they have been tested, concession was granted etc. – the system never became operational. KBNZ case is a typical example of legislative, administrative and political barriers to project implementation, leading to E3 classification of a project which could be in operation for decades already.

Mladost system is operational for 34 years, so its thermal output can be compared to the theoretical (and planned by the main mining design). According to the most recent published data (Golub et al, 2014), the annual utilization is 3 MW in capacity and 19.16 PJ of thermal energy. In comparison to Figure 41, it is visible that it is only 60% of the P90 estimate, i.e. the exploitation should be organized in a much more efficient fashion. KBNZ system is not in operation, so none of the available energy is put into useful function. Considering that the field is situated in the national capital with a number of possible users, it can be considered as an example of a resource abandoned for decades due to socio-economic circumstances.

2.10 Triassic carbonates of the Pantelleria-Linosa-Malta rift complex (Malta, T2.8)

Author: C. Galea (MFE, Continental Shelf Department)

2.10.1 Description of the pilot area

The Malta case study (T2.8) covers a surface area of 6,850 km² and includes the Maltese Islands and the surrounding marine waters located mostly southwest of the Islands. The onshore and offshore sedimentary sequences consist predominantly of limestones and dolomites interbedded with marls, clays and evaporites (Argnani 1990, 1993; Civile et al. 1990). Although there are several carbonate formations that can act as potential geothermal reservoirs within the Mesozoic - Cenozoic interval, T2.8 focuses on the upper member of the Late Triassic Kercem Formation (indicated as the HotLime Formation in Figure 44) consisting predominantly of inter-beddings of carbonate mudstone, packstone and grainstone . This formation has been encountered in only one well in Malta, a deep onshore stratigraphic well (MTZ shown in Figure 23) drilled in the study area in 1998/9. The well penetrated nearly 1300 m of this member at a depth of 6055 m below sea level.

The top of the Kercem Formation was mapped in the marine part of the study area using over 1,800 km of 2D time-migrated seismic data. A seismic well-tie was carried out at a projected well location in view of the appreciable offset between the marine seismic data and the onshore well. Away from well control, the confidence in picking the top of the Kercem Formation horizon is fair to low. The bottom of this member could not be mapped with sufficient confidence and thus there is limited well and seismic data to map the thickness of this potential reservoir. In the circumstances, given the carbonate shelf depositional setting in the Late Triassic in the study area and its environs, the thickness of the upper member of the Kercem Formation encountered in the MTZ well (1300 m) was taken as a representative thickness of the potential reservoir (Jongsma et al. 1985, Civile et al. 1990).

Limited petrophysical data is available from the MTZ well. Porosity values of between 1% and 2% have been determined from bottom cores in the formation. Although primary porosity is relatively low, interpretation of formation micro-scanner logs indicates that the upper member of the Kercem Formation is extensively fractured in places becoming less so with depth. In addition, the predominant strike of the fractures is oriented favourably with respect to the horizontal stress direction so the fractures should remain open. This was collaborated by mud losses during the drilling of the MTZ well which indicate that the fractures are open. Evidence of water flow is evident from changes in mud salinity where increases in salinity were observed.

Temperature data was extracted from the MTZ well. These indicate a temperature gradient of 27°C/km within the Kercem Formation.

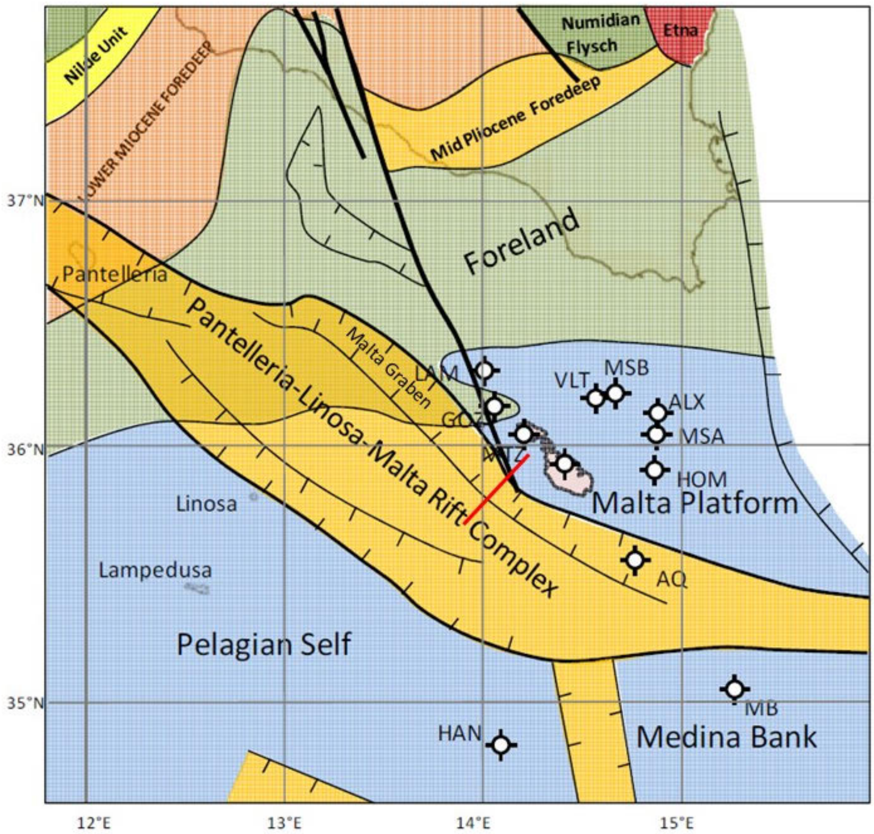

Figure 43 *Regional structural setting of the Maltese Islands showing the Pantelleria-Linosa-Malta Rift Complex (including the Malta Graben) and the location of the geological cross section (modified after Debono, 2014).*

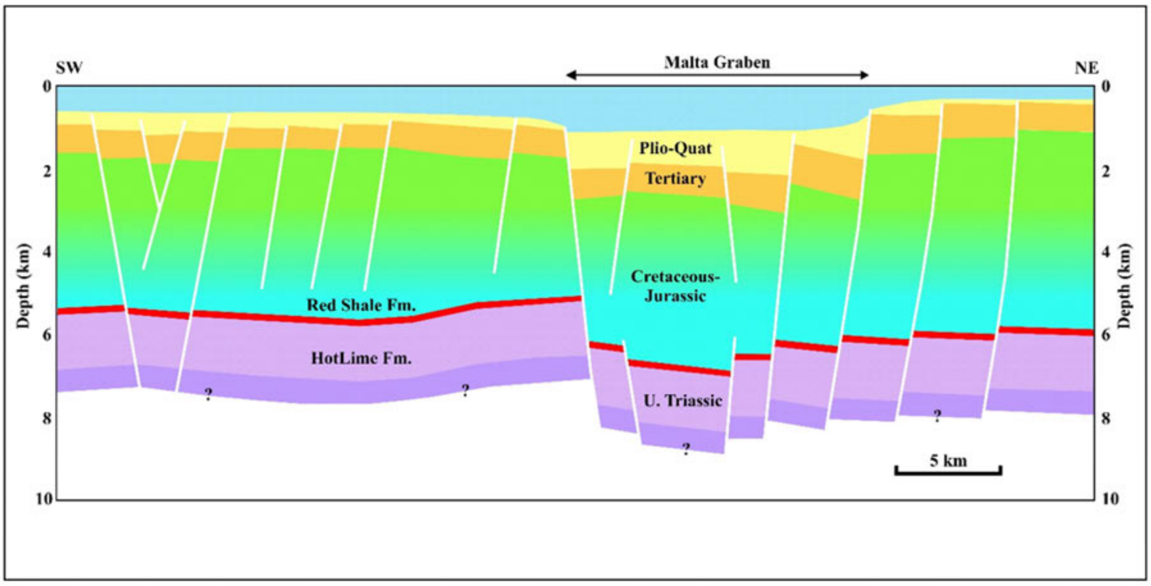

Figure 44 *NE-SW section across the Malta Graben in the study area.*

2.10.2 Heat in place

The heat in place was calculated using the method defined in Muffler & Cataldi (1978) described in chapter 1. Assuming a reservoir thickness of 1300 m, a temperature at the top the reservoir of 130°C and a temperature gradient of 2.7°C/100m within the reservoir, gives the following HIP values for a volume of reservoir rock V and injection temperatures of 18°C and 50°C respectively (Table 7).

Table 7 Heat in Place calculation results for return temperatures of 18 and 50°C.

T_{ref} [°C]	HIP [GJ/m²]
18	404
50	304

The above figures are only indicative estimates given the uncertainties in several key parameters used to calculate the HIP. In particular, limited information is available on the petrophysical properties of the potential reservoir such as porosity and permeability given that only one well penetrated this formation.

Although primary porosity of the reservoir is expected to be low in view of the considerable burial depth and carbonate diagenesis, the location of the study area within the extensively faulted Malta Graben of the Pantelleria - Linosa - Malta Rift Complex (Figure 43), fracturing is expected to contribute significantly to the enhancement of the geothermal properties of the reservoir.

2.10.3 Recommendations for further work:

The results from this case study are based on the interpretation of time domain 2D seismic data and limited well data. In this regard, additional data such as 3D depth migrated seismic data and further studies are required for fault/fracture characterization and facies mapping to understand better the geothermal properties of the potential reservoir.

2.11 Eocene carbonates of the Empordà Basin (Spain, T2.9)

Authors: M. Colomer, I. Herms (ICGC)

2.11.1 Description of the pilot area

For a detailed description of the reservoir please refer to HotLime Deliverable 2.0, Summary report of mapping and characterization. Here, only a summary is given.

The Empordà Basin (EB) is a Neogene basin located in the NE of Catalonia, close to the Pyrenees ranges. EB is internally structured by a blocky structure in the pre-Neogene bedrock, which presents a general deepening towards the north (Figure 45). Within the lithostratigraphic succession from the Paleozoic to the Paleocene, the Girona Limestones Formation (Lower Eocene) is identified as a potential hot limestone aquifer. Its thickness values range between 22m to 270m, with an average of 75m, and an increase towards to the west (Pallí 1972), to the north and in depth. The maximum depth reaches 2725 m in the study area.

In general terms, the Girona Limestones Formation registers a general transgressive trend, in accordance with a retrogradation of the carbonate platform system to the south due to basin deepening but it shows a high heterogeneity of facies. A preliminary diagenetic study (ICGC-UB, 2019) mainly indicates an early cementation and practically syn-sedimentary. On the other hand, all the outcrops show an intense stylolitization of compaction, indicative of the existence of burial previous to the current aerial exposition.

Furthermore, the Lutetian marine rocks are highly affected by faulting, mostly normal faults related to the Neogene extension. These structures, with the presence of marls between limestone beds, can produce a potential compartmentalization of the carbonate unit from the reservoir point of view.

The target aquifer covers an area of more than 400 km² in which there are only two deep wells (Girona-2 and Jafre) with available data from the hot limestone aquifer. Both wells showed an artesian behaviour with a geothermal fluid. Considering the BHT corrected values for the Girona-2 well, it was estimated the temperature gradient of the aquifer is 47°C/km. According to the BHT Jafre values, a geothermal gradient of 42°C/km measured from the top of the aquifer could also be considered. In both cases a mean annual surface temperature of 16°C has been considered. Until now, no geothermal resource assessment of the aquifer has been carried out at regional scale.

To sum up, the lateral and vertical distribution of the hydraulic permeability is difficult to predict due to the high heterogeneity of facies plus a complex diagenetic and faulting history. Despite all, a less compartmentalization in the deeper parts of the aquifer is expected towards the W, according to the current geological knowledge, and a higher hydraulic transmissivity due to a thickening of the aquifer.

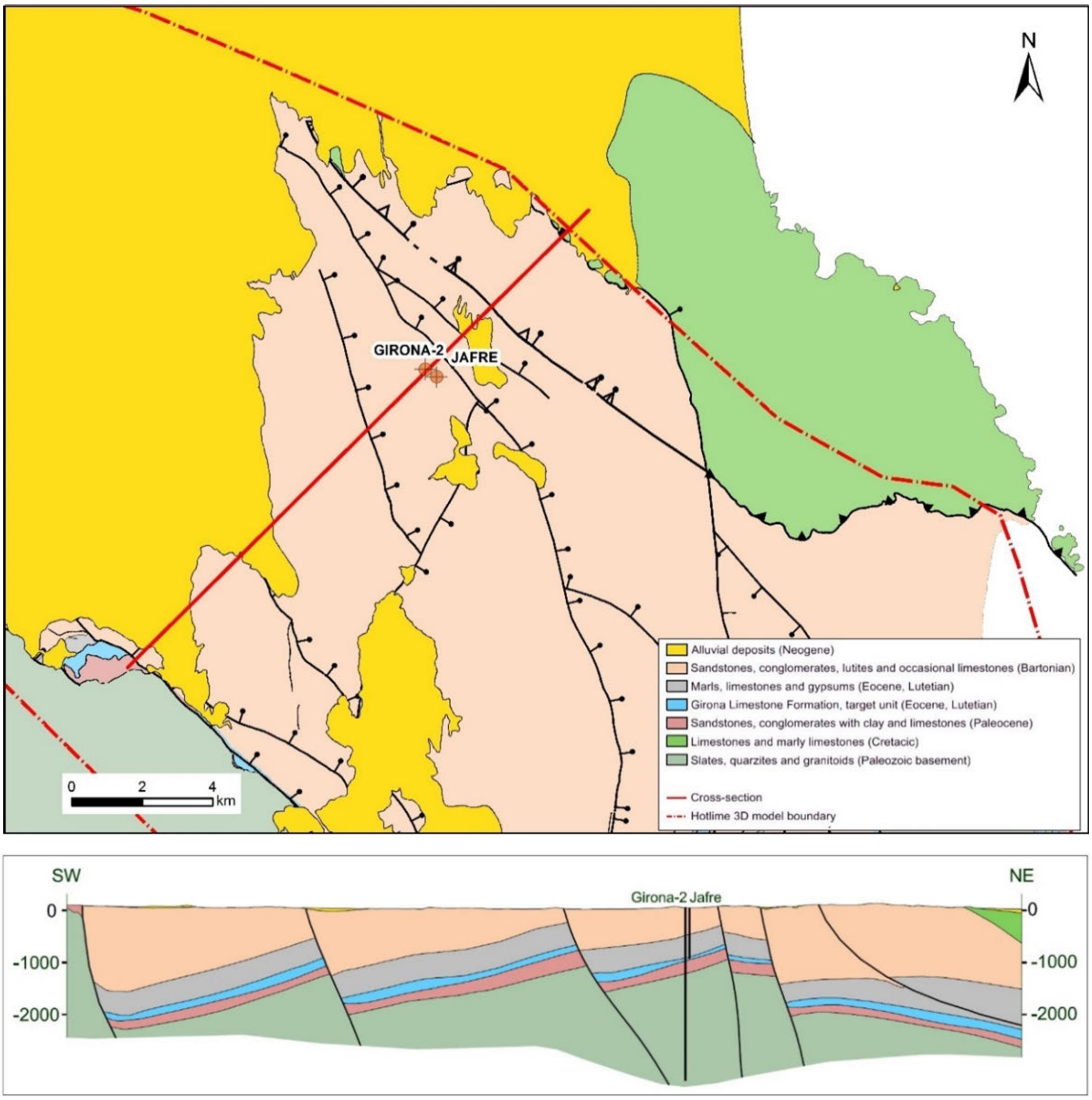

Figure 45 *A) Synthetic structural and lithological map of the study basin (modified from IGCG, 2017). The map shows the cross-section and the location of the borehole data used to build the 3D geological model; B) Synthetical cross-section showing the location of the Girona Limestone Formation.*

2.11.2 Applied methodology and results

In the Empordà Case, due to the not-well constrained context, a probabilistic approach was applied both in terms of reservoir geometry and petrophysical parameters. Thus, it was considered to generate a first 3D geological model by using a modelling software (MOVE by Midland Valley and SKUA-GOCAD by Paradigm) that honoured all available data so far. Afterwards, this preliminary model was validated by geophysical methods following a full gravity litho-constrained stochastic approach. Once the geometry of the aquifer was well constrained, a 3D thermal model was generated also using a probabilistic approach.

In order to be able to build these 3D models, new data were collected from new field campaigns: a new gravity campaign (Dec 2018- Apr 2019) was carried out by the Geophysical Techniques Unit Team of ICGC. It consists of 365 new gravimetry measurements in the study area. A second field campaign was also done by the University of Barcelona (ICGC-UB, 2019), to collect rock samples and characterize the analogues outcrops. The sampling campaign was oriented to characterize the carbonate facies of the reservoir and determined by laboratory test petrophysical parameters.

Stochastic approach was done using the 3DGeoModeller software (by Intrepid Geophysics) which allows to validate the 3D geological model according to available geophysical potential-field data (gravity) by means of forward modelling and 3D geophysical inversion following a lithological-constrained stochastic gravity inversion. This iterative process finishes until a good fit is achieved between the observed gravity data and the gravity modelled response (misfit<1.4 mGal, in this case). The input model considered covers the whole study area (400 km²) with a depth of 7 km and, as input parameter, the rock densities values following a probability density function (PDF) (i.e. a Gaussian distribution) for each geological unit (Table 8). The obtained results – a 3D voxel model with lithology and density values for each voxel cell – allow to see a thickness aquifer and the depth to top aquifer (Figure 46) which confirm the initial assumptions for the geological structure and the parametric values according to those observed in the field campaign.

Table 8 Loaded rock densities probability density functions in the 3DGeomodeller during the geophysical inversion step (Mean value / Standard deviation value) (source: Ayala et al., 2015; Husson et al., 2018; Rivero et al., 2001; Schön 2011).

geological units and lithology	**geological age**	**density [g/cm³]**	
		mean	**SD**
Conglomerates, sandstones and clays in variable proportions, associated with alluvial and deltaic fans	Neogene	2.450	0.050
Sandstones, conglomerates, lutites	Eocene (Bartonian)	2.630	0.050
Marls, limestones and gypsums	Eocene (Lutecian)	2.615	0.050
Limestones (GLF, target reservoir)	Eocene (Lutecian)	2.650	0.050
Sandstones, conglomerates, lutites and some levels limestones	Paleocene	2.575	0.050
Limestones and marly limestones	Cretaceous	2.710	0.050
Slates, quartzites and granitoids	Paleozoic	2.720	0.050

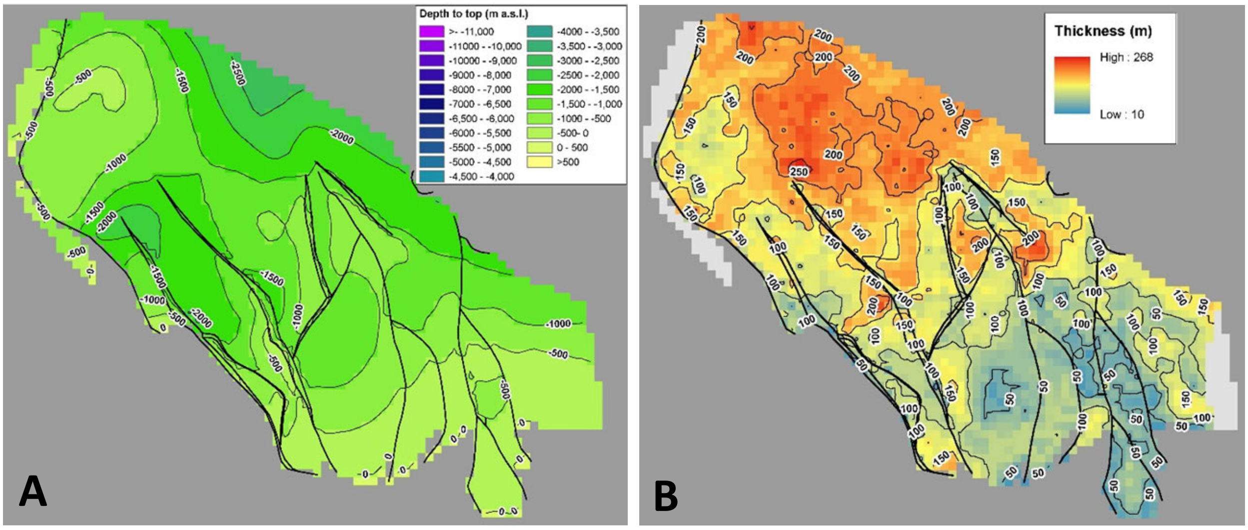

Figure 46 Outputs maps derived from the geological model: A) (left) Depth of the top of the fractured Eocene limestone. B) (right) Thickness of the fractured Eocene limestone (light grey zones represent no thickness data zones).

Once the 3D geological model was finished, the next step was to build the 3D thermal model using also the 3DGeoModeller software. In this case, a conduction dominated assumption was considered for the heat regional heat transport and steady state. The bottom and top boundary conditions used was the Dirichlet type (fixed temperature) with 155°C and 16°C (average surface temperature) respectively and no heat flux was considered by the lateral boundaries of the model. The bottom boundary condition was previously calculated by means of a lithospheric model at regional scale using LitMod3D software (Fullea et al., 2009). The process included also a “Forward Model Temperature” module and, to consider the uncertainty of the thermal parameters, a resource uncertainty algorithm (“Parameter Sweep – Heat”) which follows a quasi-stochastic approach (Intrepid-Geophysics, 2020). Therefore, the input parameters (i.e. thermal conductivity and heat production rate) were defined by a PDF (Gaussian distribution, defining the mean and the standard deviation) for each lithological unit (Table 9). This algorithm solved the heat transport equations in steady state considering conduction and it calculated the isotherms for the entire domain following. Finally, the same software allows to compile the different scenarios generated in one unique with the most probable lithology, thermal parameters and temperature in each voxel cell of the 3D model. The results fit well with the temperature values of the Girona-2 and Jafre wells with errors below 2°C.

The final 3D geological model and 3D thermal model were exported as 3D voxel-based models in ASCII format which will contain the following data: the reservoir inferred temperature, the lithology, the voxel position (X,Y,Z coordinates) and the rock density (derived from the geophysical inversion process). This format will be useful for further analysis or assessments.

Table 9 *Loaded rock thermal properties probability density functions in the Parameter Sweep algorithm - Heat resource uncertainty algorithm of 3DGeomodeller. (Mean value / Std. Standard deviation value) (source: ICGC-UB, 2019, Čermák, V. & Rybach, L., 1982; Vilà, et al., 2010; Schön, J.H., 2011; Eppelbaum, L. et al., 2014; Bär, et al. 2019)*

geological units and lithology	geological age	thermal conductivity		heat production rate	
		λ [W/mK]		HPR [W/m³]	
		mean	std	mean	std
Conglomerates, sandstones and clays in variable proportions, associated with alluvial and deltaic fans	Neogene	1.60	0.50	1.10E-06	9.19E-08
Sandstones, conglomerates, lutites	Eocene (Bartonian)	1.85	0.20	1.20E-06	6.60E-07
Marls, limestones and gypsums	Eocene (Lutecian)	2.10	0.50	8.00E-07	5.00E-07
Limestones (GLF, target reservoir)	Eocene (Lutecian)	2.80	0.30	4.77E-07	3.56E-07
Sandstones, conglomerates, lutites and some levels limestones	Paleocene	2.91	0.55	1.19E-06	6.60E-07
Limestones and marly limestones	Cretaceous	2.37	0.52	4.77E-07	3.56E-07
Slates, quartzites and granitoids	Paleozoic	3.50	0.50	2.20E-06	2.53E-07

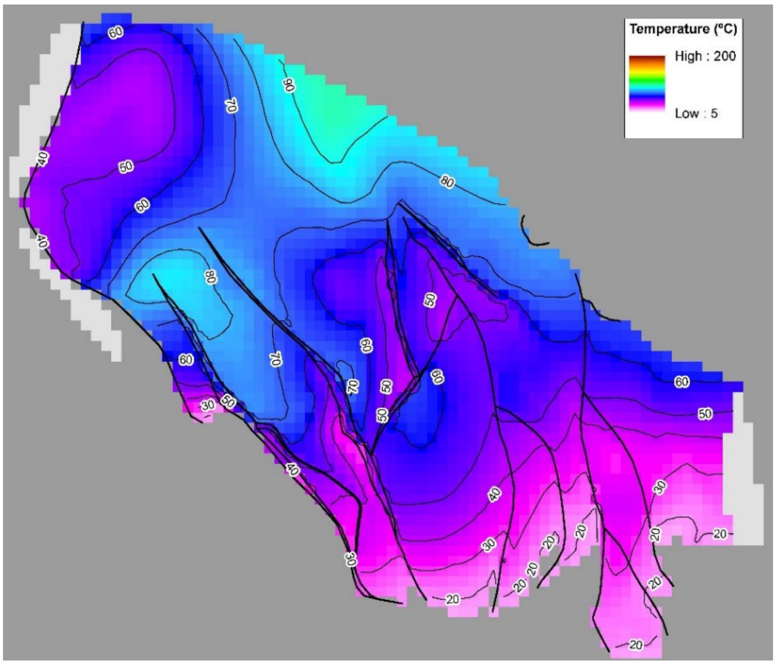

Figure 47 *Output map derived from the thermal model: temperature at top of the fractured Eocene limestone (light grey zones are no temperature data zones).*

2.11.3 Assessment of geothermal potential by HIP method

To assess the deep geothermal potential for the Girona Limestone Formation aquifer, the Heat in Place (HIP) method (Muffler and Cataldi, 1978) was applied at each voxel from the resulted 3D voxel-based model using the 3DHIP-Calculator software (V 1.1. December 2020) with a deterministic approach. This means, although the tool is ready to use for probabilistic approach (see Chapter 3), it is possible using it in a deterministic approach. In this case, values for each parameter were fixed (i.e., without using a PDF) and only considering the spatial variation defined by the geological and thermal models (see in Table 10).

The considered values for porosity and specific heat capacity of rock which correspond to the measured average value of samples measured in the field campaign carried out in the Empordà area (ICGC-UB, 2019). About the reference temperature (Tr), 3 values were considered: 18 and 50°C, in order to compare with all the study areas, and 26°C accordingly with the assumption of Limberger et al. (2018*)* for a global geothermal source assessment (considering a minimum reinjection temperature by unitarily adding 10°C to the mean air temperature at the surface of 16°C in the EB).

Table 10 Parameters introduced at the 3DHIP-Calculator (: values from the 3D geological model; **: values from the 3D thermal model).*

parameter		unit	fixed value
thickness of the reservoir (calculated for each voxel *)		m	-
area of the reservoir (calculated for each voxel *)	A	m²	-
rock density (calculated for each voxel *)	ρ_r	kg/m³	-
porosity	ϕ	-	0.055
specific heat capacity (rock) at reservoir condition	C_r	kJ/kg°C	0.858
temperature of the reservoir (°C) (calculated for each voxel)	T_i	°C	-
fluid density	ρ_w	kg/m³	1040
specific heat capacity (fluid) at reservoir condition	C_w	kJ/kg°C	3.8
reference temperature	T_f	°C	18 26 50

Once the 3DHIP-Calculator software is executed, two ASCII files are obtained from which different 2D outputs maps could be generated. In this case, we obtained the HIP maps at a several reference temperatures (at 18, 26 and 50°C respectively). Considering the study area of Case 9, the modelled Heat in Place shows a maximum value of HIP of 39.3 GJ/m2 (Tinj = 18°C), 34.8 GJ/m2 (Tinj = 26°C) and 22 GJ/m2 (Tinj = 50°C).

According to the results obtained, the most promising area is the western part of the EB before the eastern area where Girona-2 and Jafre are located. Thus, different initial assumptions were confirmed such as an increase in the thickness of limestone reservoir towards the West; a deepening towards W and N; and a decrease of compartmentalizing due to less faulting (according to the geological knowledge available so far). These characteristics have been reflected in the HIP estimation. The variation of the reference temperature involves further reducing the HIP and the extension of the promising area becoming the NW part the best to be explored in the future.

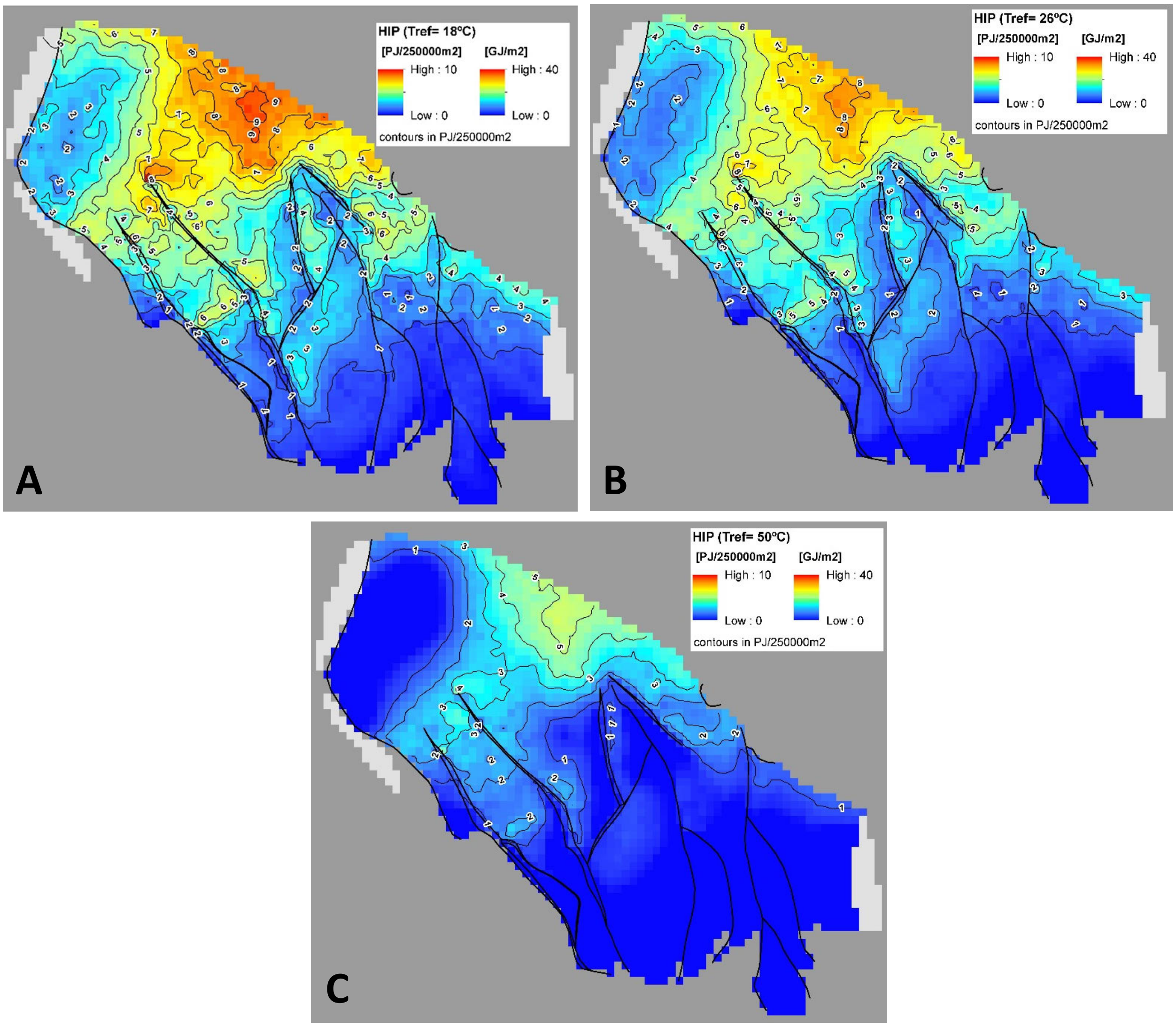

Figure 48 *Output maps of HIP assessment in the Empordà area: A) (top left) HIP with the reference temperature (Tr) at 18°C; B) (top-right) HIP with the reference temperature (Tr) at 26°C; C) HIP with the reference temperature (Tr) at 50°C (in all maps: light grey zones are no HIP data zones). Note that the legend was adapted to a maximum of 40 GJ/m2.*

2.12 Triassic carbonates in the Umbria Trough (Italy, T2.10)

Authors: A. Motti, S. Mariuccini, N. Natali, M. Ogna (Regione Umbria)

2.12.1 Description of the pilot area of the Castelviscardo Geothermal Field

The pilot area is located in Regione Umbria (Central Italy) and it covers an area about 240 km² wide. The exploration of this area started with the research carried out by the private company ENEL in the late 70s-80s for the characterization of the Castelviscardo geothermal field. During this exploration campaign, 9 deep boreholes have been drilled, most of them are about 600 or 800 m deep , while the Alfina 15 well reached a depth of 4,826 m (Buonasorte et al. 1988, 1991). Hence, the geological study of the area was made with all the available geological / hydrogeological maps, the geophysical and thermal springs information and the useful logs from the deep wells exploration campaign as well (ISPRA 2005, Regione Umbria 2013, 2019).

Geology

The geological setting of the area is represented by a fold-thrust belt showing a NNE verging trend, where (from top to bottom) the Ligurian, Tuscan and Umbria-Marche units tectonically overlap (Figure 49). Extensional tectonic acted on this compressional structure and formed NNW-SSE half-grabens later filled by marine or continental Pliocene sediments, sometimes covered by Quaternary volcanic deposits. The Ligurian unit (Cretaceous-Eocene) can be considered made mainly of limestones and ophiolites, the Tuscan Unit consists of turbidites like the Macigno and Scaglia Toscana Formations (Cretaceous-Miocene) and carbonates and evaporites (upper Triassic-Cretaceous). The Tuscan-Umbrian unit consists of the turbiditic Rentella Formation (Oligcene-Miocene), while the Umbria-Marche Unit is represented by carbonates and evaporites like the Anidriti di Burano Formation (Upper Triassic-Cretaceous) (Barsella et al. 2009).

Geological Model

According to the interpreted geological cross section (Figure 49) the geological model of the subsurface shows, in the SW portion of the section, the Tuscan nappe overlapping the Umbria Marche Succession. In our reconstruction two different reservoirs exist: the former is located inside the Tuscan carbonates and the latter inside the Umbria-Marche carbonates and evaporites, both are considered tectonically fractured and confined between low permeability units like the Scaglia Toscana Formation, the Rentella or the Ligurian Unit (Regione Umbria 2014). The 3D geological model was created across a SW- NE transect of area where the most relevant input data and reliable information was available, applying geostatistical GIS analysis to a series of 500x500m square grids, giving the value for depth and thickness of the reservoir for each vertex of the grid. The results of this model are shown in Figure 50 with a 3D geological model of the area from the 500x500m grid (black points), where the extension of the top (blue colour), the bottom (green) of the reservoir and the location of the deep wells (pink) have been traced.

Thickness of the reservoir

The map of the thickness of the reservoir in Figure 52 shows the structural condition of the reservoir, due to tectonics intensive action, the upper carbonate reservoir is almost always kept separated from the lower one by the Scaglia Toscana Formation deposits, so the highest values of thickness have only reached in the central and NE part of the transect.

Assessment of temperature values for each vertex of the 500x500m grid was achieved through the interpretation of the information from the thermal springs and wells in the area. Hydraulic conductivity of the reservoir due to fractures, karst and dissolution supplemented by (primary/secondary) porosity and permeability data, where available and meaningful also was considered in temperature prediction at various depth levels. The map of the temperature on top of the reservoir in Figure 53 shows that in the central part of the transect T, where also the top of the carbonate reservoir is closer to the ground level, values have reached about 100 °C.

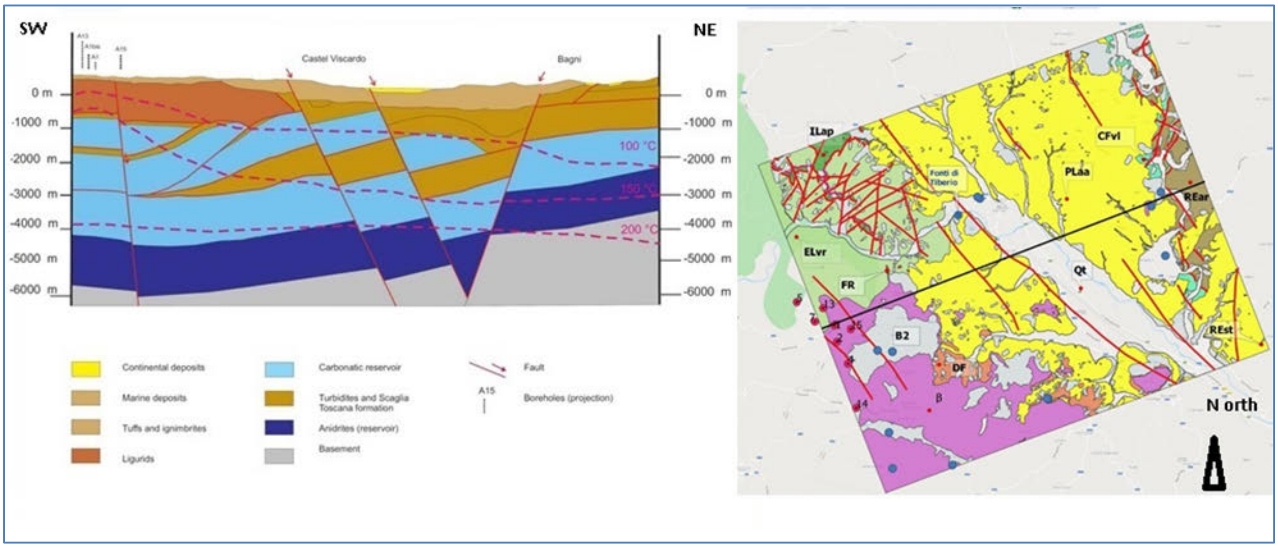

Figure 49 Geological map and the SW-NE Geological Cross Section (in black) across the study area with geothermal reservoir and temperature assessment.

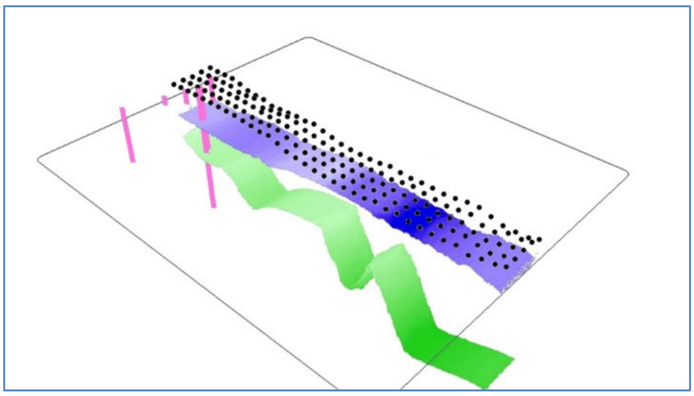

Figure 50 In the semi- central part of the area, the top of the carbonate reservoir starts at about 700 m below ground level.

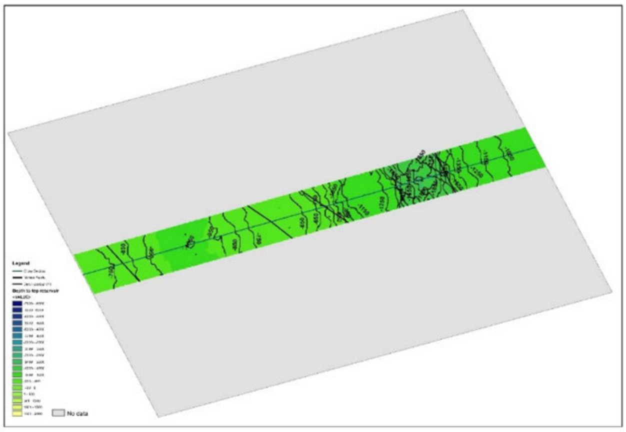

Figure 51 Top reservoir depth.

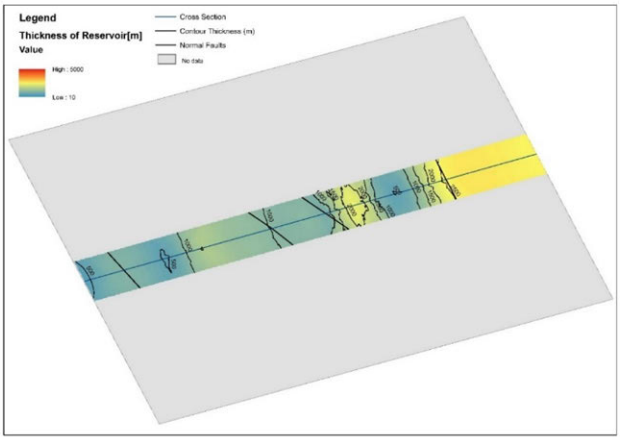

Figure 52 Thickness of the reservoir.

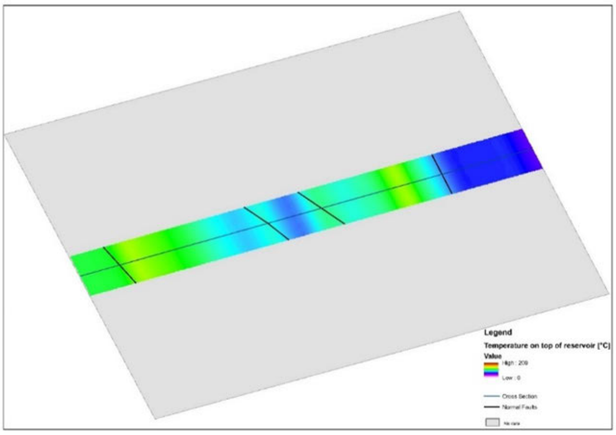

Figure 53 Temperature on top of reservoir.

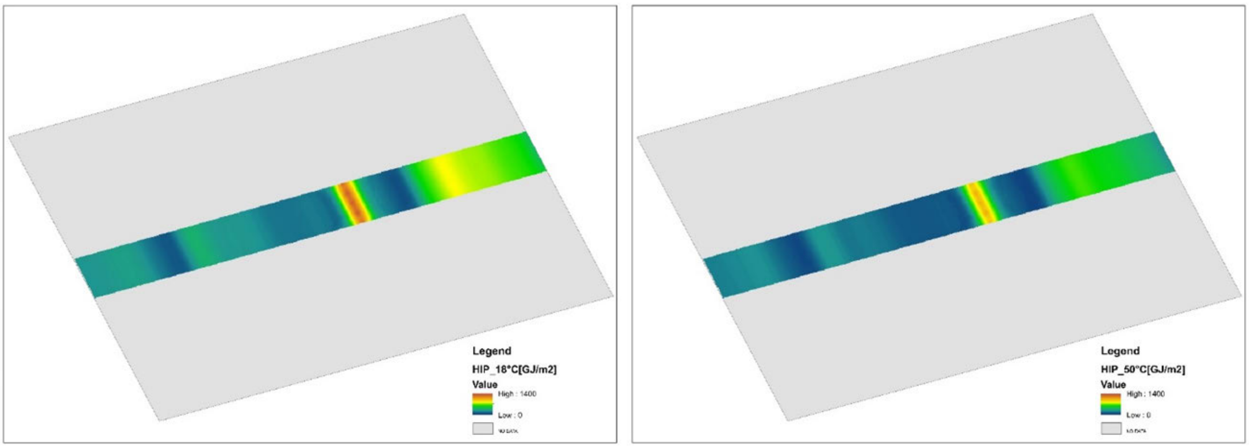

Figure 54 Heat in place for a return temperature of 18 °C (top) and 50 °C (bottom).

2.12.2 Heat in Place

The Heat in Place (HIP) was calculated according to Muffler & Cataldi (1978) using most of the parameters agreed by the HotLime team considering an injection temperature of 18 °C and 50 °C, and the data available from the 3D geological and geothermal modelling. The results are shown in Figure 54 where highest values of HIP have reached about 1328 GJ/m² for 18 °C and 1070 GJ/m² for 50 °C in the central part of the transect.

2.12.3 Conclusions

The case study area is part of a geothermal field located in the south western part of Regione Umbria where geothermal systems of medium-high enthalpy have been already explored and where one of the few authorized projects for future exploitation of geothermal resources in our territory is planned to start soon.

The synthetic maps in this report, though subject to some refinement due to the assumptions made and the not homogeneous distribution of the deep wells in the area, represent an effort to integrate all the available geological, geophysical and hydrogeological information available providing a model of the reservoir behaviour and a contribution to the geological and geothermal knowledge of the area.

In conclusion this study, integrated with further investigations like drilling new exploration wells, should help taking the next steps towards implementing sustainable energy solutions based on geothermal resources.

This study, integrated with further investigations like drilling new exploration wells, should help taking the next steps towards implementing sustainable energy solutions based on geothermal resources.

3 3DHIP Calculator (D3.1.4)

Authors: I. Herms, M. Colomer (ICGC)

A new tool to perform geothermal resource assessment maps of deep hot aquifers from 3D geological and thermal voxel models, by means of the “Heat in Place” method using Monte Carlo simulations.

3.1 Introduction

The volumetric “Heat in Place” (HIP) method, developed by the United States Geological survey (USGS), with its subsequent revisions and specific reformulations (Williams et al. 2008, Garg & Combs 2010, 2011, 2015), is still the most globally used evaluation technique to estimate the available stored and recoverable heat from deep geothermal reservoirs among geological services, research centres and companies in general. The HIP estimation is the first and the key step of any geothermal project in early exploration stages.

The methodology that was originally defined would have used the stochastic approach proposed initially by Nathenson (1978) to consider the uncertainty in the accessible geothermal resource base. The other variables used to estimate the stored energy were the volume (surface and thickness), the average temperature of the reservoir, the re-injection or reference temperature, and the properties of the water-rock system: porosity, density, and specific heat capacity.

In the simpler form of applying the HIP method, the reservoir is conceptualized as a unit model (one-cell approach) for its entire volume or considering a specific part of it, and therefore the stored heat is estimated as a whole (Arkan & Parlaktuna, 2005; Halcon et al. 2015; Yang et al. 2015, Barkaoui et al. 2017; Shah et al. 2018; Miranda et al. 2020). Therefore, the stochastic approach is inferred by the temperature of the reservoir and the properties of the water-rock system. Until now, this has been normally performed using commercial software such @Risk (Palisade) or Crystal-Ball (Oracle). This approach can be also applied nowadays using free and open-source tools (Pocasangre & Fujimitsu, 2018). Both applications regard the analysed domain as a lumped parameter model, i.e. with homogeneous distribution of parameters in the whole calculated volume.

Although originally the HIP method was thought to be applied following a stochastic approach using Monte Carlo simulations, many authors has been also applied it following a deterministic approach at regional scale (Colmenar-Santos et al. 2016; Limberger et al. 2018). To better define the volume of the reservoir in this deterministic approach many authors improve the workflow using 3D geological models to better determined the volume of the aquifers for then globally applying the deterministic HIP approach (Bär & Sass 2014; Yang et al. 2015). More recent and rigorous approaches have been implemented in the framework of nationwide projects in Netherlands (ThermoGIS project, TNO) and in specific parts of Italy (VIGOR ThermoGIS) which used 3D subsurface models and mapping techniques by means of Geographic Information Systems (GIS) to spatially and stochastically assess deep geothermal potential (Vrijlandt et al. 2019; Kramers, et al. 2012; Trumpy et al. 2016). At the moment, these tools are not designed to be used outside of the areas for which they were developed.

Therefore, with the aim of having a standard and free access tool for the entire geoscience community to allow the calculation of HIP and Heat recovery (Hrec) based on 3D data through Monte Carlo simulations, the partner Institut Cartogràfic i Geològic de Catalunya (ICGC) released in February 2020 a new free software called 3DHIP-Calculator (Piris et al. 2020). The 3DHIP methodology has been applied at the moment in two different sites in Catalonia, one of them in the framework of the GeoERA HotLime project (Herms et al. 2020, 2020b). The software was presented to the HotLime team in a webinar hold in May 20th, 2020. 10:00 – 11:30h CET.

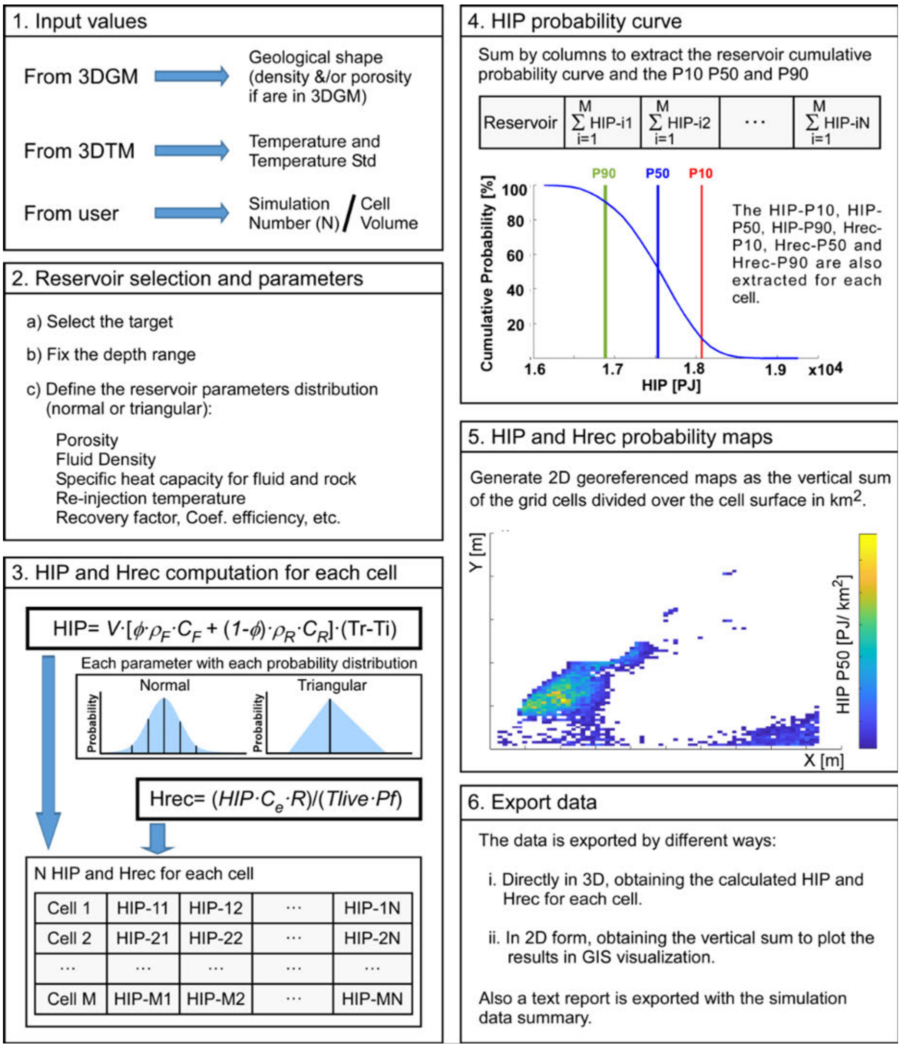

Figure 55 *3DHIP-Calculator workflow. The 3DHIP-Calculator application is structured in different tabs, where text and numerical editable files and boxes allow the user to select the properties, desired labels, and run tasks. Conceptually this workflow is divided into six main steps: 1) input values, 2) Reservoir selection and parameters, 3). HIP and Hrec computation, 4) HIP probability curve, 5) HIP and Hrec probability maps and 6) Export data.*

Tool description

The 3DHIP-Calculator is a new software which allows to assess the regional deep geothermal potential from the three-dimensional point of view using stochastically the volumetric USGS method. It allows to consider any case study from own 3D geological and thermal models and obtaining 3D evaluation geothermal potential and derived maps.

The 3DHIP-Calculator was developed using the MATLAB™ language and then compiled for Windows as a standalone application with an intuitive graphical user interface (GUI) that help their utilization. The installation files, as well as the user manual in pdf format and some examples for testing, can be freely downloaded from the Deep geothermal energy web page of the ICGC (under the Creative Commons licence Attribution 4.0 International, CC BY 4.0). The current version is v1.1. December 2020. The download, available from this link, includes examples to test the software and a manual in English.

The resulting tool is able to perform the simulations, compile the results and getting different graphs and maps with the results. As shown in Figure 55, it is organized in six main steps: firstly, the pre-processing steps include the selection of input parameters (step 1. Figure 55) and the definition of probability distribution functions (PDFs) which defined them (step 2. Figure 55). Then, the processing steps perform the HIP and Hrec calculations (step 3. Figure 55). Finally, the post-processing allows visualising the probability results (step 4. and 5. Figure 55) and export them to text files (step 6. Figure 55). For more information on how to operate the application the reader is referred to the 3DHIP-Calculator software user manual.

3.2 Approach and methods

3DHIP-Calculator is based on the HIP approach that allows estimating the geothermal resource and the recoverable fraction of a subsurface *reservoir* (Garg & Combs, 2015; Limberger et al. 2018; Muffler & Cataldi, 1978; Trumpy et al. 2016). The HIP is calculated according to the Eq. (2):

$$HIP = V \cdot [\emptyset \cdot \rho_F \cdot C_F + (1-\emptyset) \cdot \rho_R \cdot C_R] \cdot (Tr - Ti) \qquad \textit{Eq. (2)}$$

Where:

- *HIP* is the “Heat in Place”, stored heat or *accessible resource base* [*kJ*]
- *V* is the cell volume [m^3]
- $\emptyset$ is the rock porosity [parts per unit]
- ρ_R , ρ_F are the rock density and fluid density [kg/m^3]
- C_R ,C_F are the rock specific heat capacity and the fluid specific heat capacity [kJ/kg·°C]
- T_r is the reservoir temperature [°C]
- T_i is the temperature [°C] referred to either re-injection temperature, or abandonment temperature (as the threshold of economic or technological viable temperature) or the ambient temperature (i.e., the annual mean surface temperature value), or other criteria such as e.g., Limberger et al. (2018).

Then, the HIP value obtained is used to calculate the Hrec following the Eq. (3), which accounts for the producible thermal power during a given plant or project lifetime:

$$Hrec = \frac{HIP \cdot C_e \cdot R}{Tlive \cdot Pf} \qquad \textit{Eq. (3)}$$

Where:

- *Hrec* is the expected recoverable heat energy [kW]
- *HIP* is the "Heat in Place" [kJ] resulting from Eq. (1)
- R is the recovery factor [parts per unit]
- C_e is the conversion efficiency [parts per unit]. It considers the heat exchange efficiency from the geothermal fluid to a secondary fluid in a thermal plant.
- $Tlive$ is the mean plant lifetime or total project live [seconds]
- Pf is the plant or load factor [parts per unit]. Most of the direct heat applications (district heating, greenhouse heating, etc.) of geothermal energy are not continuous throughout the year. This factor considers the fraction of the total time in which the heating application is in operation.

The 3DHIP-Calculator allows combining the HIP method with probabilistic Monte Carlo simulations to regarding the reservoir uncertainties or heterogeneities as for example the porosity, rock density or the specific heat. In order to considerate it, each input parameters of Eqs. (2) and (3) is defined by a probability distribution function (PDF) (normal distribution or triangular distribution in the 3DHIP-Calculator). Thus, the calculations are repeated as many times as desired (N, number of simulations) using random values extracted from PDF's. The HIP result can be evaluated by a probabilistic way obtaining a new PDF from which the probability 10% or P10 (very low confidence of the estimation and high values), P50 and P90 (high confidence of the estimation and low values) can be extracted. Otherwise, the tool also allows the deterministic approach setting the values (i.e., without using a PDF) for each parameter and only considering the spatial variation defined by the geological and thermal models. Accordingly, the application calculates as many different HIP and Hrec values as the number of simulations defined by the user for each cell of the model.

3.3 Input data

The application requires a 3D geological and thermal models as input data.

The 3D geological model must be of the voxel type, generated from any of the most commonly used commercial geological-geophysical modelling software's – such as Petrel® E&P (Schlumberger), Leapfrog® (Seequent), GeoModeller3D® (BRGM, Intrepid-Geophysics) or GOCAD® (Paradigm), among others – and by any approach or building methodologies. It will have integrated the 3D distribution of lithology and additionally some petrophysical parameters (i.e. density or porosity rock) for each voxel in the model. When this spatial distribution of petrophysical parameters is not available, the tool can also evaluate the HIP method by assuming that each of them is either constant or varies according to the PDFs.

The 3D thermal model must follow the same georeferenced voxel format and it can be generated from purely conductive steady-state heat transport models, or more complex models considering convection flow. The distribution of thermal parameters and their outputs (i.e. temperature) will have the same 3D distribution (size cells and resolution) than the geological model. Required parameters for the 3DHIP Calculator are the temperature and its standard deviation for each voxel of the model. If the 3D thermal model is not available, the app allows inferring a rough 3D temperature field distribution within the 3D geological model using the 'temperature gradient approach' according to the following equation (Eq. 4):

$$Tz = T0 + gradT \cdot Dz \qquad \textit{Eq. (4)}$$

Where:

- Tz is the estimated temperature at depth [°C]
- $T0$ is the mean annual surface temperature [°C]
- $gradT$ is the measured thermal regional gradient [°C/km]
- Dz is the depth of the target according to the geological model

In order to run the application, this two main sets of input data must be performed to ASCII delimited text files. They will contain the cell coordinates and the other parameters in a specific order and in the required units for each voxel-cell in order to run in good way the tool.

3.4 Results and post-processing

The application provides results presented in several formats such as 2D maps and graphs (histograms and cumulative probability functions). The results are expressed in probability terms, using P10 as very low confidence of the estimation, and P50 and P90 as high confidence of the estimation. The outputs from the stochastic simulations are used to generate:

- Cumulative probability distribution for each cell, from which P10 (very low confidence of the estimation and high values), P50 and P90 (high confidence of the estimation and low values) are extracted. Furthermore, the mean and standard deviation are also calculated.
- Cumulative probability distribution for the entire investigated target (*e.g.*, geological unit, reservoir, etc.) summing the cell values and the P10, P50 and P90 are calculated. This approach is only carried out for the HIP calculation, not for the Hrec.
- 2D maps using the ratio between the vertical sum of the grid cells respect to the cell surface (in *km²*). The P10, P50 and P90 of HIP and Hrec are then estimated.

Otherwise, the application allows exporting two ASCII files with all results for further post-processing and generates an automatic report that summarizes the input data and the main results:

- The first exported file follows an ASCII format, which contains the 3D model with all the cells of the selected target. Each cell contains the initial data plus the HIP and Hrec calculations, expressed in terms of P10, P50, P90, mean and standard deviation. This file is suitable to be exported to 3D geological modelling software or for subsequent post-processing.

- The second one contains the information resulting from the 2D calculation considering the vertical sum of the HIP and Hrec values of each cell and the cell coordinates (in this case only *X* and *Y*). The values of HIP and Hrec are not divided by the cell surface and they are expressed as they have been calculated, *i.e.*, in P10, P50 and P90. This is useful for further geospatial analysis in a 2D mapping.
- Finally, the last file contains a brief report in text format that includes the data and parameters used for the simulation, as well as the main results obtained.

3.5 Application to the study case of Empordà Basin

In order to show the 3DHIP-Calculator applicability as a tool to assess the regional deep geothermal potential from the three-dimensional point of view using stochastically the volumetric Heat in Place (HIP) method (Muffler & Cataldi 1978), the Empordà Case was considered (Herms et al. 2020b). So, the 3D geological and thermal models generated in the HotLime framework were available in ASCII format and contain for each voxel cell: the voxel position (X,Y,Z coordinates); the lithology and the rock density, derived from the gravity inversion process; and the reservoir inferred temperature, from a purely 3D conductive steady-state heat transport model. For the workflow, GOCAD and 3DGeomodeller were used.

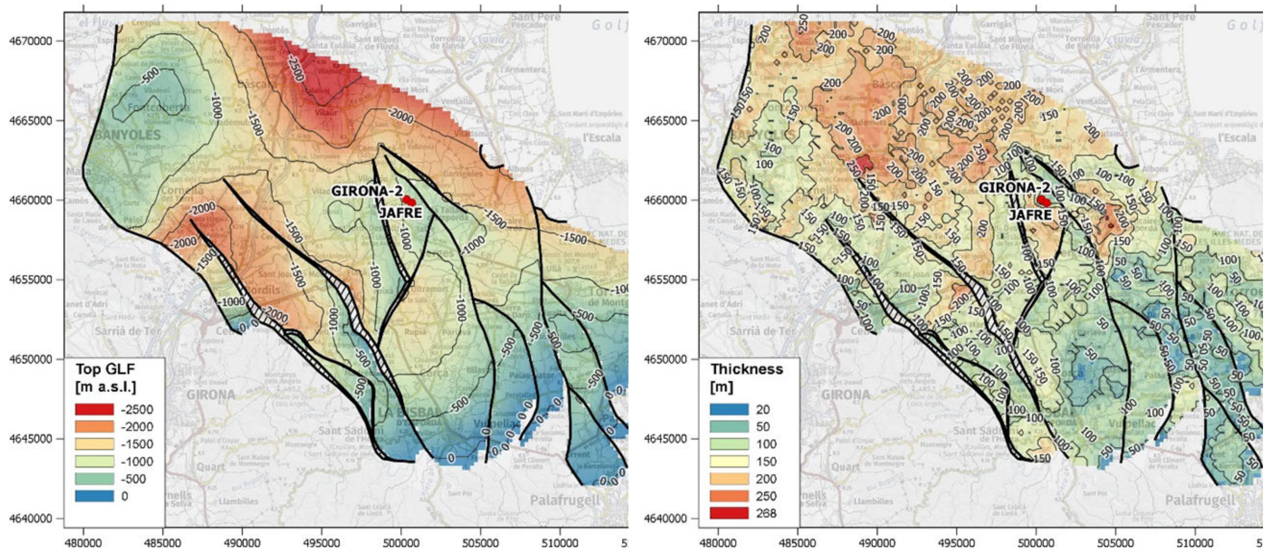

Figure 56 *Outputs maps derived from the 3D geological model: A) (left) Depth of the top of the fractured limestone GLF. B) (right) Thickness of the fractured limestone GLF.*

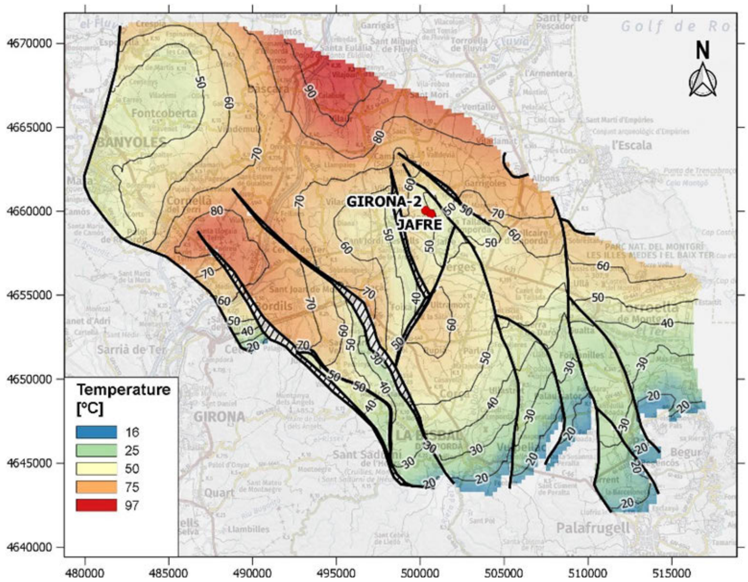

Figure 57 Output map derived from the 3D thermal model: temperature at top of the fractured limestone GLF.

In the first step (Figure 55), the tool load both models as well as the attributes to be considered. The user must also select the number of Monte Carlo simulations (e.g., 1.000 in this case), the desired target (the GLF layer for testing in this example) and the cell volume. The application then displays a graph with the temperature distribution against depth for all the cells of the selected target reservoir. Next step, still on the same tab, is selecting the depth range to be assessed (in this case, the whole aquifer depth) which it will be showed by two red lines after click on #3 Run button (Figure 58).

Going to the next tab ('Petrophysical properties and HIP distribution' tab), the user must introduce the required HIP and Hrec parameters and assign the corresponding PDFs (Table 11). In this case, the values for porosity and specific heat capacity of rock correspond to the measured average value of samples measured in the field campaign carried out in the Empordà area (ICGC-UB, 2019). The fluid density value also responds to a TDS around 5% (PH, S.A. 2003) at a temperature about 100 °C. The reference temperature (Tr) considered was 26 °C accordingly with the assumption of Limberger et al. (2018) for a global geothermal source assessment (considering a minimum reinjection temperature by unitarily adding 10 °C to the mean air temperature at the surface of 16 °C in the EB).

After assigning the petrophysical parameters and the corresponding PDFs, 3DHIP-Calculator provides the calculated histogram of the HIP frequency and the cumulative probability distribution function, with P10, P50 and P90 values for the entire target reservoir (Figure 59). Both resulting HIP and Hrec values (P10, P50 and P90) are also plotted in 2D maps as the vertical sum of the grid cells divided by the cell surface in km² (see Figure 60 for an example of HIP). In these maps, the cells with a value of zero are left without colour. Finally, the results obtained can be exported to other tools in the 'Export results' tab for post-processing.

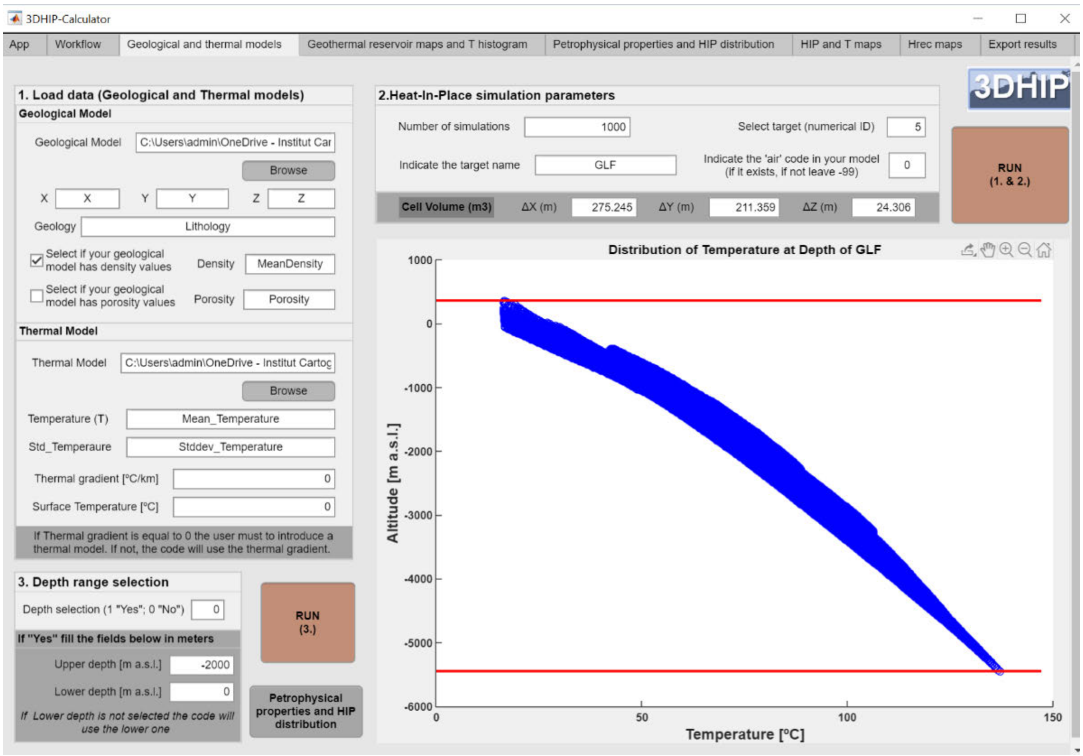

Figure 58 *Depth-temperature distribution obtained for example 2, which uses the geothermal gradient approach to calculate the temperature distribution for the Triassic unit in the geological and thermal models tab, instead of a 3D thermal model. Each blue circle corresponds to a cell corresponding the Triassic unit. The red lines indicate the fixed depth range for the HIP and Hrec calculations.*

Table 11 *Parameters introduced at the 3DHIP-Calculator (*: values from the 3D geological model; **: values from the 3D thermal model).*

parameter		**unit**	**mean**	**std**	**probability distribution**
thickness of the reservoir (calculated for each voxel*)		m	-	-	-
area of the reservoir (calculated for each voxel*)		m^2	-	-	-
rock density (calculated for each voxel*)	ρ_r	kg/m^3	-	-	-
porosity	ϕ	-	0.055	0.031	normal
specific heat capacity (rock) at reservoir condition	C_r	kJ/kg °C	0.86	0.10	normal
temperature of the reservoir [°C] (calculated for each voxel**)	T_i	°C	-	-	-
fluid density	ρ_w	kg/m^3	962.177	0.178	normal
specific heat capacity (fluid) at reservoir condition	C_w	kJ/kg °C	3.80	0.01	normal
reference temperature	T_f	°C	26	-	fixed value

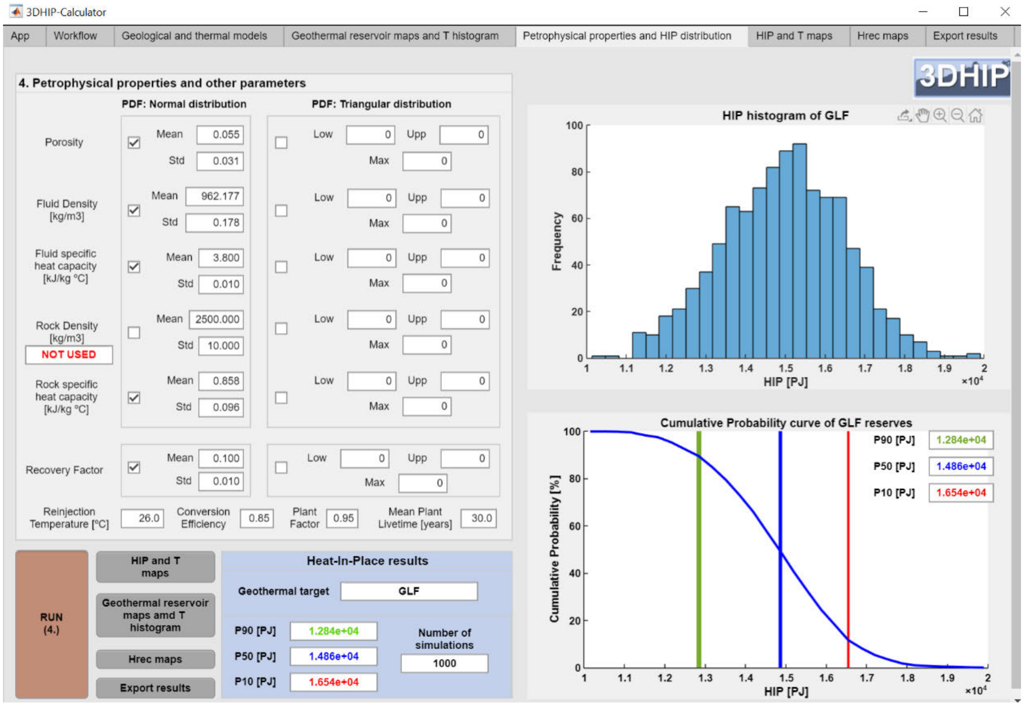

Figure 59 *Screenshot of the 'Petrophysical properties and HIP distribution' tab. In this tab the user defines the input values and the corresponding PDF.*

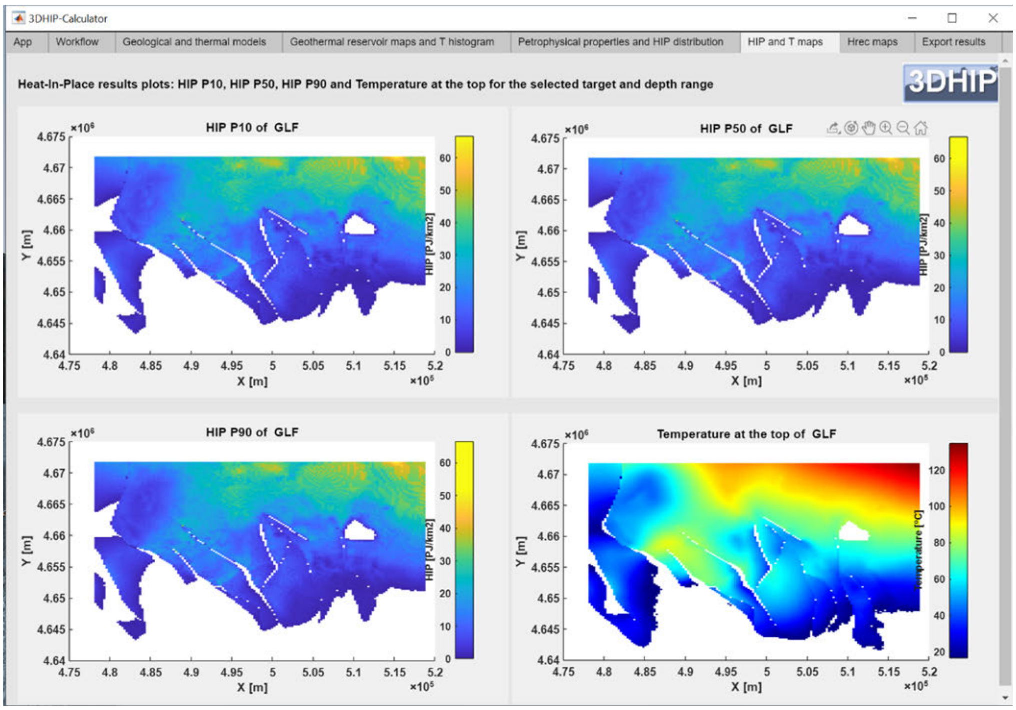

Figure 60 *Example of HIP and T maps tab where the 3D HIP results are vertically summed and divided by the cell surface area to express the results in GJ/m². The right bottom graph shows the temperature at the top of the selected target reservoir and depth range.*

The results obtained with 3DHIP-Calculator allowed to derive the HIP maps at the aquifer local scale. Figure 61 shows detailed 2D maps with different probabilities of the available resource: from 10% in HIP (P10), very low confidence of the estimation and high values; 50% in HIP (P50); and 90% in HIP (P90), high confidence of the estimation and low values. All of them were generated using the GIS software QGIS 3.16.4 'Hannover' version.

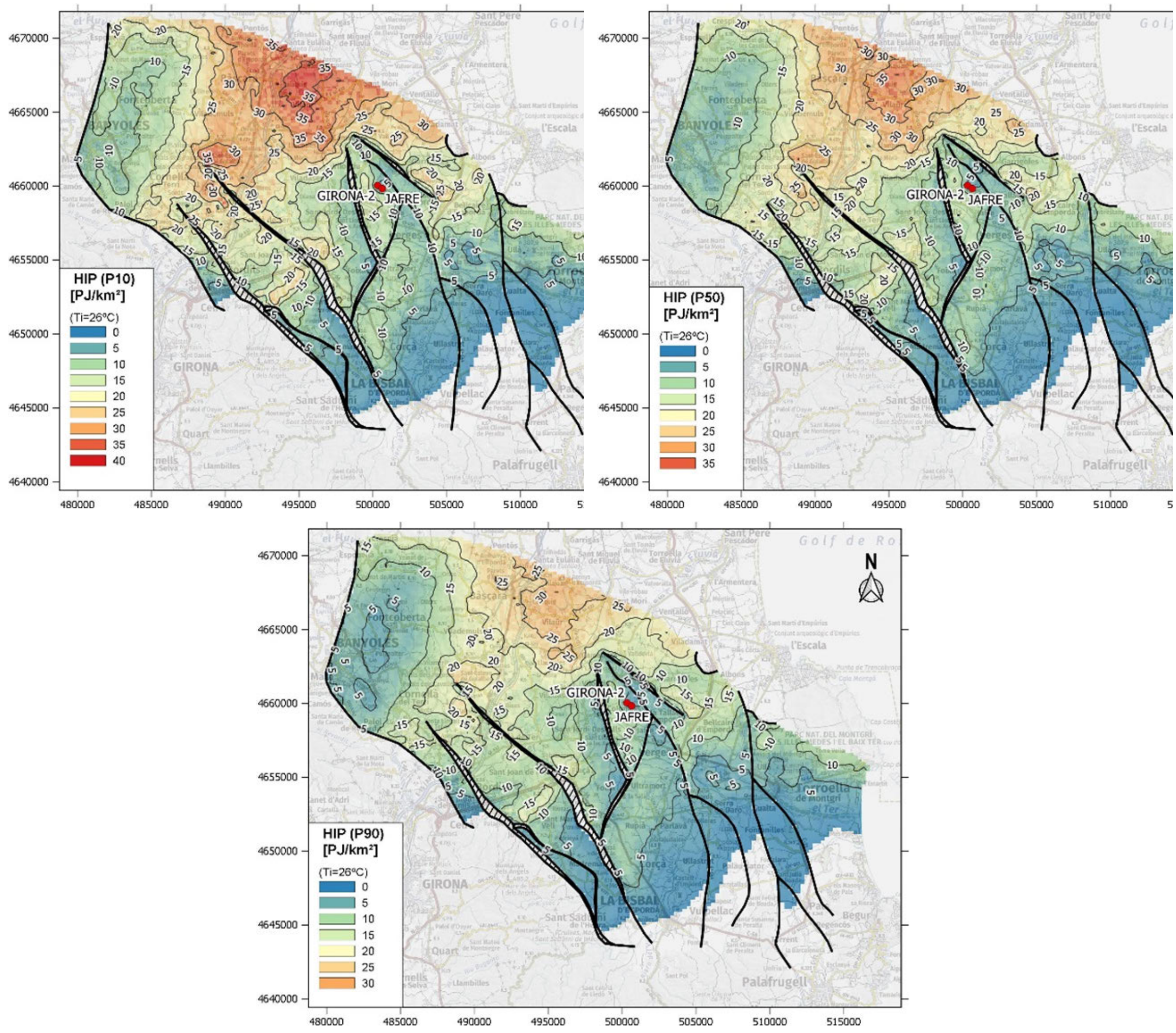

Figure 61 *Output maps of HIP assessment in the Empordà area: A) (top left) HIP map P10 map. B) (top-right) HIP map P50; C) HIP map P90.*

4 Conclusions

Author: J.G. Veldkamp (TNO)

The results of geothermal resource classification show the first ever, pan-European Heat in Place classification of 10 national and cross-border, low-enthalpy limestone reservoirs throughout Europe. In order to foster comparability between these reservoirs, a deterministic approach for Heat in Place calculation was adapted by all project partners. Input data from partners included spatial geometry of the reservoir, temperature at top of reservoir and average temperature of reservoir. Thermal parameters varied depending on the respective calculation method for the regional geothermal gradient and/or availability of a thermal model. A stochastic approach to HIP calculation was developed to incorporate uncertainty in input parameters.

During modelling and geothermal resource assessment, it became apparent that partners had to rely on very different national, geological datasets in both quantity and quality due to largely varying legal frameworks, depending to some degree on form of government (unitary or federal system) and overall data policy (liberal or restricted). Whereas some European countries have implemented a more liberal, open access policy concerning geological subsurface data (e.g. the Netherlands), others have a more restricted policy put in place in this regard (e.g. Austria).

Taking these national starting conditions into account, Heat in Place maps are not intended to offer concrete instructions for project developers to construct geothermal wells, but to indicate the overall potential of a region and identifying areas for further, localized investigation for geothermal exploration with promising values. However, as soon as reservoir maps are accessible via the EGDI platform (www.europe-geology.eu) or the HotLime map viewer https://geoera.eu/projects/hotlime6/, stakeholders can explore harmonized datasets for the respective pilot areas and identify promising locations for geothermal usage (Figure 62). Further information about the pilot areas is accessible via the attached metadata in case of inquiries by stakeholders (Geological survey responsible for data, contact details, model creator etc.).

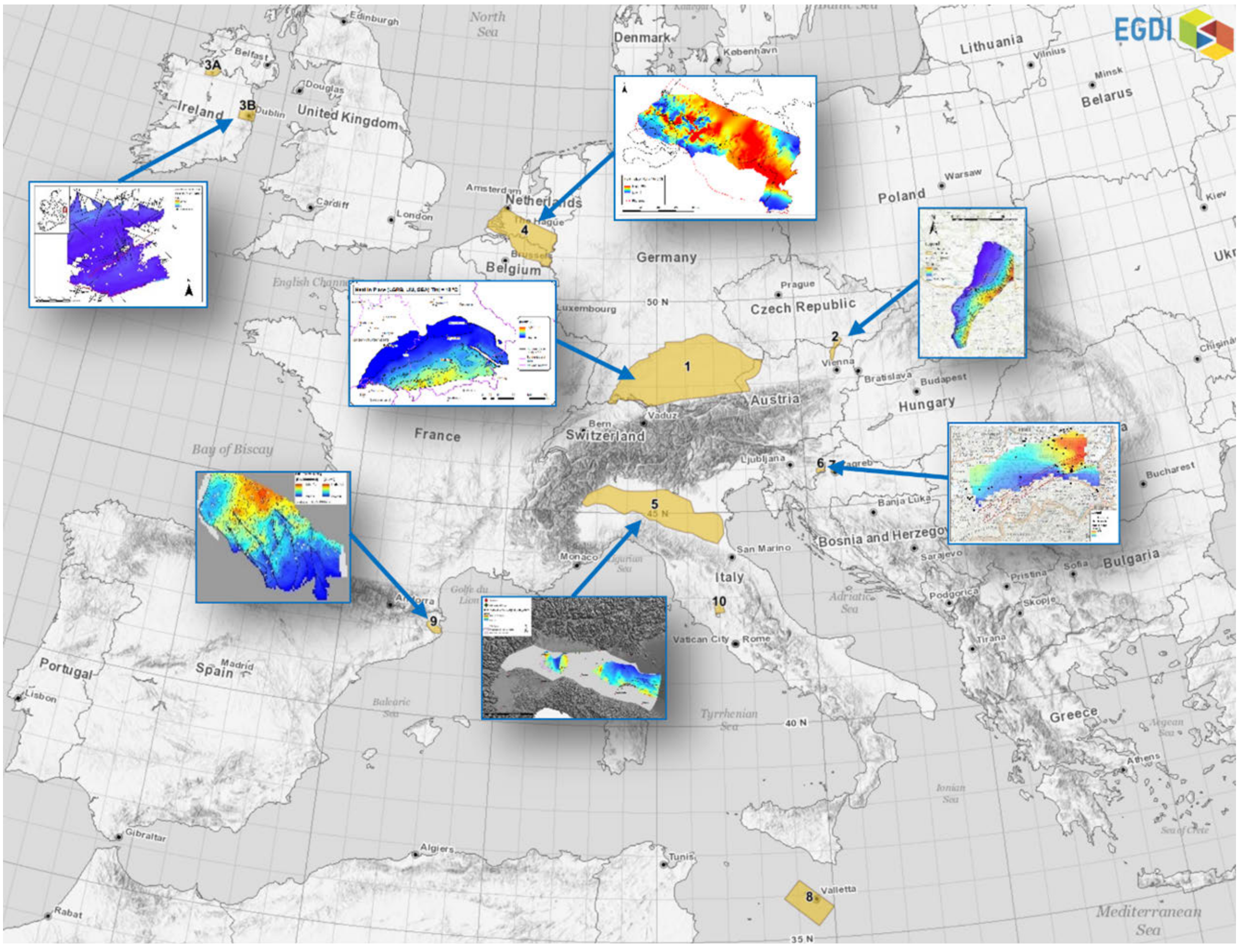

Figure 62 *Heat in Place maps from seven of the eleven pilot areas, which will be implemented to EGDI using uniform symbologies for comparability.*

Effective end of August 2021 all HIP18 maps as well as the underlying baseline parameters maps will be portrayed in HotLime's "Atlas of Carbonate Rock Geothermal Reservoirs Across Europe", a hyperlinked synopsis of the results of play and prospect evaluation in HotLime's 11 case study areas and the HotLime knowledge base, available via https://repository.europe-geology.eu/egdidocs/hotlime/hotlime_geothermal_atlas.pdf or https://geoera.eu/projects/hotlime6/. Under the latter link also the HotLime web map viewer is accessible featuring the georeferenced maps sets including metadata for further investigation.

References

Aretz, M. (2016): The Kulm Facies of the Montagne Noire (Mississippian, southern France). - In: Denayer, J. & Aretz, M. (eds.): Devonian and Carboniferous research: homage to Professor Edouard Poty. Geologica Belgica, 19 (1-2): http://dx.doi.org/10.20341/gb.2015.018

Argnani, A. (1990): The Strait of Sicily rift zone: Foreland deformation related to the evolution of a back-arc basin. - Journal of Geodynamics 1: 311-331.

Argnani, A. (1993): Neogene Basins in the Strait of Sicily (Central Mediterranean): Tectonic Settings and Geodynamic Implications. In: Boschi E., Mantovani E. & Morelli A. (eds) Recent Evolution and Seismicity of the Mediterranean Region. NATO ASI Series (Series C: Mathematical and Physical Sciences), vol 402. Springer, Dordrecht.

Arkan, S. & Parlaktuna, M. (2005): Resource Assessment of Balçova Geothermal Field. - Proceedings World Geothermal Congress 2005. Antalya, Turkey, 24-29 April 2005.

Australian Geothermal Reporting Code Committee (AGRCC) (2010): The geothermal reporting code. Australian code for reporting of exploration results.

Ayala, C., Izquierdo-Llavall, E., Félix Rubio, F., Pueyo, E., Casas, A., Oliva-Urcia, B., Adriana Rodríguez-Pintó, A., Rey-Moral, C. & Mediet, J.F. (2015): Basement characterization and cover deformation of the Linking Zone (NE Spain) from 2.5D and 3D geological and geophysical modelling. Proceedings, 8th EUREGEO 2015, ICGC, Barcelona, Spain, pp. 5-6. https://opac.geologie.ac.at/ais312/dokumente/8th_EUREGEO_2015.pdf [2021-03-28]

Bär, K. & Sass, I., (2014): 3D-Model of the Deep Geothermal Potentials of Hesse (Germany) for Enhanced Geothermal Systems. Proceedings, Thirty-Ninth Workshop on Geothermal Reservoir Engineering Stanford. https://www.researchgate.net/publication/264758168 [2021-03-28]

Bär, K., Reinsch, T. & Bott, J. (2019): P³ - PetroPhysical Property Database. V. 1.0. GFZ Data Services. https://doi.org/10.5880/GFZ.4.8.2019.P3

Barkaoui, A.-E., Zarhloule, Y., Varbanov, P.S. & Klemeš, J.J. (2017): Geothermal power potential assessment in north eastern Morocco. - Chemical Engineering Transactions 61: 1627-1632. https://doi.org/10.3303/CET1761269

Beardsmore, G. (2013): Global Review of Geothermal Reporting Terminology. Prepared for members of the International Energy Agency – Geothermal Implementing Agreement. Hot Dry Rocks Pty Ltd., South Yarra, Australia, 53 p.

Birner, J. (2013): Hydrogeologisches Modell des Malmaquifers im Süddeutschen Molassebecken. – PhD thesis Fachbereich Geowissenschaften der Freien Universität Berlin, 86 S., https://refubium.fu-berlin.de/handle/fub188/1492 [2021-03-23].

Birner, J., Fritzer, T., Jodocy, M., Savatis, A., Schneider, M. & Stober, I. (2012): Hydraulische Eigenschaften des Malmaquifers im Süddeutschen Molassebecken und ihre Bedeutung für die geothermische Erschließung. - Zeitschrift für geologische Wissenschaften 40(2/3): 133–156.

Blake, S., 2016. A multi-disciplinary investigation of the provenance, pathways and geothermal potential of Irish thermal springs. PhD thesis, National University of Ireland Galway, 179 pp., http://hdl.handle.net/10379/5926.

Bonté, D., Van Wees, J. D., & Verweij, H. (2012). Subsurface temperature of the onshore netherlands: New temperature dataset and modelling. Netherlands Journal of Geosciences, 91(4), 491-515.

Borović, S., Marković, T., Larva, O., Brkić, Ž. & Mraz, V. (2016): Mineral and thermal waters in the Croatian part of the Pannonian basin. - In: Papić, P. (Ed.) Mineral and Thermal Waters of Southeastern Europe, 31-45, Springer Intl.

Bridges, P.H., Gutteridge, P. & Pickard, N.A.H. (1995): The environmental setting of Early Carboniferous mud-mounds. In: Monty, C.L.V., Bosence, D.W.J., Bridges, P.H. & Pratt, B.R. (eds): Carbonate Mud-Mounds: Their Origin and Evolution. Special Publication of the International Association of Sedimentologists: 171-190.

Buonasorte, G. Fiordelisi, A. & Pandeli, E. (1991): The Alfina well 15: Deep geological data from northern Latium. – Boll. Soc. Geol. It. 110: 823-831.

Buonasorte, G., Cataldi R., Ceccarelli, A., Costantini, A., D'offizi, S., Lazzarotto, A., Ridolfi, A., Baldi,P.,Barelli A., Bertini, G, Bertrami, R., Calamai, A., Cameli, G., Corsi, R., Dacquino, C., Fiordelisi, A.,Ghezzo, A. & Lovari, F. (1988): Ricerca ed esplorazione nell' area geotermica di Torre Alfina. – Boll. Soc. Geol. It. 107: 265-337.

Burgess, P. M. & Gayer, R. A. (2000): Late Carboniferous tectonic subsidence in South Wales: implications for Variscan basin evolution and tectonic history in SW Britain. Journal of the Geological Society 157(1): 93-104.

Carlsen, T. (2019): Petrophysical Report of the Dinantian Carbonates in the Dutch Subsurface. Report available from www.NLOG.nl

Civile, D., Lodolo, E., Accettella, D., Geletti, R., Ben-Avhraham, Z., Deponte, M., Facchin, L., Ramella, R. & Romeo, R. (2010): The Pantelleria graben (Sicily Channel, Central Mediterranean): An example of intraplate 'passive' rift. - Tectonophysics 490: 173-183.

Colmenar-Santos, Folch-Calvo, M., Rosales-Asensio, E. & Borge-Diez, D. (2016): The geothermal potential in Spain. - Renewable and Sustainable Energy Reviews 56: 865–886. https://doi.org/10.1016/j.rser.2015.11.070

Debono, G. (2014): A preliminary assessment of the geothermal potential of Malta, (unpublished).

Deibert, L., Hjartarson, A., McDonald, I., McIlveen, J., Thompson, A., Toohey, B. & Yang, D. (2010): The canadian geothermal code for public reporting. Reporting of exploration results, geothermal resources and geothermal reserves. - Canadian Geothermal Energy Association, 34.

Diepolder, G.W., Borović, S., Herms, I. & HotLime Team (2019): HotLime – Mapping and Assessment of Geothermal Plays in Deep Carbonate Rocks. - Proceedings World Geothermal Congress 2020+1, Rey-kjavik, Iceland, Paper 16040, 9p. https://www.researchgate.net/publication/335871009 [2021-03-30].

Diepolder, G.W. & HotLime Team (2020): HotLime - Mapping and Assessment of Geothermal Plays in Deep Carbonate Rocks – summary of mapping and generic characteristics of eleven case studies. - HotLime Mid-term Summary Report: 10 pp. https://repository.europe-geology.eu/egdidocs/hotlime/hotlime_deliverable_21.pdf [2021-06-30].

Donner, E. (2020): Geologisches 3D-Modell Niederbayern. - UmweltSpezial, 35 S., Augsburg (Bayerisches Landesamt für Umwelt).

Dővényi, P. & Horváth, F. (1988): Review of Temperature, Thermal Conductivity and Heat Flow Data for the Pannonian Basin. - In: Royden, L.H. & Horváth, F. (Eds.): The Pannonian Basin – a Study in Basin Evolution. - American Association of Petroleum Geologists, Tulsa, Oklahoma, pp. 195-233.

Eppelbaum, L., Kutasov, I. & Pilchin, A. (2014): Thermal Properties of formations. Applied Geothermics (p. 757). https://doi.org/10.1007/978-3-642-34023-9

Falcone, G., Antics, M., Baria, R., Bayrante, L., Conti, P., Grant, M., Hogarth, R., Juliusson, E., Mijnlieff, H., Nádor, A., Ussher, G. & Young, K. (2017): Application of the United Nations Framework Classification for Resources (UNFC) to Geothermal Energy Resources. Selected case studies. UNECE Energy Series No. 51. UN Economic Commission for Europe, New York and Geneva, 82p.

Fullea, J., Afonso, J. C., Connolly, J. A. D., Fernandez, M., García-Castellanos, D. & Zeyen, H. (2009): LitMod3D: An interactive 3-D software to model the thermal, compositional, density, seismological, and rheological structure of the lithosphere and sublithospheric upper mantle. - Geochem. Geophys. Geosyst. 10: Q08019. https://doi.org/10.1029/2009GC002391.

Garg, S.K. & Combs, J. (2010): Appropriate use of USGS volumetric "Heat in place" method and Monte Carlos calculations. Thirty-Fourth Workshop on Geothermal Reservoir Engineering Standford University, Stanford, California, February 1-3. (2010) SGP-TR-188. https://pangea.stanford.edu/ERE/pdf/IGAstandard/SGW/2010/garg.pdf

Garg, S.K. & Combs, J. (2011): A re-examination of USGS volumetric "Heat in Place" method. - Proceedings, Thirty-Sixth Workshop on Geothermal Reservoir Engineering Standford University, Stanford, California, January 31 – February 2. (2011) SGP-TR-191. https://pangea.stanford.edu/ERE/pdf/IGAstandard/SGW/2011/garg.pdf

Garg, S.K. & Combs, J. (2015): A reformulation of USGS volumetric "heat in place" resource estimation method. - Geothermics 55: 150–158. http://dx.doi.org/10.1016/j.geothermics.2015.02.004

GEOHEAT-APP. 2014. Economische haalbaarheid van diepe en intermediaire geothermie voor het verduurzamen van de warmtevraag bij bouw-en renovatieprojecten (Economical feasability of deep and intermediary geothermal energy in supplying sustainable heat for new building and renovation projects). VITO, Grontmij Nederland & TNO, IVa.

GeoMol Team (2015): GeoMol – Assessing subsurface potentials of the Alpine Foreland Basins for sustainable planning and use of natural resources. – Project Report, 188 S., Augsburg (Bayerisches Landesamt für Umwelt). https://www.geomol.eu/report [2021-03-23].

Goodman, R., Jones, G., Kelly, J., Slowey, E., O'Neill, N., 2004. Geothermal Energy Resource Map of Ireland Final Report. Sustainable Energy Ireland (SEI), Dublin.

Götzl, G., Hoyer, S., Fuchsluger, M., Weilbold, J., Lipiarsky, P., Ramberger, R. & Zekiri, F. (2012): OMV Thermal. Final report, Geological Survey of Austria, 159p.

Halcon, R. M., Kaya, E. & Penarroyo, F. (2015): Resource Assessment Review of the Daklan Geothermal Prospect, Benguet, Philippines. - Proceedings World Geothermal Congress 2015 Melbourne, Australia.

Hantschel, T., & Kauerauf, A.I. (2009): Fundamentals of basin and petroleum systems modeling. - 492 pp., Springer. http://dx.doi.org/10.1007/978-3-540-72318-9

Heidbach, O., Reinecker, J., Tingay, M., Müller, B., Sperner, B., Fuchs, K. & Wenzel. F. (2007): Plate boundary forces are not enough: Second- and third-order stress patterns highlighted in the World Stress Map database. - Tectonics 26: TC6014. http://dx.doi.org/10.1029/2007TC002133

Herms, I., Colomer, M., Diepolder, G.W., Piris, G., Arnó, G., Gomez-Rivas, E., Gabas, A., Cantarero, I., Bellmunt, F., Trave, A., Macau, A., Griera, A., Benjumea, B., Sedano, J., Figuereas, S., Martin-Martin, J., Bover-Arnal, T. & Healy, D. (2020b): 3D Modeling and Geothermal Potential Assessment of a Fractured Carbonate Reservoir in the South-Eastern Pyrenees - the Empordà Case Study in NE Catalonia - GeoERA HotLime Project. - Proceedings World Geothermal Congress 2020+1, Reykjavik, Iceland, [Abstract].

Herms, I., Piris, G., Colomer, M., Peigney, C., Griera, A., Ledo, J. (2020a): 3D Numerical Modelling Combined with a Stochastic Approach in a Matlab-based Tool to Assess Deep Geothermal Potential in Catalonia: The Case Test Study of the Reus Valls Basin. Proceedings World Geothermal Congress 2020+1 Reykjavik, Iceland, [Abstract].

Horváth, F., Musitz, B., Balázs, A., Végh, A., Uhrin, A., Nádor, A., Koroknai, B., Pap, N., Tóth, T. & Wórum, G. (2015): Evolution of the Pannonian basin and its geothermal resources. - Geothermics 53: 328-352.

Husson, E. Guillen, A. Séranne, M., Courrioux, G., and Couëffé, R. (2018): 3D Geological modelling and gravity inversion of a structurally complex carbonate area: application for karstified massif localization. - Basin Research 2018: 1-17. https://doi.org/10.1111/bre.12279

ICGC (1994): Mapa geològic 1:25.000. Torroella de Montgrí 296-2-2 (78-24)

ICGC (1995): Mapa geològic 1:25.000. Cornellà de Terri 296-1-1 (77-23)

ICGC (1995b): Mapa geològic 1:25.000. l'Escala 296-2-1 (78-23)

ICGC (1997): Mapa geològic 1:25.000. Sarrià de Ter 296-1-2 (77-24)

ICGC (2001): Mapa geològic 1:25.000. la Bisbal d'Empordà 334-2-1 (78-25)

ICGC (2003): Mapa geològic 1:25.000. Girona 334-1-1 (77-25)

ICGC (2017): Mapa de les unitats estructurals majors de Catalunya 1:1.000 000. ICGC, Barcelona, España. http://www.icgc.cat/

ICGC-UB (2019): Fieldworks and laboratory test for the determination of petrophysical properties for the evaluation of the geothermal potential of the deep carbonate reservoirs of the Empordà basin. 355p. (unpublished).

Intrepid-Geophysics (2020): Forward modelling & inversion with 3D GeoModeller. Geomodeller documentation. https://docs.intrepid-geophysics.com/geomodeller/index.html

Jongsma, D., Van Hinte, J.E. & Woodside, J. M. (1985): Geologic structure and neotectonics of the north African continental margin south of Sicily. - Marine and Petroleum Geology 2: 156-179.

Kombrink, H., Besly, B.M., Collinson, J.D., Den Hartog Jager, D.G., Drozdzewski, G., Dusar, M., Hoth, P., Pagnier, H.J. M., Stemmerik, L., Waksmundzka, M.I. & Wrede, V. (2010): Carboniferous. In: Doornenbal, J.C. & Stevenson, A.G. (eds): Petroleum geological atlas of the Southern Permian Basin area. Houten, the Netherlands, EAGE, 342pp.

Kombrink, H., 2008. The Carboniferous of the Netherlands and surrounding areas; a basin analysis. - Geologica Ultraiectina, Mededelingen van de Faculteit Geowetenschappen. Universiteit Utrecht (Utrecht): 294: 1-184.

Kombrink, H., Doornenbal, J., Duin, E., Den Dulk, M., ten Veen, J., & Witmans, N. (2012): New insights into the geological structure of the netherlands; results of a detailed mapping project. Netherlands Journal of Geosciences, 91(04), 419-446.

Kramers, L., Van Wees, J.D., Pluymaekers, M., Kronimus, A. & Boxem, T. (2012): Direct heat resource assessment and subsurface information systems for geothermal aquifers; the Dutch perspective. - Netherlands Journal of Geosciences 91/4: 637-649. https://doi.org/10.1017/S0016774600000421

Lawless, J. V., Ward, M., & Beardsmore, G. (2010): The Australian code for geothermal reserves and resources reporting: Practical experience. Paper presented at the World Geothermal Congress, Bali, Indonesia. 5.

Limberger, J., Boxem, T., Pluymaekers, M., Bruhn, D., Manzella, A., Calcagno, P., Beekman, F., Cloetingh, S. & Van Wees, J. D. (2018): Geothermal energy in deep aquifers: A global assessment of the resource base for direct heat utilization. - Renewable and Sustainable Energy Reviews 82: 961-975. https://dx.doi.org/10.1016/j.rser.2017.09.084

Lučić, D., Saftić, B., Krizmanić, K., Prelogović, E., Britvić, V., Mesić, I. & Tadej, J. (2001): The Neogene evolution and hydrocarbon potential of the Pannonian Basin in Croatia. Marine and Petroleum Geology 18: 133-147.

Mijnlieff, H., Van Kempen, B., Tolsma, S., De Vries, C., Martins, J. E., Veldkamp, H. & Van Wees, J. D. (2019): Dutch geothermal resource reporting. A first attempt of dutch nationwide geothermal resource using the UNFC resource classification system, status date january 2019. Paper presented at the European Geothermal Congress, Den Haag, Netherlands.

Miranda, M.M., Raymond, J. & Dezayes, C. (2020): Uncertainty and Risk Evaluation of Deep Geothermal Energy Source for Heat Production and Electricity Generation in Remote Northern Regions. - Energies 2020, 13(16), 4221. https://doi.org/10.3390/en13164221

Moeck, I. S. (2014): Catalog of geothermal play types based on geologic controls. - Renewable and Sustainable Energy Reviews 37: 867-882. http://dx.doi.org/10.1016/j.rser.2014.05.032

Moeck, I. S., Dussel, M., Weber, J., Schintgen, T. & Wolfgramm, M. (2020): Geothermal play typing in Germany, case study molasse basin: A modern concept to categorise geothermal resources related to crustal permeability. Netherlands Journal of Geosciences - Geologie en Mijnbouw 98: e14. https://doi.org/10.1017/njg.2019.12

Mozafari, M., Gutteridge, P., Riva, A., Geel, C.R., Garland, J., & Dewit, J. (2019). Facies analysis and diagenetic evolution of the Dinantian carbonates in the Dutch subsurface: overview and synthesis. Report available from www.NLOG.nl

Muffler, L. J. P., & Cataldi, R. (1978). Methods for regional assessment of geothermal resources. - Geothermics 7 (2-4): 53-89. https://dx.doi.org/10.1016/0375-6505(78)90002-0

Nádor, A. (2018): Training on UNFC-2009 geothermal specifications, and case studies in the Central and SE-European region – DARLINGe project examples. Presentation, 25 April 2018, UNECE Geneva, (2018). https://www.unece.org/fileadmin/DAM/energy/se/pp/unfc_egrm/egrc9_apr2018/25.04/p.5_DARLING_Nador.pdf [2019-07-26]

Nádor, A., Rman, N., Szöcz, T., Ádám, L. et al. (2018): D.6.3.1. Manual on the use of the transnational tool-box. DARLINGe – Danube Region Leading Geothermal Energy. Interreg Danube Transnational Programme, 62 pp.

Narkiewicz, M., 2007. Development and inversion of Devonian and Carboniferous basins in the eastern part of the Variscan foreland (Poland). Geological Quarterly, 51 (3): 231-265.

Nathenson, M. (1978): Methodology of determining the uncertainty in the accessible geothermal resource base of identified hydrothermal convection systems. Open-File Report 78-1003. https://doi.org/10.3133/ofr781003

Oncken, O., von Winterfeld, C. & Dittmar, U., 1999. Accretion of a rifted passive margin; the late Paleozoic Rhenohercynian fold and thrust belt (middle European Variscides). Tectonics, 18(1): 75-91.

Pallí, L. (1972): 'Estratigrafía del Paleógeno del Empordà y zonas limítrofes'. Publicaciones de Geología, Universidad Autónoma de Barcelona, 338 pp.

Paschen, H., Oertel, D., Grünwald, R. (2003): Möglichkeiten geothermischer Stromerzeugung in Deutschland – Sachstandsbericht. Büro für Technikfolgen-Abschätzung beim Deutschen Bundestag (Hrsg.) TAB-Arbeitsbericht 84: 124 S. (Berlin, TAB).

PH, S.A. (2003): Proyecto General de aprovechamiento de un manantial de agua termal y mineromedicinal, situado en el término municipal de Jafre (Girona), 197p. (unpublished).

Piris, G., Herms, I., Griera, A., Gómez-Rivas, E. & Colomer, M. (2020): 3DHIP-Calculator (v1.0) [Software]. Institut Cartogràfic i Geològic de Catalunya, Universitat Autònoma de Barcelona. CC-BY 4.0. (accessible from ICGC website)

Pluymaekers, M., Kramers, L., Van Wees, J. D., Kronimus, A., Nelskamp, S., Boxem, T., & Bonté, D. (2012). Reservoir characterisation of aquifers for direct heat production: Methodology and screening of the potential reservoirs for the netherlands. Netherlands Journal of Geosciences, 91(04), 621-636.

Pocasangre, C., & Fujimitsu, Y. (2018): A Python-based stochastic library for assessing geothermal power potential using the volumetric method in a liquid-dominated reservoir. - Geothermics 76: 164-176. https://doi.org/10.1016/j.geothermics.2018.07.009

Rajver, D. & Ravnik, D. (2003): Geothermal characteristics of the Krško basin, Slovenia, based on geophysical research. - Phys. Chem. Earth 28: 443-455.

Rajver, D., Rman, N., Lapanje, A. & Prestor, J. (2020+1): Geothermal country update report for Slovenia, 2015-2019. Proceedings. World Geothermal Congress 2020+1, Reykjavik, Iceland, Paper 10075, 16 p.

Regione Umbria – Servizio Geologico (2013): Cartografia Geologica Informatizzata vettoriale della Regione Umbria. h ttp://www.regione.umbria.it/, h ttp://dati.umbria.it

Regione Umbria (2014): Studio delle Potenzialità geotermiche del territorio regionale Umbro. - http://www.geoelec.eu/wp-content/uploads/2013/10/10-Checcucci-Umbria.pdf [2021-04-07].

Regione Umbria, Regione Emilia-Romagna, Regione Marche, Regione Toscana, Università Siena Cgt (2019): Geological Map of the Northern Apennines. - https://www.regione.umbria.it/paesaggio-urbanistica/intesa-interregionale [2021-04-07].

Reijmer, J. J. G., ten Veen, J. H., Jaarsma, B., & Boots, R. (2017). Seismic stratigraphy of Dinantian carbonates in the southern Netherlands and northern Belgium. Netherlands Journal of Geosciences 96 (4): 353-379.

Rivero, L., Vilas, M., Pinto, V. & Casas, A. (2001): Modelización gravimétrica 2D de la fosa de l'Empordà (NE de la Península Ibérica). - Acta Geologica Hispanica 36: 97-113. https://www.raco.cat/index.php/ActaGeologica/article/view/75633

Rupf, I., Diepolder, G.W. & HotLime Team (2020): Summary report of resources mapping and characterization. including descriptive reports on the case studies T2.1 - T2.10. - HotLime Deliverable 2.0: 130 pp. https://repository.europe-geology.eu/egdidocs/hotlime/hotlime_deliverable_20.pdf [2021-06-30].

Saula, E., Picart, J., Mató, E., Llenas, M., Losantos, M., Berástegui, X. & Agustí, J. (1996): 'Evolución geodinámica de la fosa del Empordà y las Sierras Transversales'. - Acta geológica hispánica 29(2-4): 55-75. https://www.raco.cat/index.php/ActaGeologica/article/view/75472/98282 [2021-04-07].

Schejbal, B. (2003): New considerations about Aquae Balissae and the Iassi people. - Opvuscula archaeologica 27: 393-416.

Schön, J.H. (2011): Physical Properties of Rocks: A Workbook: Volume 8 (Handbook of Petroleum Exploration and Production). ISBN: 978-0-444-53796-6.

Serra-Kiel, J., Mató, E., Saula, E., Travé, A., Ferràndez-Cañadell, C., Busquets, P., Samsó, J.M. Tosquella, Barnolas, A., Àlvarez-Pérez, G., Franquès, J. & Romero, J. (2003b): An inventory of the marine and transitional Middle/Upper Eocene deposits of the Southeastern Pyrenean Foreland basin (NE Spain). Geologica Acta 1(2): 201-229. https://doi.org/10.1344/105.000001610

Serra-Kiel, J., Travé, A., Mató, E., Saula, E., Ferràndez-Cañadell, C., Busquets, P., Tosquella, J. & Vergés, J. (2003a): Marine and Transitional Middle/Upper Eocene Units of the Southeastern Pyrenean Foreland Basin (NE Spain). - Geologica Acta 1(2): 177-200. https://doi.org/10.1344/105.000001609

Shah, M., Vaidya, D., & Sircar, A. (2018): Using Monte Carlo simulation to estimate geothermal resource in Dholera geothermal field, Gujarat, India. Multiscale and Multidisciplinary Modeling, Experiments and Design, (March). https://doi.org/10.1007/s41939-018-0008-x

SLR, 2009. Deep Geothermal Exploration Newcastle, South County Dublin VOLUME 1 - Phase 2 Deep Geothermal Exploration Report. SLR Consulting Ireland, Dublin. 72 pp.

Tari, V. & Pamić, J. (1998): Geodynamic evolution of the northern Dinarides and the southern part of the Pannonian Basin. - Tectonophysics 297: 269-281.

Ten Veen, J., De Haan, H., de Bruin, G., Holleman, N. Schöler, W. (2019): Seismic Interpretation and Depth Conversion of the Dinantian carbonates in the Dutch subsurface. Report available from www.NLOG.nl

TNO (2014): DoubletCalc, a program for calculating the indicative power of a geothermal doublet, v. 1.4.3. https://www.nlog.nl/en/tools [2019-07-22].

Trumpy, E., Botteghi, S., Caiozzi, F., Donato, A., Gola, G., Montanari, D., Pluymaekers, M.P.D., Santilano, A., Van Wees, J.D. & Manzella, A. (2016): Geothermal potential assessment for a low carbon strategy: A new systematic approach applied in southern Italy. Energy 103: 167–181. https://doi.org/10.1016/j.energy.2016.02.144

UNECE (2016): Specifications for the application of the United Nations framework classification for fossil energy and mineral reserves and resources 2009 (UNFC-2009) to geothermal energy resources. UNECE / International Geothermal Association.

UNFC (UNFC Geothermal Working Group) (2016): Specifications for the application of the United Nations Framework Classification for Fossil Energy and Mineral Reserves and Resources 2009 (UNFC-2009) to Geothermal Energy Resources. http://www.unece.org/fileadmin/DAM/energy/se/pdfs/UNFC/UNFC_GEOTH/UNFC.Geothermal.Specs.pdf [2021-03-28].

Van Hulten, F.F.N. & Poty, E. (2009): Dinantian Reefs underneath the Netherlands. EAGE 71th Conference and Technical Exhibition. EAGE, Amsterdam. W039: 1-5.

Van Leverink D. & Geel C.R. (2019): Fracture characterization of the Dinantian carbonates in the Dutch Subsurface. Report available from www.NLOG.nl.

Van Wees, J. D., Kronimus, A., Van Putten, M., Pluymaekers, M., Mijnlieff, H., Van Hooff, P., Kramers, L. (2012): Geothermal aquifer performance assessment for direct heat production–Methodology and application to rotliegend aquifers. Netherlands Journal of Geosciences, 91(04), 651-665.

Van Wees, J. D., Veldkamp, J.G., Brunner, L.G., Vrijlandt, M., de Jong, S., De Jong, S. & Peijster, J. (2020): Accelerating geothermal development with a play-based portfolio approach. - Netherlands Journal of Geosciences - Geologie en Mijnbouw 98: e14. https://doi.org/10.1017/njg.2020.4

Veldkamp J.G. & Hegen D. (2019): Temperature modelling of the Dutch subsurface at the depth of the Dinantian. Report available from www.NLOG.nl

Velić, J., Malvić, T., Cvetković, M. & Vrbanac, B. (2012): Reservoir geology, hydrocarbon reserves and production in the Croatian part of the Pannonian Basin System. - Geologia Croatica, 65(1): 91-101.

Vilà, M., Fernández, M., & Jiménez-Munt, I. (2010): Radiogenic heat production variability of some common lithological groups and its significance to lithospheric thermal modelling. Tectonophysics 490(3–4): 152–164. https://doi.org/10.1016/j.tecto.2010.05.003

Vrijlandt, M.A.W., Struijk, E.L.M., Brunner, L.G., Veldkamp, J.G., Witmans, N., Maljers, D. & Van Wees, J. D. (2019): ThermoGIS update: A renewed view on geothermal potential in the Netherlands. Paper presented at the European Geothermal Congress, The Hague, The Netherlands.

Williams, C.F., Reed, M.J. & Mariner, R.H. (2008): A review of methods applied by the U.S. Geological Survey in the assessment of identified geothermal resources. - U.S. Geological Survey, Open-File Report 2008-1296, 27 pp., https://pubs.usgs.gov/of/2008/1296/ [2021-03-23].

Yang, F., Liu, S., Liu, J., Pang, Z. & Zhou, D. (2015): Combined Monte Carlo Simulation and Geological Modeling for Geothermal Resource Assessment: a Case Study of the Xiongxian Geothermal Field, China. - Proceedings World Geothermal Congress 2015, Melbourne, Australia.

Zelić, M., Čubrić, S., Kulenović, I., Kušek, M., Marčan, B. et al.: Main mining design of the Zagreb Geothermal Field. INA plc., Zagreb, (1995). (in Croatian)

Ziegler, P.A., 1990a. Geological atlas of Western and Central Europe. Shell International Petroleum Maatschappij B.V., 237 pp.

Ziegler, P.A., 1990b. Tectonic and palaeogeographic development of the North Sea Rift system, In: Blundell, D.J. & Gibbs A.D. (eds): Tectonic Evolution of the North Sea Rifts. Oxford Science Publications (Oxford): 1-36.

Appendix 1: UNFC axes categorization

E category classification and subclassification of the present project – Čatež geothermal field

Category	***UNFC-2009 definition***	***Reasoning for classification***
E1	Extraction and sale have been confirmed to be economically viable	
E1.1	Extraction and sale are economic on the basis of current market conditions and realistic assumptions of future market conditions	• The project has been operating for 11 to more than 50 years (at 3 different users) and based on all experiences it is foreseen to run at least another 25 years. At surface, the heat may be transferred to another working fluid through heat exchangers. • It has positive and quantified effects on the reduction of gas consumption and decreased CO_2 emission.

F category classification and subclassification of the present project – Čatež geothermal field

Category	***UNFC-2009 definition***	***Reasoning for classification***
F1	Feasibility of extraction by a defined development project has been confirmed.	
F1.1	Extraction of available heat is currently taking place.	The gradually expanding project has been operating at Terme Čatež d.d. since 1964, at AFP Dobova since 1996 and at Paradiso Dobova since 2010. It is believed all production licences are available and secured in the long-term.

G category classification and subclassification of the present project – Čatež geothermal field

Category	***UNFC-2009 definition***	***Reasoning for classification***
G1	Quantities associated with a known deposit (resource) that can be estimated with a high level of confidence.	Based on a production forecast that about 2500 TJ of heat energy to be extracted can be foreseen with a moderate level of confidence for the next 25 years (25 x 100 TJ).
G2	Quantities associated with a known deposit (resource) that can be estimated with a moderate level of confidence.	

UNFC-2009 classification and quantification of the future potential project(s)

E category classification of the potential project – extension of the Čatež geothermal field

Category	*UNFC-2009 definition*	*Reasoning for classification*
E3	Extraction and sale is not expected to become economically viable in the foreseeable future* or evaluation is at too early stage to determine economic viability.	Based on the current project experiences and market conditions a similar project(s) is expected to become economically viable in the next 5-10 years (at least so long) to exploit the still available resources.
E3.2	Sub-category	Economic viability of extraction cannot yet be determined due to insufficient information (e.g. during the exploration phase when the one is ongoing)

*see explanation in: Falcone et al. (2017), p.36.

F category classification of the potential project – extension of the Čatež geothermal field

Category	*UNFC-2009 definition*	*Reasoning for classification*
F3	Feasibility of extraction by a defined development project or mining operation cannot be evaluated due to limited technical data.	Very preliminary studies (e.g. during the exploration phase), which may be based on a defined (at least in conceptual terms) development project or mining operation, indicate the need for further data acquisition in order to confirm the existence of a deposit in such form, quality and quantity that the feasibility of extraction can be evaluated.
F3.2	Sub-category	Local geological studies and exploration activities indicate the potential in a specific part of a geological province but requires more data acquisition and/or evaluation, in order to have sufficient confidence to warrant drilling or testing that is designed to confirm the existence of a deposit (resource) in such form, quality and quantity that the feasibility of extraction can be evaluated.

G category classification of the potential project – extension of the Čatež geothermal field

Category	*UNFC-2009 definition*	*Reasoning for classification*
G2-G3	Quantities associated with a known deposit (resource) that can be estimated with a medium to low level of confidence.	Moderate to low confidence estimate (best or high estimate incremental to G1 or G2, respectively). Uncertainties include both variability in the Renewable Energy Source and the efficiency of the extraction.